RADIOACTIVITY TRANSPORT IN WATER--

MATHEMATICAL MODEL FOR THE TRANSPORT OF RADIONUCLIDES

Technical Report--12

to the

U. S. Atomic Energy Commission
Contract AT-(11-1)-490

by

Chia Shun Shih
Research Engineer

Earnest F. Gloyna
Project Director

CENTER FOR RESEARCH IN WATER RESOURCES
Environmental Health Engineering Research Laboratory
Civil Engineering Department
The University of Texas

EHE-04-6702
CRWR-18

June 1, 1967

ACKNOWLEDGMENT

The financial support of the U. S. Atomic Energy Commission has made these studies possible. The interest and direction of Mr. Walter Belter, Chief, and Mr. Craig Roberts, Sanitary Engineer, of the Environmental and Sanitary Engineering Branch, Division of Reactor Development, U. S. Atomic Energy Commission, are most gratefully appreciated. Special acknowledgments are extended to Mr. Hal Bernard, former Sanitary Engineer, U.S.A.E.C., and to Professors W. W. Eckenfelder, W. L. Moore, E. J. Prouse, W. F. Bradley, K. B. Bischoff, J. O. Ledbetter, and J. F. Malina, all of The University of Texas, for their suggestions and comments. Appreciation is also due Mrs. Linda D. Eschman, Mr. Frank Hulsey, and Professor J. R. Holmes for their contributions to this report.

ABSTRACT

The purpose of this study was to develop a mathematical model which describes the transport of radionuclides injected instantaneously in a stream. Particular emphasis was directed to the influence of sediments on transport.

Instantaneous release of dye and continuous release of ^{85}Sr, respectively, were used to measure the dispersion and mass transfer coefficients. Aquaria and model river experiments were undertaken to determine various parameters which define the mechanism of sorption and desorption of radionuclides by sediments. Instantaneous injection of ^{85}Sr into the model river provided data for establishing the relationship between the analytical solution and a proposed mathematical model. Fortran programs were designed for the analyses of gamma spectra, dispersion coefficients and transport equations.

Some of the important factors affecting the transport of ^{85}Sr in the model river were studied. The mass transfer coefficient was found to increase with increased velocity. High uptake of ^{85}Sr by sediments may be provided by increased temperature and the presence of an organic pollutant. An exponential relationship was established between the Sherwood's number and the Reynold's number for the model river.

CONCLUSIONS

1. The transport function of radionuclides, instantaneously injected into a model river system having a bottom sediment with high adsorption capacity may be expressed as follows:

$$C(x, t) = \frac{Mx}{2AU\sqrt{\pi D_x}} \; e^{\left(\frac{Ux}{2D_x} - k_1 t\right)} \; N(x, t)$$

Where

$$N(x, t) = \int_o^t I_1 \left[2\sqrt{dk_1 K_s (t-\tau)\tau}\right] \sqrt{\frac{dk_1 K_s}{t-\tau}} \; \frac{1}{\tau} \; e^{-\left(\frac{X^2}{4D_x \tau} + B\tau\right)} d\tau$$

$$B = \frac{U^2}{4D_x} + d\,K_s - k_1$$

$$d = \frac{k_1}{H \cdot a}$$

H = depth of water

a = sampling area of the sediment

k_1 = mass transfer coefficient of the radionuclide through the interface of the flowing water and the bottom sediments

K_s = equilibrium distribution coefficient of the sediments

I_1 = the modified Bessel function of the first order of first kind

D_x = longitudinal dispersion coefficient

U = average velocity of flow

And the impulse for the radionuclides in the bottom sediments may be expressed:

$$M(x, t) = k_1 K_s \int_0^t e^{-k_1(t-\lambda)} C(x,\lambda)\, d\lambda$$

2. The transport function of radionuclides instantaneously injected into a model river system containing selected aquatic plants could be expressed as follows:

$$C(x, t) = \frac{Mx}{2AU\sqrt{\pi D_x}} e^{(\frac{Ux}{2D_x} - K_2 t)} N'(x, t)$$

Where

$$N'(x, t) = \int_0^t I_1 \left[2\sqrt{m_b K_2{}^2 K_c (t-\tau)\tau}\right] \sqrt{\frac{m_b K_2{}^2 K_c}{t-\tau}} \frac{1}{\tau} e^{-(\frac{x^2}{4D_x\tau} + B'\tau)} d\tau$$

$$B' = \frac{U^2}{4D_x} + m_b K_2 K_c - K_2$$

m_b = biomass per unit volume

K_2 = mass transfer coefficient through the interface of water and aquatic plants

K_c = the equilibrium concentration factor of the aquatic plant for the radionuclide released

3. The mass transfer coefficient, k_1, for the ^{85}Sr into the bottom sediments of the model river was found to be a function of turbulence:

$$k_1 = -\frac{1}{t} \ln \frac{K_s C_w - M}{K_s C_w}$$

Where

K_s = the distribution coefficient at equilibrium

state(~140 dpm/core/dpm/ml)

M = the total ^{85}Sr associated with the sediments in each sediment core, 0.6 sq. in. (cross section) x 6 in. (depth)

C_w = ^{85}Sr in the water, constant value for the case of continuous release

The k_1 values were found to be 0.0045 hr^{-1} and 0.011 hr^{-1} for flow conditions having a Reynold's number 2440 and 3700, respectively.

4. The longitudinal mixing in the model river can be approximated by the relationship between Sherwood's number and the Reynold's number as follows:

$$S_h = 3.78 \ (R_e)^{-0.08}$$

Where

S_h = Sherwood's number

R_e = Reynold's number

and the range of R_e = 2,500~10,000

5. The vertical distribution of radionuclides in the sediments may be represented by the radionuclides penetration function:

$$C_s(w, t) = C_{so} \ e^{-p'(t)w}$$

Where

$C_s(w, t)$ = the radionuclide concentration at the depth

of w accumulative weight from the interface and after contact time t

$p'(t)$ = the probability to be retained in the sediments per travel length of each radionuclide

C_{so} = the saturated concentration of radionuclide at interface

For the ^{85}Sr associated with the sediments in the model river, the function for $p'(t)$ is analyzed and expressed as follows:

$$p'(t) = mt^{-n}$$

Where

$n = 0.167\ (1.002)^{(T-25)}$

$m = 0.60\ (1.03)^{(T-25)}$

T = temperature (^{o}C)

t = contact time (days)

6. The concentration factor for ^{85}Sr by bottom sediments in the model river, K_s, is a function of contact time, t, and the temperature between $10^{o}C$ and $30^{o}C$. The functional relationship may be expressed as:

$$K_s = 19.5\ t^{0.64}$$

Where

t = contact time (days)

The K_s value for the equilibrium condition was found to be in the range of 130~160 dpm/core/dpm/ml.

7. The concentration factor of ^{85}Sr by Vallisneria, K_p, was found to be dependent on both the contact time and the temperature. Its functional relationship may be expressed empirically:

$$K_p = k_p\, t^{-0.1}$$

t = contact time in days

$$k_p = 250 + (T^{\circ} - 10)$$

8. The transport of ^{85}Sr was influenced by the presence of biodegradable pollutants. For each additional 1.0 mg/l of COD added, the total ^{85}Sr associated with each sediment core was increased by~100 dpm.

9. A generalized mathematical model describing the overall transport phenomena may be written as follows:

$$\frac{\partial C_j}{\partial t} = \frac{\partial}{\partial x}\left(E_x \frac{\partial C_j}{\partial x}\right) + \frac{\partial}{\partial y}\left(E_y \frac{\partial C_j}{\partial y}\right) + \frac{\partial}{\partial z}\left(E_z \frac{\partial C_j}{\partial z}\right)$$

$$+ D_m \nabla^2 C_j - U \frac{\partial C_j}{\partial x} + \sum_{i=1}^{n} \alpha_i\, k_{ij}\, \left[C_{ij} - g_j(C_j)\right]$$

$$+ k_{d_j} \frac{P}{A}\,(C_{d_j} - C_j);\quad \frac{\partial C_{d_j}}{\partial t} = k_{d_j} \frac{P}{A_d}\,(C_j - C_{d_j})$$

and

$$\frac{\partial C_{ij}}{\partial t} = k_{ij}\, \left[g_j(C_j) - C_{ij}\right]$$

$i = 1, 2, \ldots, n.$

$j = 1, 2, \ldots, m.$

Where

C_j = concentration of j^{th} radionuclide in water

α_i = total weight of i^{th} sorbent per unit volume

C_{ij} = the concentration of j^{th} radionuclide in i^{th} sorbent

$g_j(C_j)$ = equilibrium concentration relationship

k_{ij} = mass transfer function for j^{th} radionuclide associated with i^{th} sorbent

i = index variable for the sorbent in the system = 1, 2, ..., n

j = index variable for the radionuclides in the mixture of source = 1, 2, ..., m

C_{d_j} = concentration of j^{th} radionuclide in the dead zone

P = wetted contact length

A_d = dead zone area

k_{d_j} = mass transfer coefficient for j^{th} radionuclide in the dead zone

D_m = molecular diffusivity

E_x = turbulent diffusivity along x direction

E_y = turbulent diffusivity along y direction

E_z = turbulent diffusivity along z direction

TABLE OF CONTENTS

TABLE OF CONTENTS (Cont'd.)

TABLE OF CONTENTS (Cont'd.)

TABLE OF CONTENTS (Cont'd.)

LIST OF TABLES

LIST OF TABLES (Cont'd.)

LIST OF FIGURES

LIST OF FIGURES (Cont'd.)

LIST OF FIGURES (Cont'd.)

LIST OF FIGURES (Cont'd.)

Chapter 1

INTRODUCTION

The transport of radionuclides in an aquatic environment becomes important because of the fast growing nuclear industry. Many studies describing the behavior of radionuclides in the aquatic environment have been reported (53, 40, 43, 35, 37, 4, 42). However, the overall transport of radionuclides has not been established quantatively.

The movement of radionuclides in a stream is a function of hydrodynamic mixing and interaction between the liquid phase and various solid phases, e.g., the biota, the bottom sediments, and the suspended debris, etc. (41, 37). The detention caused by the chemical and biological interactions are manifested in the time-concentration relationships (53, 40, 42, 4).

Objective

The objective of this research was to present a mathematical model with analytical solutions defining the distribution and transport of radionuclides in an aquatic environment.

Scope

The study includes the following investigations:

(a) the development of a transport function

(b) a laboratory study based on the uptake and release of ^{85}Sr by various aquatic systems;

(c) dye experiments to evaluate the longitudinal dispersion coefficients;

(d) model river studies with steady state influx of ^{85}Sr;

(e) instantaneous release of ^{85}Sr; and,

(f) the evaluation of the effects of an organic pollutant on the transport of ^{85}Sr in an aquatic environment.

Chapter II

LITERATURE REVIEW

The fate of radionuclides dispersed in a stream system depends on many complex factors. In view of the development of an useful mathematical model, the understanding of all the factors involved in the transport of radionuclides in surface waterways is required. The hydrodynamic mixing is believed to be the predominant factor involved, but it is recognized that the interaction of radionuclides associated with different components of a stream may produce a significant effect on the net transport of radionuclides (4, 42, 53, 40, 19, 9).

Diffusivity and Dispersion Coefficient

Diffusivity is the characteristic variable which describes the physical property of the transport activity along a certain direction in the space of diffusant movement (38, 39), whereas the dispersion coefficient is the overall apparent diffusivity of a fluid mixture (49). Thus, both molecular and turbulent diffusion describe the mixing phenomena without consideration of the velocity gradient. The dispersion term includes the mixing caused by both molecular and turbulent diffusion and that due to convective transport. The physical character of both diffusion and dispersion can be

illustrated mathematically either by writing a differential mass balance or developing a dispersion model (3, 49).

Based on the principle of conservation of mass, the molecular diffusion, as expressed in Cartesian coordinates, for dilute liquid solutions with constant density and diffusivity may be stated:

$$\frac{\partial C}{\partial t} + U\frac{\partial C}{\partial x} + V\frac{\partial C}{\partial y} + W\frac{\partial C}{\partial z} + \frac{r}{\rho} = D_m \nabla^2 C \qquad (2\text{-}1)$$

Where

C = concentration of diffusant

D_m = molecular diffusivity

U = laminar velocity in x direction

V = laminar velocity in y direction

W = laminar velocity in z direction

r = rate of production of mass by chemical or biological process in unit volume

ρ = density of the mixture

For the condition of turbulent flow, the diffusion equation becomes:

$$\frac{\partial \bar{C}}{\partial t} + \bar{U}\frac{\partial \bar{C}}{\partial x} + \bar{V}\frac{\partial \bar{C}}{\partial y} + \bar{W}\frac{\partial \bar{C}}{\partial z}$$

$$= D_m \nabla^2 \bar{C} + \frac{\partial}{\partial x}\left(E_x \frac{\partial \bar{C}}{\partial x}\right) + \frac{\partial}{\partial y}\left(E_y \frac{\partial \bar{C}}{\partial y}\right) + \frac{\partial}{\partial z}\left(E_z \frac{\partial \bar{C}}{\partial z}\right) + \frac{r}{\rho} \qquad (2\text{-}2)$$

in which

$C = \bar{C} + c'$

$U = \bar{U} + u'$

$V = \bar{V} + v'$

$W = \bar{W} + w'$

$E_x \frac{\partial \bar{C}}{\partial x} = \overline{u'c'}$

$E_y \frac{\partial \bar{C}}{\partial y} = \overline{v'c'}$

$E_z \frac{\partial \bar{C}}{\partial z} = \overline{w'c'}$

Where

$\bar{C}$ = mean concentration of diffusant, practically this value is the slowly varying part of C (x, y, z, t)

c' = rapidly fluctuating part of diffusant concentration

$\bar{U}$ = mean velocity component along x axis

$\bar{V}$ = mean velocity component along y axis

$\bar{W}$ = mean velocity component along z axis

u' = instantaneous deviation from mean velocity along x axis

v' = instantaneous deviation from mean velocity along y axis

w' = instantaneous deviation from mean velocity along z axis

E_x = eddy or turbulent diffusivity along x axis

E_y = eddy or turbulent diffusivity along y axis

E_z = eddy or turbulent diffusivity along z axis

For the dispersed flow model (49), Eq. 2-2 is simplified into a one dimensional function, Eq. 2-3. The dispersion coefficient, D_x, has replaced all the terms involving molecular diffusivity, turbulent diffusivity and convection along all directions. It is recognized that Eq. 2-3 may hold when the concentration variations in the lateral and vertical directions are small (15).

$$\frac{\partial \bar{C}}{\partial t} + U\frac{\partial \bar{C}}{\partial x} = \frac{\partial}{\partial x}\left(D_x \frac{\partial \bar{C}}{\partial x}\right) + \frac{r}{\rho} \qquad (2\text{-}3)$$

Where

$U = \frac{Q}{A}$ = average velocity for the whole cross section

x = the x axis usually describes the longitudinal section of the stream channel

D_x = the longitudinal mixing coefficient

Evaluation of the Dispersion Coefficient

The dispersion coefficient for the stream system, in general, is a function of discharge and the location of interest. Many investigators have attempted the evaluation of D_x by using basic hydraulic derivations.

Sir G. I. Taylor (49) first attempted the theoretical prediction of D_x for pipe flow by using the solution of Eq. 2-3 and the empirical velocity distribution presented by Stanton,

Pannell and Nikuradese. Assuming isotropic turbulence and using the Reynold's analogy, Taylor integrated the transport equation using cylindrical coordinates as shown in Eq. 2-4.

$$D_x = 10.1\, a\, U_* \qquad (2\text{-}4)$$

Where

a = radius of pipe

U_* = $\sqrt{\frac{\tau_o}{\rho}}$ = shear velocity

τ_o = shear stress

ρ = fluid density

Following Taylor's concept, Thomas (50) derived an expression of D_x for unidirectional flow in an infinitely wide channel, and assuming a power law velocity distribution, $U = (y/d)^n$.

The equation derived by Thomas for D_x was a multiple integration form which involved the exponential value n.

$$D_x = -d^2 \int_0^1 u'\, dy' \int_0^y \frac{1}{E_y}\, dy' \int_0^{y'} u'\, dy' \qquad (2\text{-}5)$$

Where

y' = y/d

y = Cartesian coordinates in vertical direction

d = depth of the flow

Elder derived a simpler expression for Eq. 2-5, assuming a logarithmic velocity profile.

$$D_x = \frac{0.404}{\gamma^3} d\, U_* \qquad (2\text{-}6)$$

Where

γ = Von Karman Constant

$u' = \frac{U_*}{\gamma} (1 + \ln y')$

Elder assumed that the additive effect of turbulent diffusion was equal to the average of E_y over the cross section, $\bar{E}_y$.

$$\bar{E}_y = \frac{\gamma}{6} d\, U_*$$

and presented Eq. 2-7.

$$D_x = 5.93\, d\, U^* \qquad (2\text{-}7)$$

As Fischer (16) pointed out, the results calculated from Eq. 2-5 and Eq. 2-7 were quite similar.

By taking p^{th} moment in the direction of flow according to Eq. 2-8,

$$C_p (y, z, t) = \int_{-\infty}^{\infty} x^p C (x, y, z, t)\, dx \qquad (2\text{-}8)$$

Aris (2) obtained the solution of Eq. 2-2 by using the cross sectional average of C (y, z, t) and its changing rate. It is recognized that Aris' solution can be applied to the flows presented by Taylor and Elder, and the results obtained are identical.

Fischer (16) considered three dimensional flow and developed Eq. 2-9 for prediction of the dispersion coefficient.

$$D_x = \frac{1}{A} \int_0^W u'(z)D(z) \left\{ \int_0^z \frac{1}{E_z D(z)}\, dz \int_0^z \int_0^{D(z)} u'\, dy\, dz \right\} dz \qquad (2\text{-}9)$$

Where

A = area of channel

w = width of channel

D(z) = depth of channel at point z

u'(z) = local depth average velocity deviation

$$= \frac{1}{D(z)} \int_0^{D(z)} u\, dy$$

Determination of the Dispersion Coefficient from Experimental Data

Various techniques have been developed for the determination of D_x from experimental data. With the aid of electronic computers, the change of moment method (2, 49, 14) becomes useful for describing steady flow conditions. From data measured at a fixed station, the time-concentration can be plotted, and the mean flow through time can be calculated, Eq. 2-10.

$$\bar{t} = \frac{\int_0^\infty t\, C\, dt}{\int_0^\infty C\, dt} \qquad (2\text{-}10)$$

Where

$\bar{t}$ = mean flow through time

C = concentration of tracer for time t

t = time variable

The variance of the time-concentration curve, σ_t^2, would be obtained by Eq. 2-11.

$$\sigma_t^2 = \frac{\int_0^\infty (t-\bar{t})^2 \, C \, dt}{\int_0^\infty C \, dt} \qquad (2\text{-}11)$$

The variance was transferred in terms of distance through the relationship,

$$\sigma_x^2 = U^2 \, \sigma_t^2$$

and

$$d\,\sigma_x^2 = U^2 \, d\,\sigma_t^2$$

then by Einstein's equation,

$$D_x = \frac{1}{2} \frac{d\,\sigma_x^2}{dt}$$

the dispersion coefficient may be computed as (15, 16)

$$D_x = \frac{1}{2} U^2 \frac{\Delta \sigma_x^2}{\Delta t} \qquad (2\text{-}12)$$

The graphical method could be used to verify D_x as computed with Eq. 2-12.

The graphical method has been presented by many investigators (49, 25, 12). With the nature that r = 0, solution of Eq. 2-3 was derived as Eq. 2-13,

$$C\,(x,\,t) = \frac{M}{A\sqrt{4\pi D_x t}} \; e^{-\left(\frac{x-Ut}{4D_x t}\right)^2} \qquad (2\text{-}13)$$

Where

M = the weight of the injected tracer

Therefore, C (x, t) may be rewritten as

$$\ln Ct^{\frac{1}{2}} = \ln \frac{M}{A\sqrt{4\pi D_x}} - \frac{(x-Ut)^2}{4D_x t}$$

and then, the slope of the plot of $\ln ct^{\frac{1}{2}}$ versus $\frac{(x-Ut)^2}{t}$ on semi-log paper is equal to $(4\ D_x)^{-1}$.

Retaining Effects in the Transport of Radionuclides

Of the many factors which may determine the dynamic behavior of the radionuclides introduced into a stream, the effect of detention caused by various components of the stream has attracted most attention. The uptake of radionuclides by both bottom sediments and aquatic biota was recognized to be functions of the hydrodynamic movement and various interactions between the radionuclides and the environment. The dominant reactions probably involve sorption and desorption of the radionuclides by bottom sediments and aquatic biota.

Others using the same physical model (53, 40, 42, 19) have reported the release of ^{85}Sr, ^{137}Cs, ^{58}Co and ^{65}Zn in Table 2-1 and Fig. 2-1. Under the same mean flow through time, 10 hrs., the dye study showed that more than 90 percent of the Rhodamine B injected discharged through the flume within one day, whereas only 24.1%, 18.4%, 11.1% and 28%, respectively, of the ^{85}Sr, ^{137}Cs, ^{58}Co and ^{65}Zn passed. Bhagat (4) also reported the same comparison for both the chloride and nitrosyl forms of ^{103}Ru, Table 2-2. The mean flow through

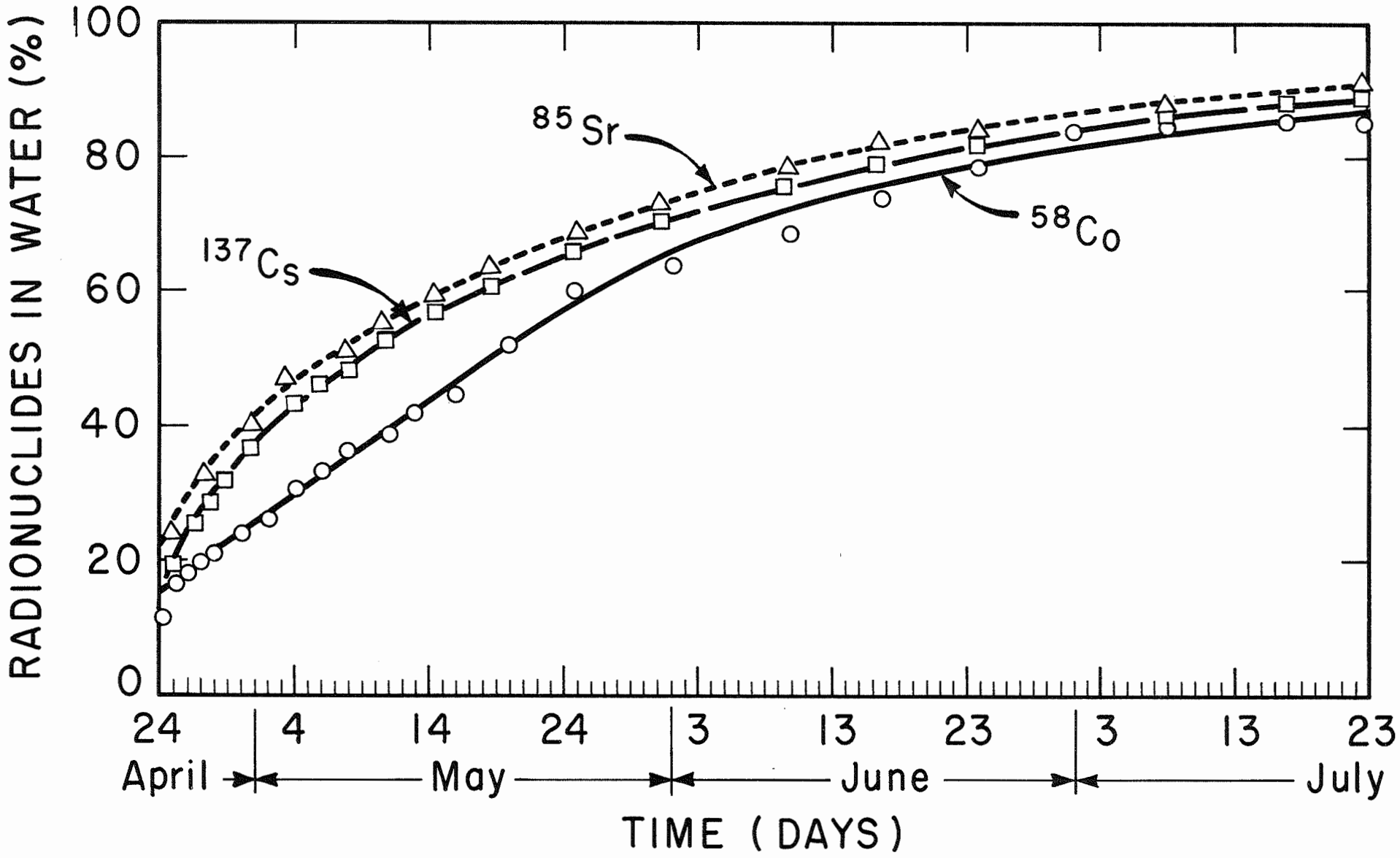

FIG. 2-1. RADIONUCLIDES DISCHARGED THROUGH FLUME

Table 2-1. Longitudinal Transport of Radionuclides in the Model River

Time Elapsed (No. of T)	Percent of Total Released Radionuclides Discharged			
	^{85}Sr	^{137}Cs	^{58}Co	^{65}Zn
2.0	21.0	17.5	10.5	25.0
5.0	30.0	26.0	16.7	32.0
10.0	35.2	31.0	20.0	25.5
20.0	42.5	40.0	26.5	42.5

T = mean flow through time = 10 hours

Table 2-2. Transport of ^{103}Ru in the Model River

Time Elapsed (No. of T)	Percent of Total ^{103}Ru Discharged	
	Chloride	Nitrosyl
8	84	92
16	88	96

T = mean flow through time = 3 hours

time for Bhagat's experiment was only 3 hours, and the biomass was much less than that of Rowe's.

Thus, it can be shown that the detention of radionuclides will effect the overall transport of radionuclides in a stream. The discrepancy between the observed and the hydrodynamic dispersed ^{58}Co concentration in the water phase has been reported by Gloyna and Yousef (53).

Strontium in the Bottom Sediments

Sorption of strontium from solutions by minerals may occur as a result of both non-specific electrostatic adsorption and specific adsorption (5, 46). Generally, it is believed that the non-specific electrostatic adsorption is the predominant method of sorption of isotopes by the coarser grained soils such as silts, sands and gravels, whereas the ion exchange is the predominant method of sorption of isotopes by the finer grained soils such as clays (37).

The distribution coefficient, K_d, is defined as the ratio of the concentration of ionic species in solid and liquid phases (23). The K_d values for strontium for various soils and minerals varies from 35 to 2,470 ml/gm (24).

The sorption capacity of cations by bed materials was reported as shown in Table 2-3 (24). These numbers are average data of nine rivers.

Table 2-3. Sorption Capacity of Bottom Sediments (% of Total Sorbed)

	Bed Materials			Suspended Materials		
Range	Sand	Silt	Clay	Sand	Silt	Clay
Average	25	45	31	10	21	68
Maximum	92	85	62	36	45	90
Minimum	4	3	2	1	8	52

The U. S. Geological Survey also found that the sands were responsible for as much as 92 percent of the exchange capacity of the bed materials in some rivers (24).

The uptake of ^{85}Sr by various clay minerals and sediments from the Clinch River has been studied at the Oak Ridge National Laboratories (29, 30, 31, 33). The data for the uptake of ^{85}Sr in distilled water are shown in Table 2-4.

Table 2-4. Percent Strontium-85 Sorption by Clay and Associated K_d Values (37)

Material	Contact Time	Average % Activity Sorbed pH 6	pH 9	Average K_d pH 6	pH 9	Ratio of Clay to Solution
Illite	1 hr	23.42	31.67	306	316	0.1 g/100 ml
	3 days	26.69	41.05	364	696	
	7 days	26.88	43.17	368	760	
Kaolinite	1 hr	62.77	71.24	3372	4954	0.1 g/200 ml
	3 days	67.49	68.55	4152	4358	
	7 days	66.44	66.28	3959	3930	
Montmoril-lonite	1 hr	70.85	71.88	2430	2555	0.1 g/100 ml
	3 days	66.88	68.65	2019	2189	
	7 days	67.21	68.67	2059	2163	
Vermucu-lite	1 hr	77.45	67.14	172	102	1 g/50 ml
	2 days	96.95	96.46	1590	1364	
	8 days	97.33	98.73	1821	3874	
Clinch River Sediment	1 hr	21.42	24.79	545	659	0.1 g/200 ml
	3 days	45.79	63.87	1690	3537	
	7 days	41.83	66.80	1438	4024	

The uptake of ^{90}Sr is affected by the concentration of sodium ions and total salt content; however, the presence of calcium will cause the greatest reduction in uptake. Furthermore, the presence of stable isotopes of the strontium or other stable ions of the same group in the periodic table may influence the uptake of the radiostrontium by sediments (30, 33).

Reynolds and Gloyna studied the transport of ^{89}Sr in both freshwater and marine systems (37). They found that the most important factors affecting the uptake of ^{89}Sr by river and lake sediments were the cation exchange capacity, CED, of the sediments, the concentration of competing cations in water, and the mass-action coefficients for the system. The mass-action coefficients were relatively constant as long as the potassium concentration in the solution did not vary appreciably. Thus, the mass-action coefficients were relatively uniform for freshwater systems; however, this was not the case for marine waters. The average mass-action coefficients were:

$$K^{Sr}_{Ca+Mg} \approx \frac{q_{Sr}}{C_{Sr}} \frac{C_{Ca+Mg}}{q_{Ca+Mg}} \approx 1.55$$

Where q and C represent the respective cation concentration in solid and liquid phases.

Reynolds and Gloyna also studied the basic property and the interactions of radiostrontium (^{89}Sr was used) and the sediments which were used in the model river of this study.

The selectivity constants, K_{Na}^{Ca+Mg} and K_{K}^{Ca+Mg}, for the equilibrium system involving the Lake Austin sediments were studied. It was found that the K_{Na}^{Ca+Mg} value was relatively constant over a wide range in Na^+ concentrations, whereas the K_{Ca}^{Ca+Mg} value increased appreciably with an increasing K^+ concentration. The cation exchange capacity for the Lake Austin sediments was determined to be 0.33 Meq/gm.

Moreover, Reynolds and Gloyna (97) have shown that the uptake of ^{89}Sr was proportional to the concentration of sediment. They also found that the percent sorption of ^{89}Sr increased with pH.

Based on the Guadalupe River studies, the K_d-Sr values were 72 and 128, respectively, for the sediments located at the headwaters and the mouth of the river, Table 2-5.

Table 2-5. ^{89}Sr Uptake and Release Data of Guadalupe River

	Uptake		Release
Variables	Fresh Water	Salt Water	Salt Water
f_s (%)*	9.0	2.0	57.5
f_l (%)**	91.0	98.0	42.5
k_d (mg/l)	198	40.8	2520

* f_s = Fraction of total ^{89}Sr concentration sorbed on the sediments

** f_l = Fraction of total ^{89}Sr concentration which was in liquid

Shih and Gloyna (42) found the percent of ^{85}Sr associated with the bottom sediments in the model river increased with decreasing biomass. The migration of ^{85}Sr into the sediments was shown to be exponential with depth.

Strontium in the Biota

Biological uptake of radiostrontium by organisms may be achieved by sorption to the surface, engulfment, or metabolic processes. Elimination of radioactive materials in organisms may occur by surface exchange, excretion through natural physiological channels, or through cell lysis after death (27).

The degree of specificity for radiostrontium by organisms varies from species to species. The concentrating ability of organisms is usually expressed by the concentration factor, K_c, which is

$$K_c = \frac{\text{concentration of activity in the organism}}{\text{concentration of activity in the water}} .$$

Bacteria, as would be expected, have been found to possess the greatest concentrating ability among organisms (27).

The pH variations affect biological uptake indirectly because there is an optimum pH range for microbial and biological activity. Since temperature affects the rate of metabolism of microorganisms, plants, and cold-blooded animals,

the seasonal differences in temperature will cause changes in the rate of radionuclide uptake (27). Light intensity will affect the rate of radionuclide uptake since light intensity affects photosynthesis (26).

In an aquatic system, there are two main types of photosynthetic plants, the rooted or large floating plants and phytoplankton (26). The phytoplankton tend to concentrate the induced radioactive products to a greater extent than the fission products because the the transition elements formed by fission have the ability to form complexes with the microplankton (28). Furthermore, the phytoplankton are able to concentrate elements such as Co, Zn, and Fe to the extent necessary to meet the metabolic requirements of the higher aquatic organisms (36).

The concentration of ^{90}Sr in plants found in White Oak Lake at Oak Ridge was less than that of ^{137}Cs and ^{60}Co, as cited in Table 2-6 (33).

Table 2-6. Uptake of Radionuclides by Various Plants

	Concentration (μc/gm of oven dry wt.)		
Plant Genus	Cs^{137}	Co^{60}	Sr^{90}
Festuca	1.60	1.42	0.38
Festuca (stem)	1.36	1.08	0.34
Polygonium	2.85	6.20	1.33
Tupatorium	1.50	1.99	0.38
Rumex	1.83	3.42	2.05

Based on the Sr/Ca ratio, Bowen (5) presented some estimates of concentration factors of Sr for some marine organisms as shown in Table 2-7.

Table 2-7. Concentration Factors in Marine Organisms

Organism	Concentration Factors (Wet wt. - Vol. basis) Sr
Calanus	0.8
Ommestrepes	(0.3)
Saggita	70
Euphausia	(0.3)

Shih and Gloyna (42) have studied the uptake of ^{85}Sr by aquatic plants in a model river, and they found the immediate uptake of ^{85}Sr was about 14% of total released for the system with biomass 13 gm/sq. ft. Table 2-8 shows the concentration factors for various aquatic plants in the model river and the maximum K_c values. In order to determine the degree of sorption, the plants were washed with citric acid. The release of ^{85}Sr is given in Table 2-9. The relative uptake of ^{85}Sr by aquatic plants was found to be:

Spirogyra sp. > Potamogeton sp. > Zannichellia sp. > Myriophyllum sp. > Chara sp. > Cladophora sp.

Table 2-8. Maximum Concentration Factor, K_c, of ^{85}Sr for Freshwater in the Flume

Plant	Maximum K_c of ^{85}Sr
Macroplants	
1. Zannichellia sp.	8,060
2. Potamogeton sp.	12,400
3. Myriophyllum sp.	7,450
Algae	
1. Spirogyra sp.	14,500
2. Cladophora sp.	3,400
*3. Chara sp.	5,700

*Macroalgae

Table 2-9. Release of ^{85}Sr from Aquatic Plants After Washing with Citric Acid

Plant	Release of ^{85}Sr (%)
Macroplants	
1. Zannichellia sp.	37
2. Potamogeton sp.	20
3. Myriophyllum sp.	29
Algae	
1. Spirogyra sp.	23
2. Cladophora sp.	12
3. Chara sp.	19

Chapter III

ANALYSES OF DATA FROM 512 CHANNEL GAMMA SPECTROMETER

The purpose of this chapter is to present a flexible computation system which can be used to accept the output from the RCL 512-channel gamma spectrometer. The computer programs written in Fortran-63 language were developed to calculate the counting efficiency, the contribution coefficients, the self-absorption constant, and the net radionuclide concentration. A subroutine program was also developed to translate and select data initially registered on paper tape.

Procedure

The reduction of data involves the following steps: Punching data on tape, transference of data to magnetic tape, and translation of data by the computer.

Paper Tape: A binary number system was used, and each channel was furnished with space for six digits. As shown in Fig. 3-1, each row represents a numerical value in the digital system, and each column represents a digit of the digital number. It is recognized that the value of each perforated hole in row i is $2^{(i-2)}$ where $i \geq 2$, and the perforated holes in row 1 only indicate the position of the digits. The perforated holes in column j designate the multiplication factor of $10^{(j-1)}$ where $j \leq 6$. However, the

perforated hole at column 7 always falls in row 6, and it gives the signal for the starting of a channel. For example, the perforated holes in Fig. 3-1 represent 124830 and 609735 from left to right.

All samples with the same counting time, decay period and self-absorption constant were grouped; and the paper tape was arranged into one roll. At the beginning of each roll of tape, the appropriate background information was attached. Stop codes were attached at both ends of each roll of the paper tape. This code is the binary column with combination of punches which was not identical with the standard punches normally provided by the tape unit of the gamma spectrometer.

Magnetic Tape: The paper tapes were read into the paper tape reader, such as CDC 160A, and the images of the data were transferred to magnetic tape. The conversion program was put in according to the character mode. The record length was selected to be 62_8 words. In case of necessity, the record length could be another octal number other than 62_8.

Accordingly, an input and an output buffer were utilized in this transference operation. Paper tape with the counting data was read and placed in the input buffer until 62_8 words of information were contained in this buffer. Then the input buffer information was transferred to an output buffer according to the character mode. The information was finally put on output magnetic tape.

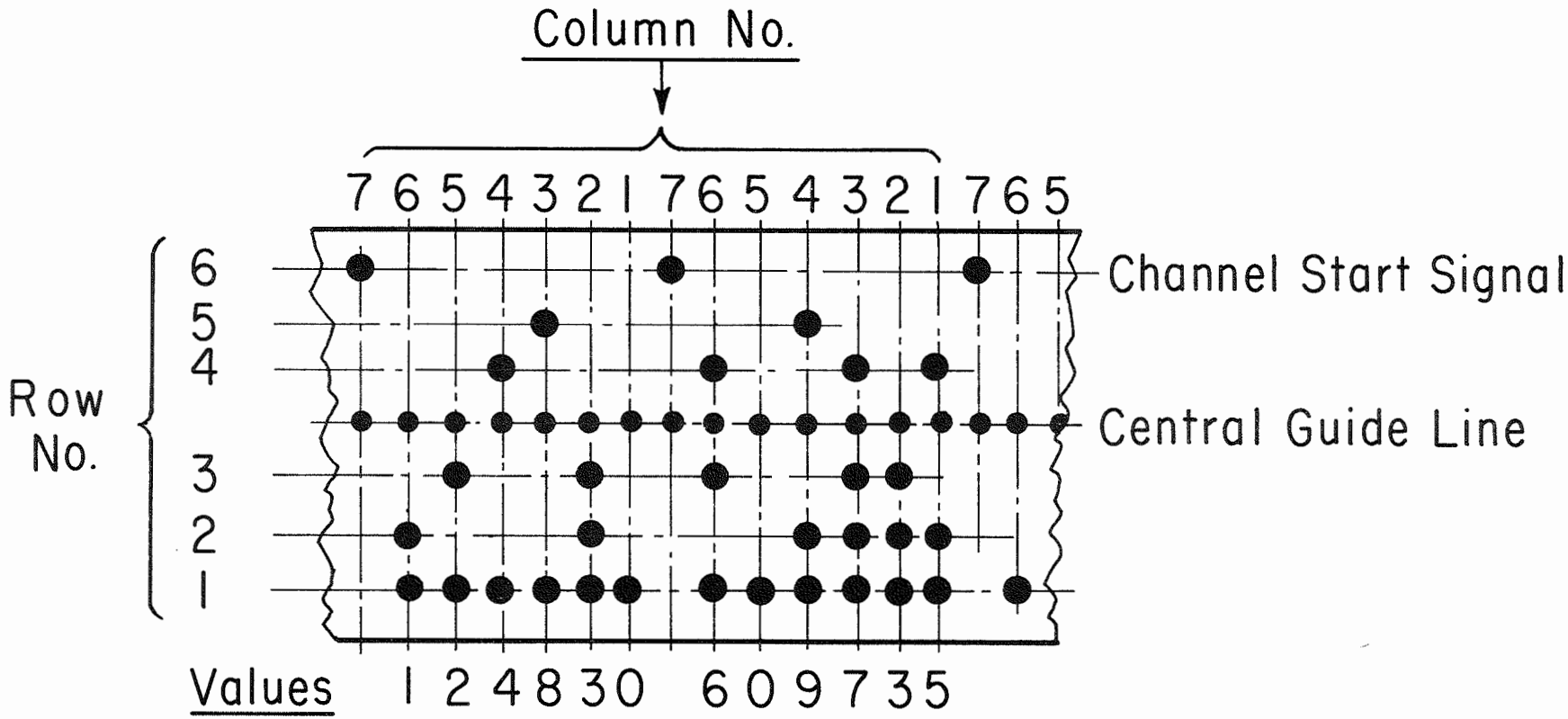

FIG. 3-1. BINARY COLUMN CODE ON PAPER TAPE

Computer Translation: Those images stored on magnetic tape were translated into the true information which the combination of punches represented. The paper tape reader accepted the punches in row i as a value of $2^{(i-1)}$ and registered this on magnetic tape. Thus, a systematic formulation for data translation was designed:

$$N_j = \frac{(N_j' - 1)\, 10^{(j-1)}}{2} \quad ; \; j = 1, 2, \ldots, 6. \qquad (3\text{-}1)$$

Where

N_j = the true value of the combined punches in j^{th} column

N_j' = the value registered by the paper tape reader on the magnetic tape

j = the number of column punches

The true counts of each channel could then be formulated as:

$$X_\ell = \sum_{j=1}^{6} N_j = \sum_{j=1}^{6} \frac{(N_j' - 1)\, 10^{(j-1)}}{2} \qquad (3\text{-}2)$$

and

$$X_\ell = \sum_{j=1}^{6} \frac{\left[\sum_{i=1}^{5} P_{ij}\, (2)^{(i-1)} - 1\right] 10^{(j-1)}}{2} \qquad (3\text{-}3)$$

Where

X_ℓ = the total counts of channel ℓ^{th}

P_{ij} = the signal for the punches of i^{th} row j^{th} column

$$P_{ij} = \begin{cases} 1 & \text{punched} \\ 0 & \text{unpunched} \end{cases}$$

i = the number of row of punches

It is important to note the designation of row and column of the punches was not the same as that of an ordinary matrix array.

Subroutine Program CON (IABC)

The subroutine program, CON (IABC), was designed for the translation and selection of the input data. It is recognized that any kind of erratic operations on the paper tape punching unit can cause difficulties. However, the undesired punches seem to follow some systematic pattern, such as: continuous extra punches along one line, superfluous spaces furnished for a channel, blank spaces, incompleted spectrum, etc. CON (IABC) is capable of picking out the useless data, abandoning it, and at the same time translating the useful data.

Though the subroutine CON (IABC) was developed mainly for acquisition of data from the gamma spectrometer, it can be utilized for other similar purposes with a few modifications. The improper punches that have been encountered in the gamma spectrum and treated in the subroutine CON (IABC) are as follows:

a. continuous punches in top row

b. extra binary columns for each channel

c. unpunched sections used for recording the description of the next spectrum

d. incompleted data with the loss of a section

In order to translate the true counting images on magnetic tape, the following Boolean Statements were used, Eq. 3-4:

$$I_{(\ell-1),\,k} \neq 16 \wedge I_{(\ell-1),\,k} \neq 0 \wedge I_{(\ell+1),\,k} = 16 \wedge I_{(\ell+1),\,k} \neq 0 \wedge I_{\ell k} = 16 \equiv f \qquad (3\text{-}4)$$

Where

$I_{\ell k}$ = the total digital value of the images on magnetic tape at ℓ^{th} binary column and after the k^{th} signal of channel start

f = equalities in data translation as follows:

$$f: \quad C_{ik} = \left[I_{(\ell-1),\,k} - 1\right] 10^{(i-1)} / 2 \qquad (3\text{-}5)$$

$$J_n^{\,s} = \sum_{i=1}^{6} C_{ik} \quad ; \quad n = k - \left[\frac{k}{N}\right] N \qquad (3\text{-}6)$$

Where

C_{ik} = the true counting data along the binary column i columns ahead of k^{th} channel start signal

$J_n^{\,s}$ = the total counts at n^{th} channel of the $(s+1)^{th}$ spectrum from the beginning point of the roll

N = total number of channels in each spectrum, 256 for gamma spectrum

$\left[\frac{k}{N}\right]$ = bracket function of $(\frac{k}{N})$

s = $\left[\frac{k}{N}\right]$; 0, 1, 2, ...

The arguments used in the subroutine CON (IABC) are described as follows:

IABC - error flag for the data information punched on paper tape

0 indicates acceptable spectrum

1 indicates rejected spectrum

2 indicates the beginning or the end of a roll of paper tape

II (I)- value of the digital number which the punches on paper tape represent at the I^{th} binary column from the last stop code

L - the subscript defining the integer between 1 and the limit of each record length, 50

J - the subscript defining the starting binary column of each record

K - the subscript defining the ending binary column of each record; thus, K = J + 49

MXN - the total number of binary columns on paper tape for an acceptable spectrum

Ii - the translated value of the image on magnetic tape, where i = 1, ...6., increasing along the direction of buffer-in

Efficiency of Detection Device

In the calibration of a spectrometer, the efficiency of detection is important. It is recognized that a spectrum is usually expressed with another dimensionally independent variable such as energy level, frequency of vibration, time, wavelength, etc. In order to attain accurate quantitative results, it is required to have the analysis on multiplicate internal standards with different concentrations spanning the expected range of the variation for each object involved in the study. The GAMA 3 was programmed specifically for producing the counting efficiency, but it can be used for the analysis of other types of spectra with slight modification.

The calculations involve primarily arithematical processes, Fig. 3-2.

$$B_n = J_n^{S_o}; \qquad S_o = \left[\frac{k}{N}\right] = 0$$

$$NJ_n^{(s)} = J_n^{(s)} - B_n \frac{Ts}{Tb}; \qquad s = \left[\frac{k}{N}\right] > 0$$

$$A_i(s) = \sum_{n=p}^{q} NJ_n^{(s)}/Ts; \qquad p = r-R$$

$$E_i(s) = \frac{A_i}{D_i^{(s)}} \qquad q = r+R \qquad (3\text{-}7)$$

Where

B_n = background count at n^{th} channel

$NJ_n^{(s)}$ = net counts of standard at n^{th} channel of s^{th} spectrum in the roll

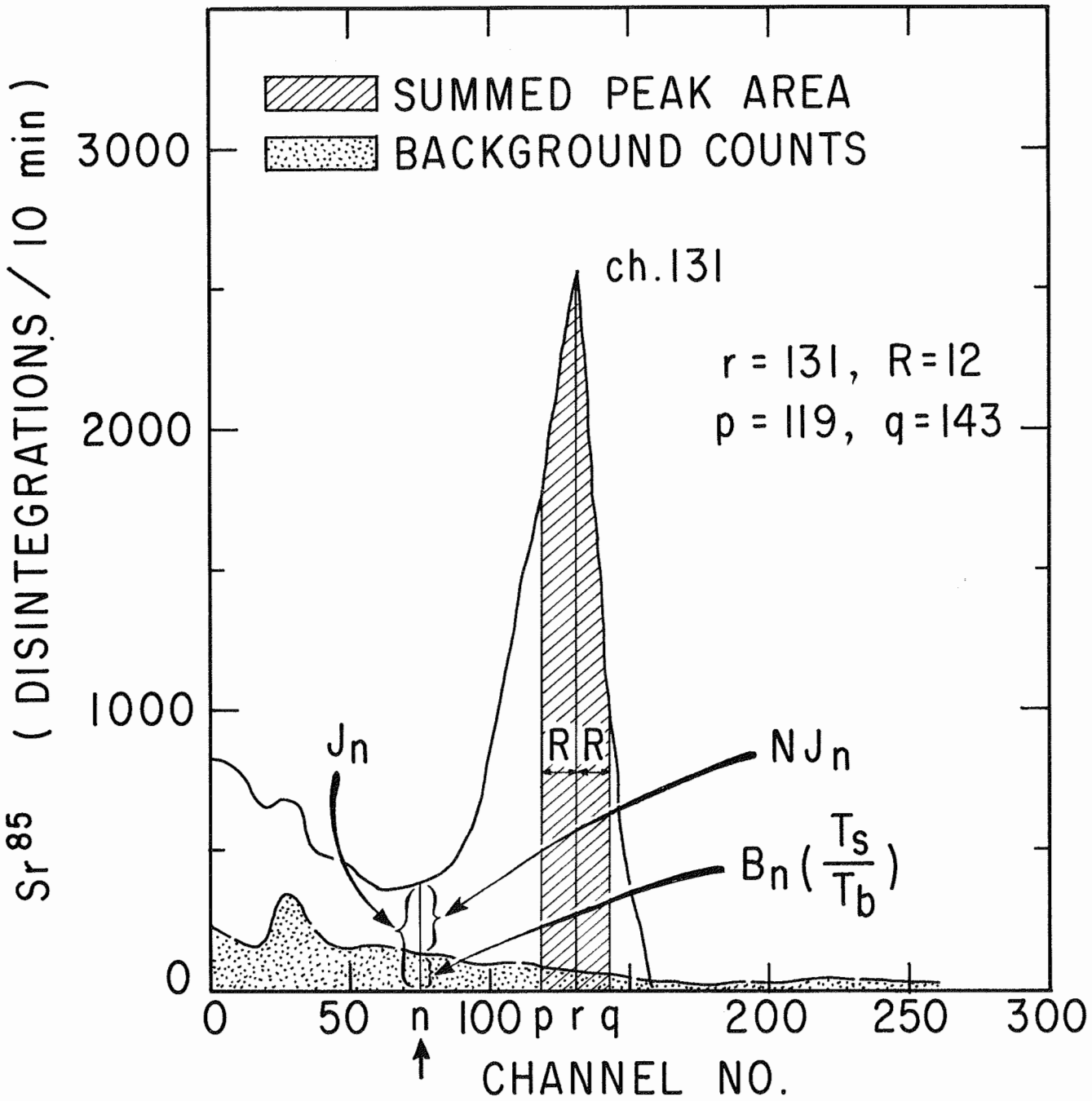

FIG. 3-2. STANDARD SPECTRUM

A_i = total counts under the peak area for i^{th} isotope punched in s^{th} spectrum. The value of i was given uniquely for each isotope.

$D_i(s)$ = ultimate counts of the known standard for i^{th} isotope located in the s^{th} spectrum

$E_i(s)$ = detection efficiency for i^{th} isotope based on the data in the s^{th} spectrum

r = channel number for a standard spectrum peak

R = selected range of summation of peak area in terms of numbers of channels

All the symbols used above are described in Fig. 3-2.

The arguments involved in GAMA 3 are as follows:

NB - total number of roll of paper tapes

IBOX - the number of roll of tapes which has been executed

IBADX - the number of roll of unacceptable tapes

NBOX - catalog number of the roll of tapes being executed

ISPECT- total number of spectrum contained in the roll being executed

DPM (I)-known concentration for standard of I^{th} spectrum

JKK - theoretical lower limit of summed channels

IKK - theoretical upper limit of summed channels

ISO - name of the isotope for the standard being analyzed

BMM - background counting time

CMM - standard counting time

DAYS - delayed time in days

HAFLY - half life of the radioactive decay in days

CPM - total counts of standard sample detected by gamma spectrometer

EFF - efficiency of detection

IBAD - no. of the unacceptable spectrum

IGOOD - no. of the accepted spectrum

Contribution Coefficient

The contribution coefficient defines the fraction of total peak area of the spectrum of one isotope contributed to the peak area of another isotope which may be present. Because of the scattering effects and the statistical distribution of a certain isotope, the spreading of the non-peak area in its standard spectrum has a constant pattern.

The physical sense of contribution coefficients can be explained in Fig. 3-3 and in the formulations.

$$A_{ii}^{(s)} = \sum_{n=p_i}^{q_i} NJ_{in}^{(s)} \quad ; p_i = r_i - R;\ q_i = r_i + R \qquad (3\text{-}9)$$

$$A_{ij}^{(s)} = \sum_{n=p_j}^{q_j} NJ_{in}^{(s)} \quad ; p_j = r_j - R;\ q_j = r_j + R \qquad (3\text{-}10)$$

$$C_{ij} = A_{ij}^{(s)} / A_{ii}^{(s)}$$

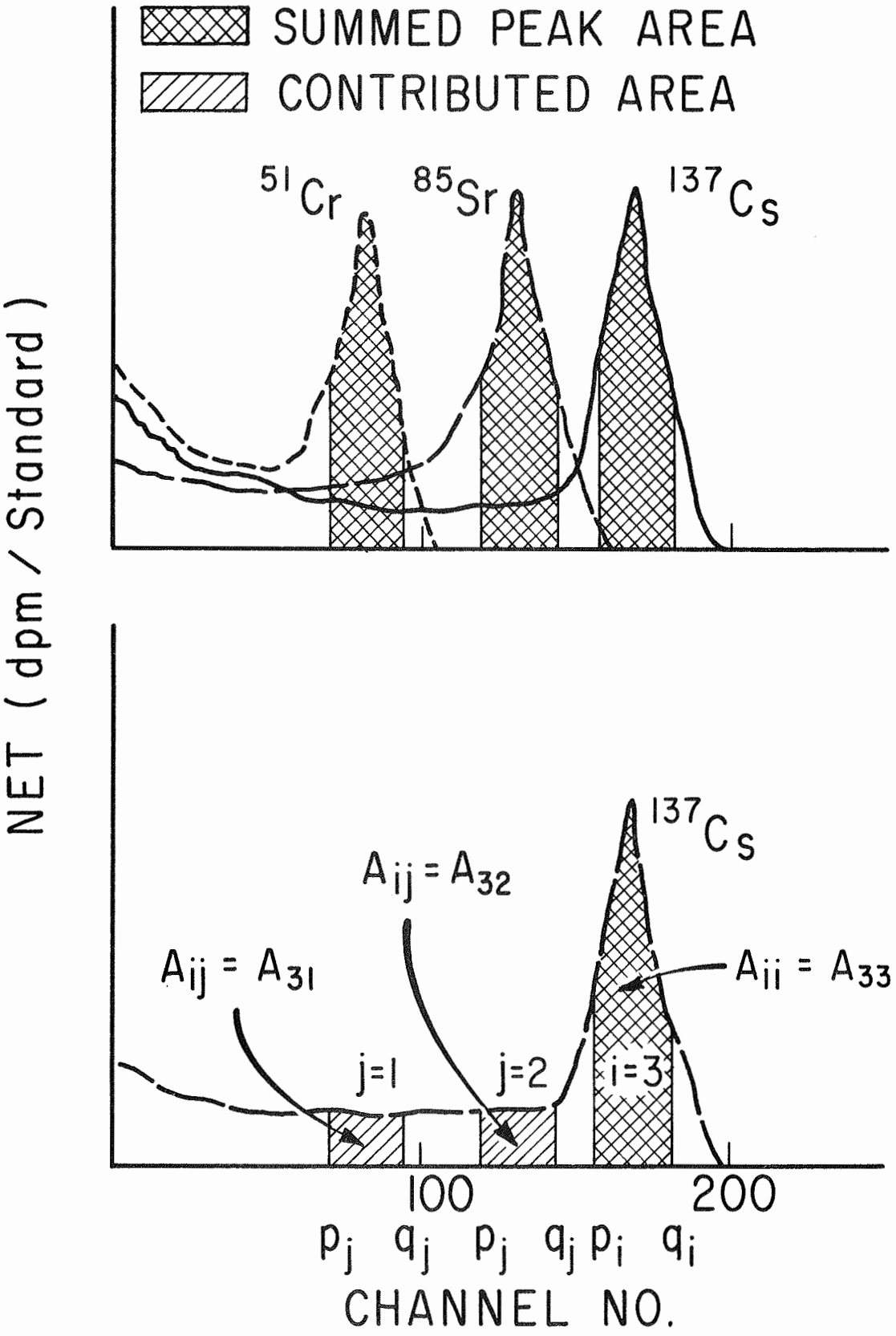

FIG. 3-3. CONTRIBUTION IN THE COMPLEXED SPECTRUM

Where

$A_{ii}^{(s)}$ = total peak area of i^{th} isotope in its s^{th} standard spectrum

$A_{ij}^{(s)}$ = contributed counts at the channel summed for the peak area of j^{th} isotope in the s^{th} standard spectrum of i^{th} isotope

C_{ij} = contribution coefficient of i^{th} isotope with respect to j^{th} isotope

$NJ_{in}^{(s)}$ = net counts of n^{th} channel of the s^{th} standard spectrum for i^{th} isotope

r_i = peak channel of i^{th} isotope

r_j = peak channel of j^{th} isotope

The matrix which consists of the contribution coefficients has unit value along its diagonal, e. g., $C_{ii} = 1.0$.

$$\underset{\sim}{C} = \begin{vmatrix} C_{11} & C_{12} & \cdots & C_{ij} & \cdots & C_{in} \\ C_{21} & C_{22} & & & & \\ \vdots & & & & & \\ C_{i1} & & C_{ii} & C_{ij} & \cdots & C_{in} \\ \vdots & & & & & \\ C_{n1} & C_{2n} & & C_{nj} & \cdots & C_{nn} \end{vmatrix} \qquad (3\text{-}11)$$

The GAMA 1 was designed for the calculation of the contribution coefficient. In a gamma spectrum, if the i value was chosen along with the order of the energy level of

the radionuclides, the matrix $\underset{\sim}{C}$ would be triangularized automatically; and the values for the elements in the matrix $\underset{\sim}{C}$ could be summarized:

$$C \begin{cases} = 0 & \text{when } j > i \\ = 1.0 & \text{when } j = i \\ < 1.0 & \text{when } j < i \end{cases}$$

The arguments used in GAMA 1 are as follows:

M - variable representing the serial number given to each isotope involved in the spectrum

ISO(M) - common name of the isotope with the serial number M, such as SR(85), CS(137), etc.

IKK(M) - lower limit of summed channels in calculating the peak area in the standard spectrum of M^{th} isotope

JKK(M) - upper limit of summed channels in calculating the peak area in the standard spectrum of M^{th} isotope

NBOX - catalog number of the reel of paper tape to be analyzed

ISPECT - total spectra contained in the reel

IO - serial number of the isotope

A(M) - area under the standard spectrum of 10^{th} isotope within the channels summed for the peak area of M^{th} isotope

FRAC(J)- contribution where J = j
and IO = i for C_{ij} designation mentioned in matrix $\underset{\sim}{C}$.

Self-Absorption Function

Self-absorption is another correction which must be applied. The amount of radioactivity absorbed by the sample is proportional to the thickness of the sample. In view of the inconvenience of measuring the sample thickness, the weight of the sample, spread evenly over the planchet, is used as the independent variable for the self-absorption function.

The program GAMA 4 was designed for the evaluation of self-absorption corrections. The weight and the type of the sorbent used in the standard for self-absorption have to cover the range that the experimental samples may contain. The first standard spectrum in the reel of the paper tape must be the one with infinitesimal thickness, e. g., water sample.

The formulations involved in the GAMA 4 are as follows:

$$G_i = A_i^{(s_1)} \quad ; \quad s_1 = 1$$

$$S_b^{(s)} = \frac{A_i^{(s)}}{G_i} \quad ; \quad s > 1 \qquad (3\text{-}12)$$

Where

G_i = total counts of the standard with infinitesimal thickness for i^{th} isotope arranged as first spectrum after background

S_b = self-absorption correction value

The self-absorption function for ^{85}Sr is shown in Fig. 3-4. As shown in Eq. 3-13, it should follow the first order reaction because the macroscopic cross-section for the absorption of gamma rays is constant.

$$A_i(w) = A_i(0)\ e^{-\mathcal{f}w}$$

$$S_b(w) = A_i(w)/A_i(0) = e^{-\mathcal{f}w}$$

Where

$A_i(w)$ = gamma rays detected for the samples with (w) grams of sorbent. (This term can be correlated to $A_i(s)$ based on the spectrum catalog of counting data.)

$A\ (0)$ = $A_i(s_1)$

$\mathcal{f}$ = macroscopic cross-section of absorption of the sorbent involved in the standardization (The dimensional numerical value is the slope of the semilogarithmic plot as cited in Fig. 3-4. For ^{85}Sr in Lake Austin sediments, $=0.021\ gram^{-1}$.)

Complex Spectrum Analysis

The Fortran program GAMA 2 was developed for the general use of gamma spectrometer data analyses. With slight modification, it can be used for similar spectrum analyses.

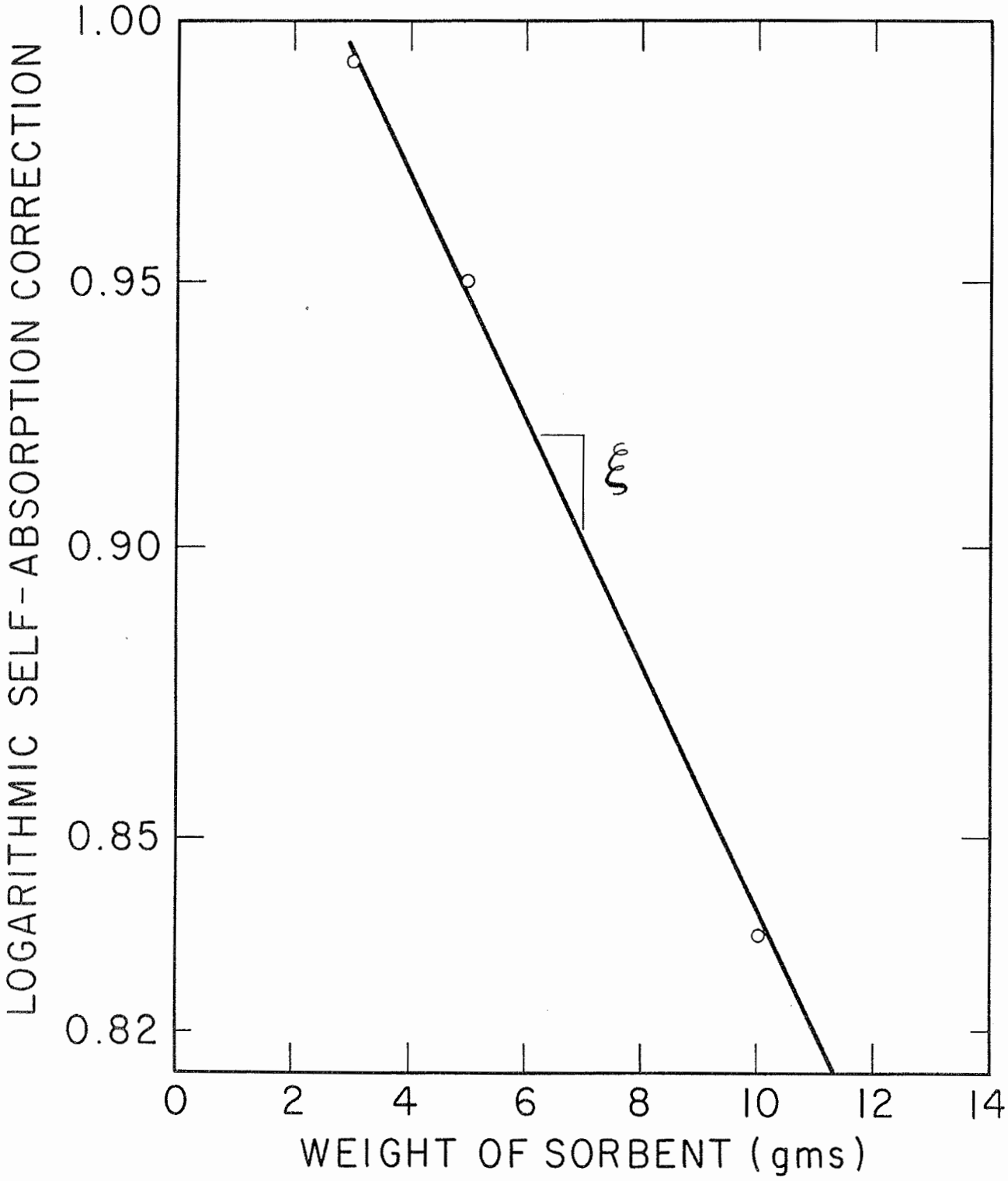

FIG. 3-4. SELF-ABSORPTION FUNCTION OF ^{85}Sr BY LAKE AUSTIN SEDIMENTS

GAMA 2 searches for the peak produced by each isotope, and then calculates the area under each peak with corrections for decay, detection efficiency, contributions, and the self-absorption. For each element or isotope contained in the sample, a linear algebraic equation can be established with the contribution coefficients related to that element. Since the peak area for j^{th} isotope in the complex spectrum was the sum of the true peak area of the j^{th} isotope and the contributed area from other isotopes, Eq. 3-14 can be formulated as:

$$C_{1j} X_1 + C_{2j} X_2 + \cdots\cdots + C_{ij} X_i + \cdots + C_{nj} X_n = b_j$$

$$j = 1, 2, \ldots\ldots, n \qquad (3\text{-}14)$$

Where

C_{ij} = contribution coefficients of i^{th} isotope with respect to j^{th} isotope

X_i = true peak area of i^{th} isotope in the complex spectrum

b_j = peak area for the j^{th} isotope summed from the entire spectrum

Thus, the matrix consisting of the coefficients of the simultaneous equations is the transposed matrix of the contribution coefficient matrix $\underset{\sim}{C}$. The solutions of these simultaneous equations were obtained through the use of Gaussian elimination techniques with row pivoting and back substitution.

Finally, subroutine Gauss 2 was called for the solution after the vector $\underset{\sim}{b}$ was calculated

The mathematical steps are summarized in Eqs. 3-15 through 3-21.

$$\underset{\sim}{C}^T \underset{\sim}{X} = \underset{\sim}{b} \tag{3-15}$$

Where

$$\underset{\sim}{X} = \begin{vmatrix} X_1 \\ X_2 \\ \vdots \\ X_n \end{vmatrix} \tag{3-16}$$

$$\underset{\sim}{b} = \begin{vmatrix} b_1 \\ b_2 \\ \vdots \\ b_n \end{vmatrix} \tag{3-17}$$

$$\underset{\sim}{C}^T = \begin{vmatrix} C_{11} & C_{21} & - - - - - & C_{i1} & - - - & C_{n1} \\ C_{12} & C_{22} & - - - - - & C_{i2} & - - - & C_{n2} \\ \vdots & & & & & \\ C_{1n} & C_{2n} & - - - - - & C_{in} & - - - & C_{nn} \end{vmatrix} \tag{3-18}$$

After $\underset{\sim}{C}^T$ and $\underset{\sim}{b}$ have been through the Gaussian elimination process, they were represented by the (n) x (n+1) matrix $\underset{\sim}{F}$.

$$\underset{\sim}{F} = \begin{vmatrix} f_{11} & f_{12} & \cdots & f_{ij} & \cdots & f_{in} & f_{i,\,n+1} \\ 0 & f_{22} & & & & & \\ & 0 & & & & & \\ & & & f_{ii} & & f_{jn} & f_{j,\,n+1} \\ & & & 0 & & & \\ 0 & 0 & & 0 & 0 & f_{nn} & f_{n,\,n+1} \end{vmatrix} \qquad (3\text{-}19)$$

The solution to the simultaneous equations was obtained by back substitution

$$X_i = \frac{f_{i,\,n+1} - S}{f_{ii}} \quad ; \quad i = 1, 2, \ldots, n. \qquad (3\text{-}20)$$

and when

$$i = n \; ; \qquad S = 0$$

and when

$$i \neq n \; ; \qquad S = \sum_{k=i+1}^{n} f_{ik} X_k \qquad (3\text{-}21)$$

The final calculation for the concentration of radionuclides was to convert the X_i's to disintegrations per minute of i^{th} radionuclide per unit weight of analyzed sample. The transformation formula is as follows:

$$N_i = \frac{X_i \exp^{(0.693t/T_i)}}{E_i \cdot M \cdot A_i(w) \cdot W} \qquad (3\text{-}22)$$

Where

N_i = disintegration per minute per unit weight of sample content of i^{th} isotope

X_i = solution for i^{th} isotope from simultaneous equations

t = time interval between the counting date and the reference date, usually the date of isotope release

T_i = half life of i^{th} isotope

E_i = counting efficiency of gamma spectrometer for i^{th} isotope

M = counting time of the analyzed sample in minutes

$A_i(w)$ = self-absorption correction of i^{th} isotope for w grams sample content

w = sample content in grams

The arguments used in GAMA 2 are defined as follows:

N - number of isotopes to be analyzed on each spectrum

MMN - number of rolls of paper tape to be analyzed

I - order for isotopes to be analyzed, such as 1, 2, 3, ...

KJJ(I)- channel number of lower limit for summation range of i^{th} isotope derived from standards

KJI(I)- channel number for photo-peak of i^{th} isotope

KII(I)- channel number of upper limit for the summation range of i^{th} isotope derived from standards

ISO(I)- name of each isotope, such as SR(85), CS (137)

EFF(I)- efficiency of counting by the RCL gamma spectrometer for the i^{th} isotope

DECAY(I)-half life of i^{th} isotope in days

FRAC(I,J)-contribution coefficient on a specific isotope i, from another isotope j

CNN - counting time for background in minutes

AMM - counting time for samples in minutes

DAYS - number of days between release date and counting date

BOX - arbitrary catalog number to identify the roll of paper tape

ABS(J)- self-absorption coefficient for typical sample j

JJJ(I)- net counts of i^{th} channel after stripping out the corresponding background counts

IRLM - order number of spectra in each paper tape roll

IJK(IX)-total summed counts between the two summation limits for ix^{th} isotope

A(IX) - total summed counts between the two summation limits in real number for ix^{th} isotope

IX 2 - check to determine if spectrometer has drifted excessively

IDELT 1-number of channels between two summation limits derived from standard of specific isotope

IDELT 2-number of channels between two summation limits figured from sample spectrum

F(I,J) - the matrix array for the coefficients and constant term of simultaneous equations

LKL - error flag (fixed-point)
1 indicates no error
2 indicates that the equations are inconsistent

IKI(I) - channel number of photo-peak of i^{th} isotope in spectrum

COUNT(I)-solution of simultaneous equations for i^{th} isotope

DIS(I) - radioactivity of i^{th} isotope in the sample in disintegrations per minute

WT - weight of sample content

Details in the Utilization of GAMA 2

Data cards were arranged in the following manner:

(1) Number of isotopes and total number of reels of paper tape involved.

(2) Information for each isotope is read in as:

a. number to denote the order and name of isotope

b. channel number for the lower limit of integration, peak value, and higher limit of integration

c. counting efficiency

d. half-life in days

e. contribution coefficients derived from internal standards. (The contribution coefficients are arranged in square matrix format. The first row is the contribution coefficient for first isotope. The second row is those for second isotope, and so on.)

$$\hat{C} = \begin{vmatrix} C_{11} & C_{12} & - - - - - & C_{1j} & - - - & C_{1n} \\ C_{21} & C_{22} & - - - - - & C_{2j} & - - - & C_{2n} \\ & & & & & \\ C_{i1} & C_{i2} & - - - - - & C_{ij} & - - - & C_{in} \\ & & & & & \\ C_{n1} & C_{n2} & - - - - - & C_{nj} & - - - & C_{nn} \end{vmatrix}$$

← data card for 1st isotope

← data card for ith isotope

(3) Specific data about each roll of paper tape are included:

a. background counting time in minutes

b. sample counting time in minutes

c. time delay before sample counted (days)

d. catalog number for paper tape

e. sample content in the planchet

(4) Self-absorption for each isotope is put in according to the order used in (2).

Chapter IV

UPTAKE OF ^{85}Sr IN A STAGNANT AQUEOUS ENVIRONMENT

This series of experiments was undertaken to study the distribution of ^{85}Sr in the water, bottom sediments, and plants of an aquaria. Emphasis was directed to the uptake of ^{85}Sr by the bottom sediments and Vallisneria, the function describing the uptake of ^{85}Sr by sediments and Vallisneria, the penetration coefficients associated with the migration of ^{85}Sr in the bottom sediments, and the effects of temperature on the uptake of ^{85}Sr by various solid phases.

Physical System and Techniques

Sixteen aquaria, each with a layer of Lake Austin sediments and controlled biomass of Vallisneria, were used, Fig. 4-1. This contained ecosystem simulated a plug flow. The dimensions of each aquarium were 60 cm x 26 cm x 36 cm. Each aquarium was equipped with a stirrer which was immersed 7 cm into the water as shown in Fig. 4-1. The depth of the sediments was about 3 inches. A constant freeboard (~6 cm) was maintained in each unit. Distilled water was added to compensate for evaporation losses. All aquaria except units No. 5 and 6 were placed in constant temperature rooms, and fluorescent lights with constant intensity (600 foot-candles)

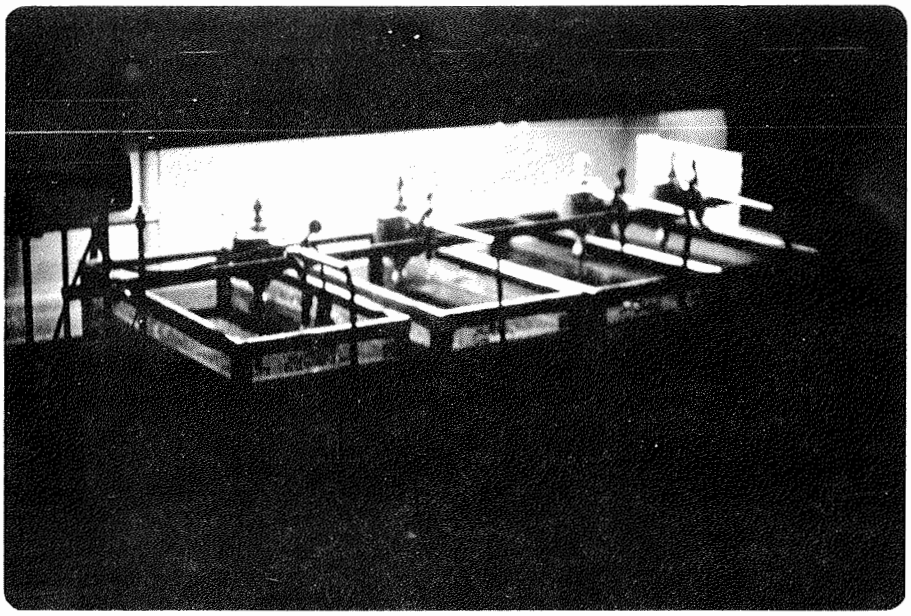

FIG. 4-1. AQUARIA STUDIES

were on 12 hours per day. For each temperature environment, three different initial concentrations of ^{85}Sr were used. These details are presented in Table 4-1. The biomass of Vallisneria was maintained constant for each of the units with the same ecological system. However, the biomass was quite different for those aquaria with different temperature conditions, Table 4-1. Separate descriptions for the flowing aquaria, units No. 5 and 6, will be reported in Chapter 5.

Table 4-1. Physical Description of Aquaria

Unit No.	Average Depth of Sediments (cm)	Total Biomass (gms)	Temperature (°C)	Initial Concentration of ^{85}Sr (MPC) (1)
1	9.5	3.8	24.5	0.119
2	6.5	4.4	24.5	0.223
3	8.1	6.48	24.5	0.477
4	8.3	3.10	24.5	0.466(2)
5	8.0	33.6	Ambient	0.370(3)
6	8.0	26.9	Ambient	0.520(3)
7	9.0	0.8	10.0	0.119
8	9.5	0.2	10.0	0.238
9	9.0	0.4	10.0	0.476
10	10.0	2.23	29.5	0.125
11	9.5	2.42	29.5	0.239
12	9.5	2.28	29.5	0.477
13	7.2	3.15	24.2	0.046
14	8.0	1.44	24.2	0.240
15	8.3	0.90	24.2	0.720
16	7.5	2.01	24.2	0.705

(1) MPC = maximum permissible concentration of ^{85}Sr in surface water according to NBS Handbook No. 62, 10^{-3} μc/ml

(2) the aquaria with initial clay suspension of 50 mg/l

(3) the flowing aquaria with continuous release of ^{85}Sr (total flow rate of 50 ml/min)

The samples of water, sediments, and Vallisneria were collected according to a predetermined schedule. In an attempt to investigate the immediate uptake of ^{85}Sr by sediments and Vallisneria, the short sampling times were set during the first day after release. The total sampling period for each unit was about one month.

A simplified procedure of sample collection was developed for the aquaria studies. Ten ml of water solution were withdrawn and processed directly for each water sample. Sediment samples were collected as previously described (42). Vallisneria leaves were picked individually with steel tongs. The sediment and Vallisneria samples were dried, ground, and weighed before placement into planchets.

Special techniques were used in evaluating the migration of ^{85}Sr into the sediment. Sediment sample cores were frozen and cut into five sections at depths of $\frac{1}{4}$, $\frac{1}{2}$, 1, 2, 3 inches from the interface of the sediment and water. Each section was dried at 110°C, weighed, and counted. All the details of collection and processing are presented in Appendix II.

^{85}Sr Variation in Water Solution

The concentration of ^{85}Sr in the water decreased with increasing time after release. As presented in Fig. 4-2, the corrected concentration of ^{85}Sr in liquid phase decreased

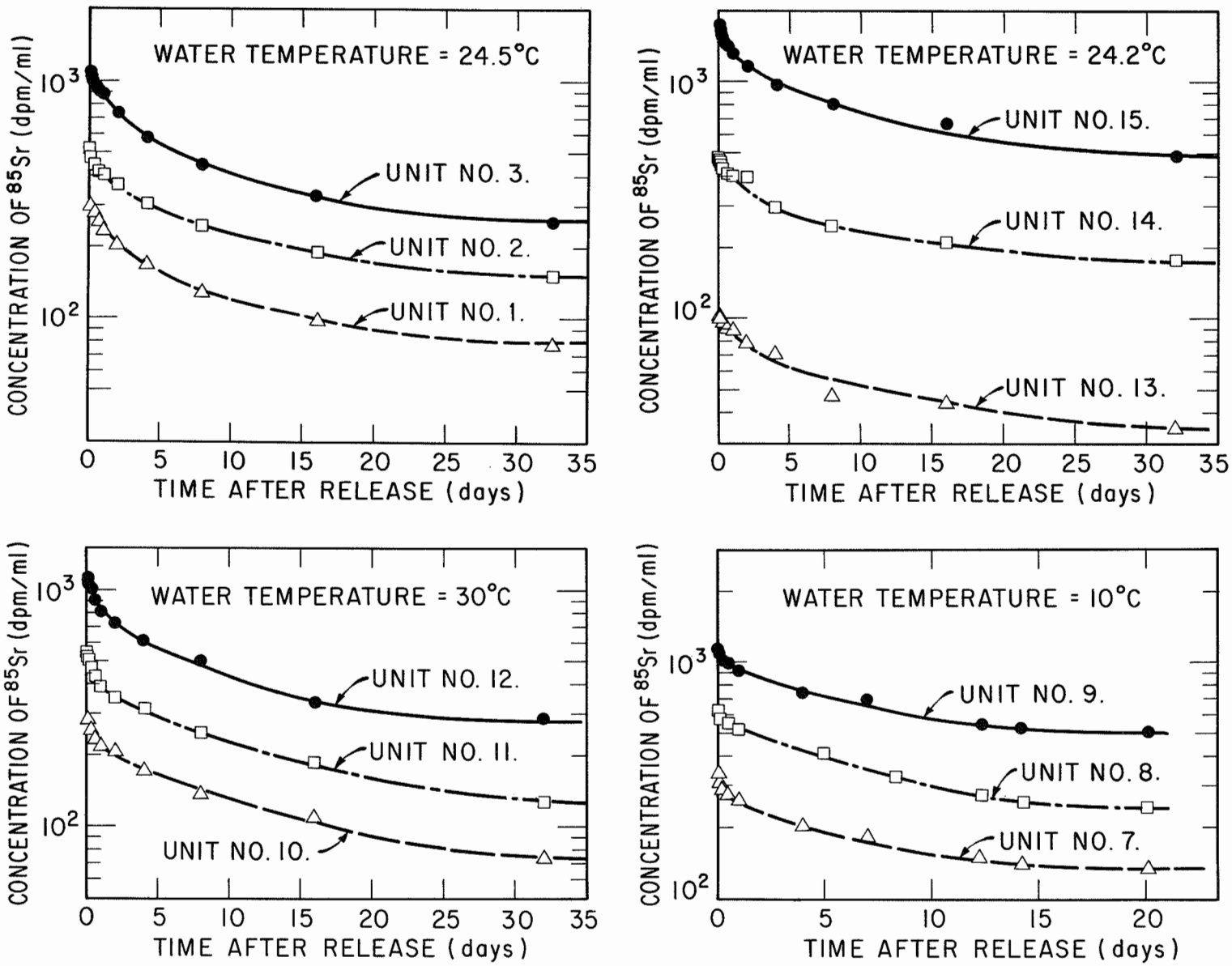

FIG. 4-2. ^{85}Sr IN THE LIQUID PHASE OF THE CONTAINED ECOSYSTEM

very rapidly during the first day after the introduction of ^{85}Sr, but the concentration leveled off to a constant value after 30 days. Four sets of aquaria were studied with water temperatures of 24.5°C, 24.2°C, 10°C, and 30°C. Units No. 2 and No. 14 were duplicate systems designed for the evaluation of reproducibility and accuracy of the data, Fig. 4-2.

The total uptake by sediments and Vallisneria are shown in Table 4-2. The discrepancy was expressed in terms of the decreasing percentage of the initial ^{85}Sr in the water. Uptake of ^{85}Sr was found to be a function of temperature, that is, the higher the temperature, the greater the uptake, Fig. 4-2.

Table 4-2. Total Decrease of ^{85}Sr in the Liquid Phase of Contained System

Temperature (°C)	Unit No.	Total Decrease (%)
10.0	7	61
10.0	8	58
10.0	9	56
24.2	13	64
24.2	14	63
24.2	15	72
24.5	1	74
24.5	2	72
24.5	3	78
30.0	10	75
30.0	11	78
30.0	12	75

The equilibrium occurred as ^{85}Sr in the water decreased to a constant value. But after 30 days, the decreasing rate of ^{85}Sr in water became practically zero and a quasi-equilibrium state was established.

^{85}Sr Associated with the Bottom Sediments

The ^{85}Sr associated with sediments increased with time as shown in Fig. 4-3. A quasi-equilibrium concentration of ^{85}Sr was also reached after 30 days of interaction time. Higher uptake of ^{85}Sr was observed to occur at higher temperatures. Ratios of total ^{85}Sr associated with sediments at higher temperatures to that at 10°C are shown in Table 4-3.

Table 4-3. Ratio of Total Uptake of ^{85}Sr by Sediments

Initial ^{85}Sr Concentration (MPC)	$\frac{^{85}Sr \text{ of } 24.5^{\circ}C}{^{85}Sr \text{ of } 10^{\circ}C}$	$\frac{^{85}Sr \text{ of } 30^{\circ}C}{^{85}Sr \text{ of } 10^{\circ}C}$
0.120	1.90	2.23
0.235	1.25	1.40
0.477	1.26	1.28

^{85}Sr Penetration into the Sediments

As reported by others (53, 4, 42, 40), radionuclides migrate into the sediments through the diffusion mechanism. Shih and Gloyna (42) found the migration function to be a first order reaction. Based on the mass balance

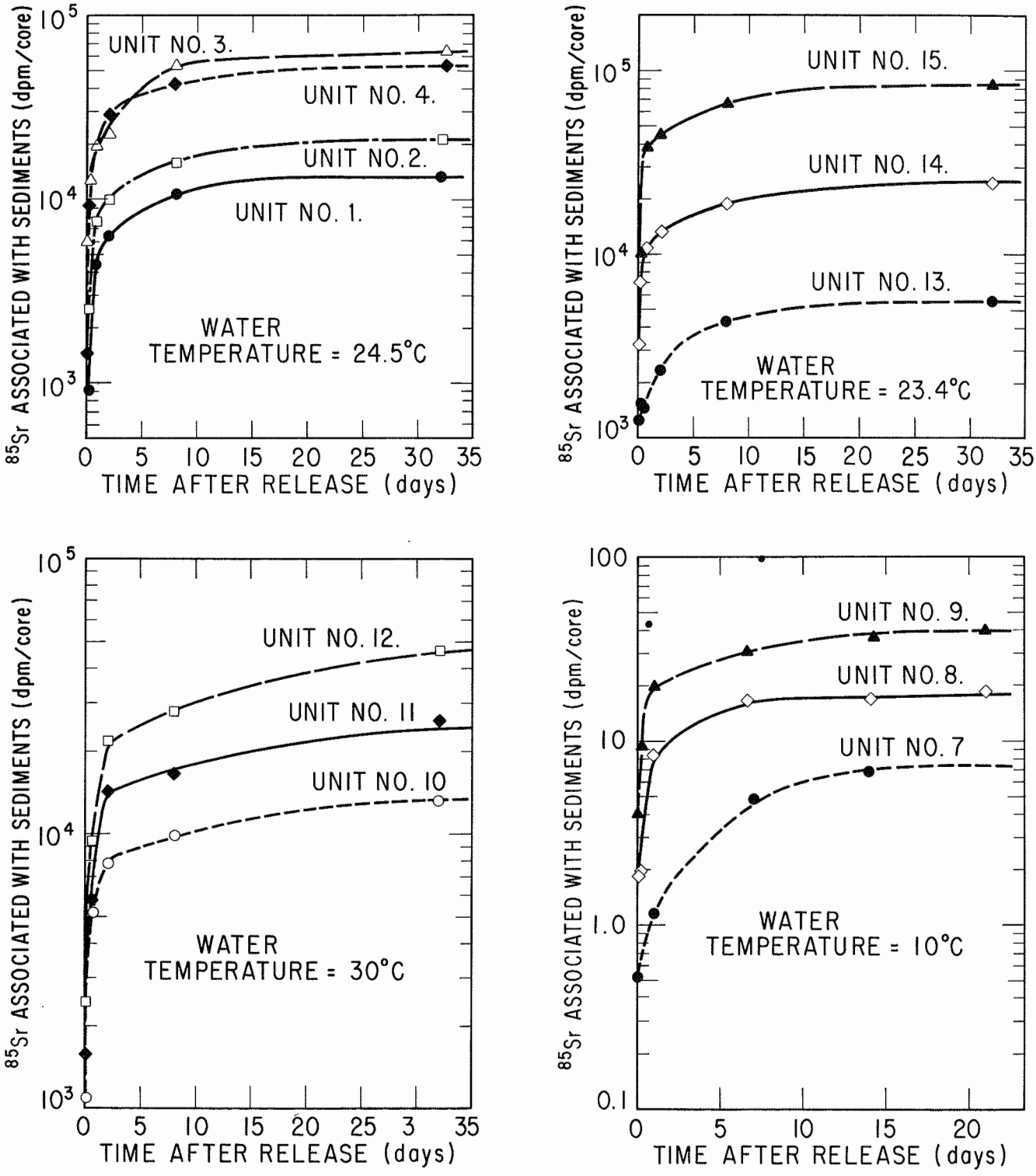

FIG. 4-3. Sr ASSOCIATED WITH SEDIMENTS

relationship, the total number of radionuclides retained in a cube of sediment with infinitesimal depth and unit area was:

$$N(d, t) - N(d+\Delta d, t) = P\left[\frac{N(d, t) + N(d+\Delta d, t)}{2}\right]\Delta d \quad (4\text{-}1)$$

Where

$N(d, t)$ = total number of radionuclides per unit area at depth d and migration time of t

$N(d+\Delta d, t)$ = total number of radionuclides per unit area at depth $(d+\Delta d)$ and migration time of t

Δd = infinitesimal depth

$p(t)$ = probability of being retained in the sediments for each radionuclide per unit of depth for time t

Then, taking limit for $\Delta d \rightarrow 0$

$$\lim_{\Delta d \rightarrow 0} \frac{N(d, t) - N(d+\Delta d, t)}{\Delta d} = \lim_{\Delta d \rightarrow 0} p(t) \quad \frac{N(d, t) + N(d+\Delta d, t)}{2}$$

gives

$$-\frac{dN}{dd} = p(t)\, N(d, t)$$

and

$$N(d, t) = N_o\, e^{-p(t)d} \quad (4\text{-}2)$$

Where

N_o = number of radionuclides per unit area at interface

Because of the difficulty of measurement, the depth d was transferred into weight of sediments by Fig. 4-4. The average dry weight of sediments (0.1 inches of depth) having a cross section of 0.6 sq. in. was calculated to be 1.1 gms. Therefore, Eq. 4-2 can be translated in terms of the radionuclides concentration per unit weight of dried sediments (dpm/gm), Eq. 4-3.

$$C_s(w, t) = C_{s_o} e^{-p(t)d} \qquad (4\text{-}3)$$

$$= C_{s_o} e^{-p'(t)w}$$

Where

$C(w, t)$ = number of radionuclides per unit weight of dried sediments at the depth with w cumulative weight from the interface

C_{s_o} = saturated interface concentration of the radionuclides associated with sediments in terms of the number of radionuclides per unit weight of dried sediments

p' = penetration coefficient for 0.09 inches of depth which is a function of contact time

The penetration of ^{85}Sr into the sediments is shown in Figs. 4-5, 4-6, 4-7, and 4-8. The penetration coefficients, p', for each unit are given in Table 4-4. It was found that the p' values were about equal to one another for the units

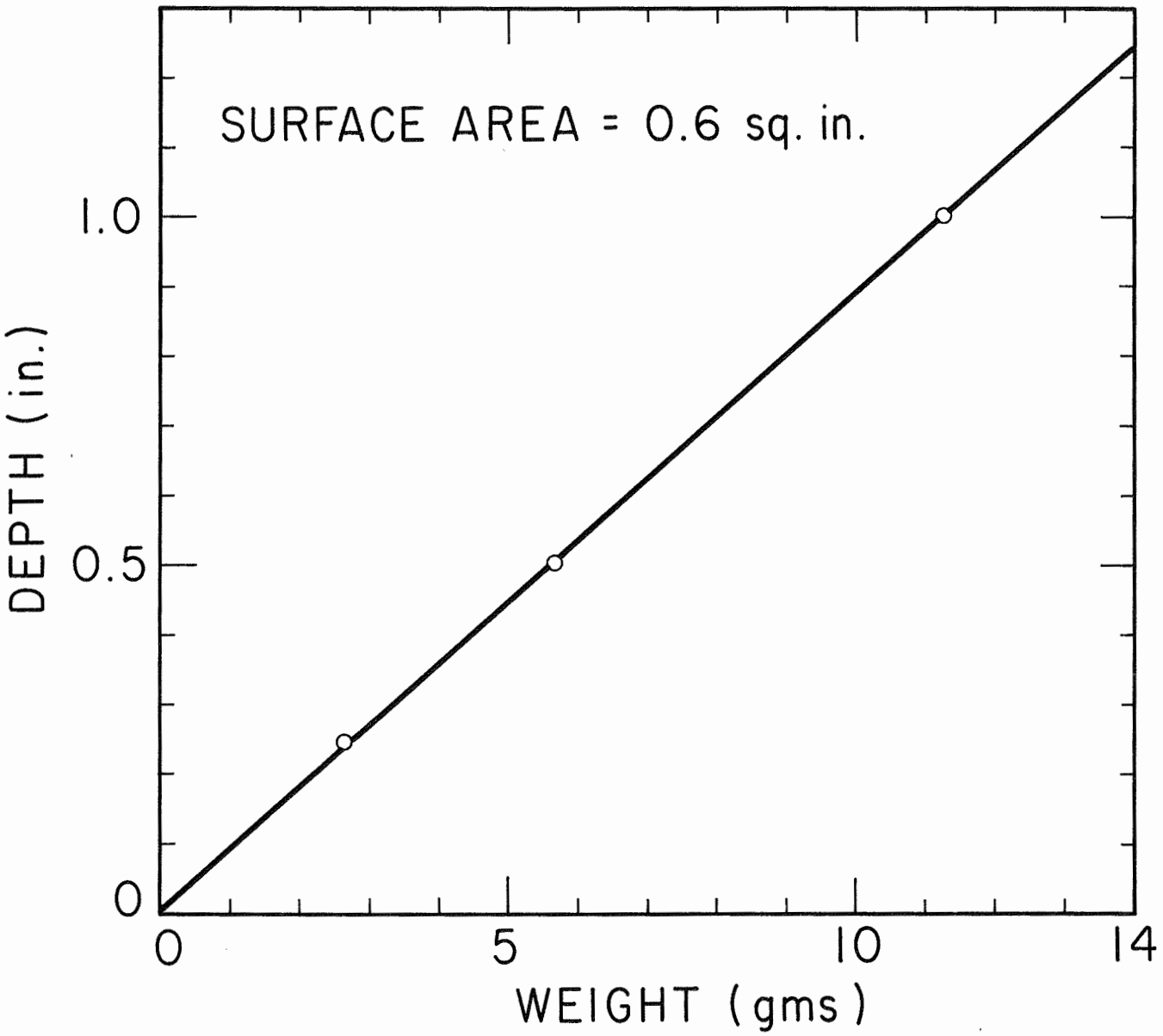

FIG. 4-4. LAKE AUSTIN SEDIMENTS WEIGHT-DEPTH RELATIONSHIP

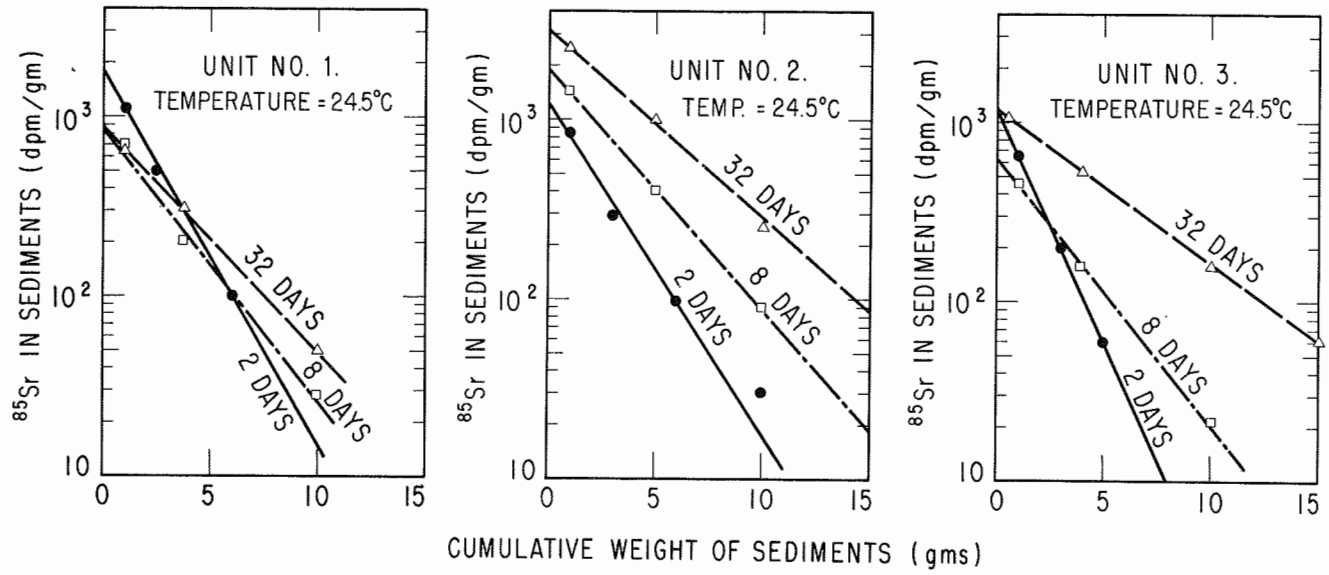

FIG. 4-5. ^{85}Sr PENETRATION INTO THE SEDIMENTS AT 24.5°C

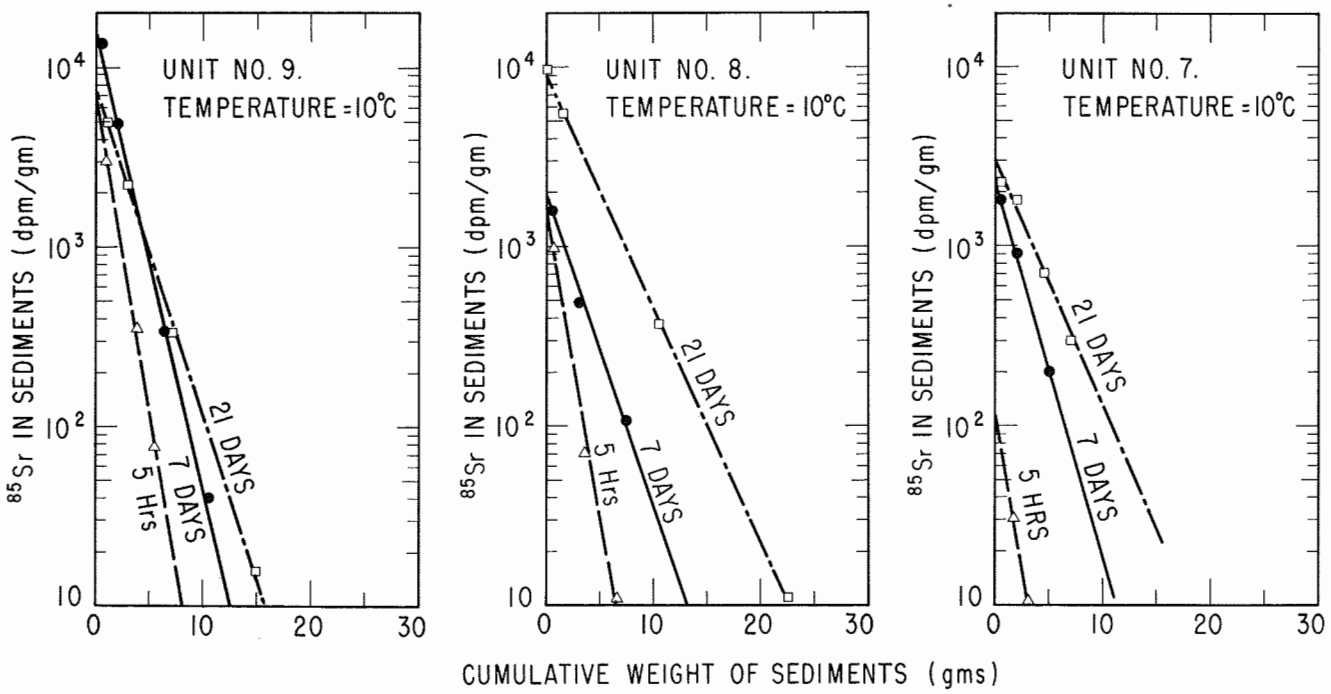

FIG. 4-6. ^{85}Sr PENETRATION INTO THE SEDIMENTS AT 10°C

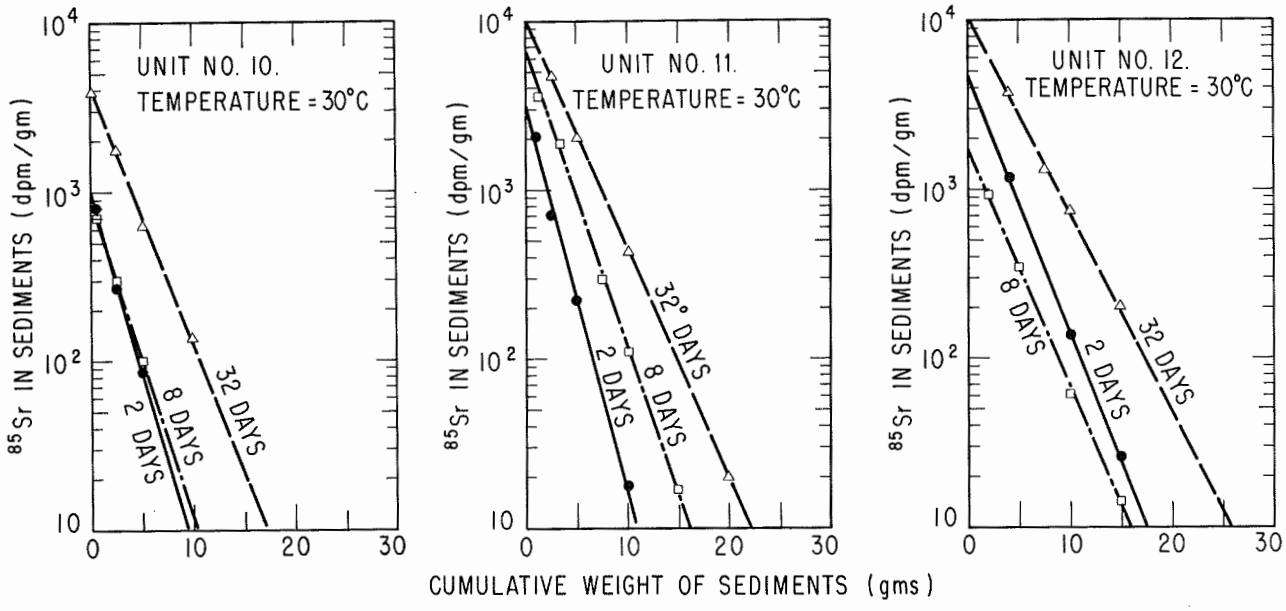

FIG. 4-7. ^{85}Sr PENETRATION INTO THE SEDIMENTS AT 30°C

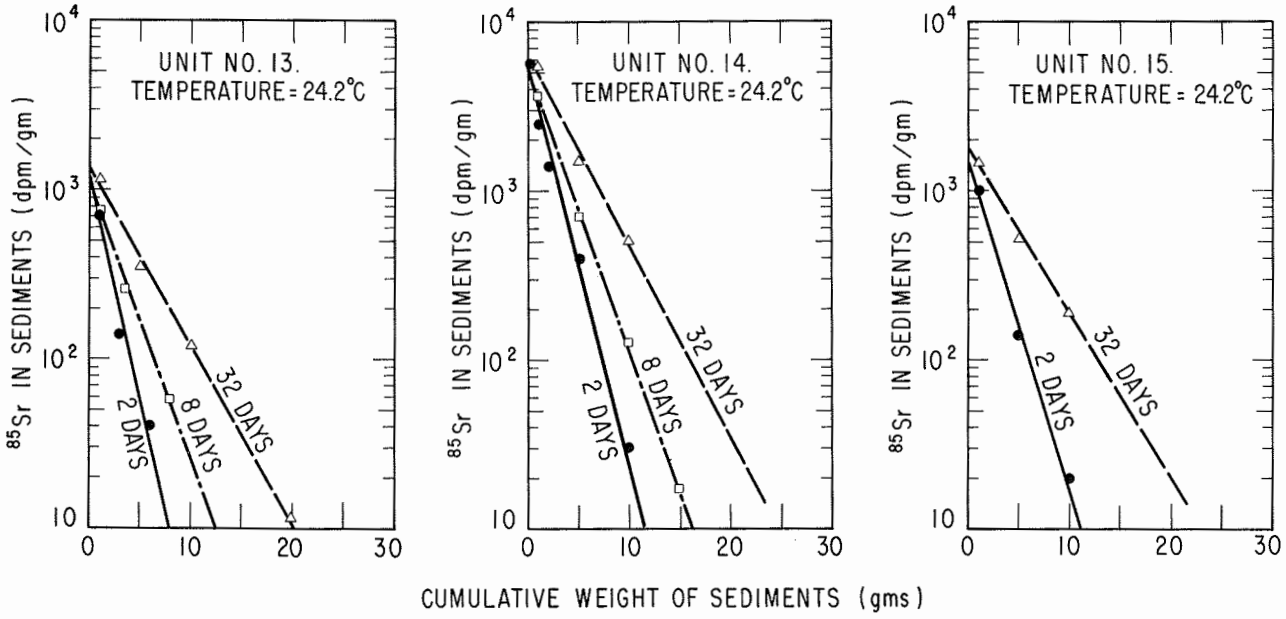

FIG. 4-8. ^{85}Sr PENETRATION INTO THE SEDIMENTS AT 24.2°C

with the same water temperatures, Table 4-4. The ^{85}Sr concentration in the water did not seem to affect the p' value as the theoretical derivation indicated. The temperature effect was studied and shown in Fig. 4-9.

Table 4-4. Penetration Coefficients for ^{85}Sr in the Sediments of Aquaria

Water Temperature (°C)	Unit Number	Penetration Coefficients (Gm^{-1}) Time after Introduction of ^{85}Sr		
		2 days	8 days	32 days
24.5	1	0.479	0.352	0.291
24.5	2	0.49	0.37	0.286
24.5	3	0.54	0.365	0.270
10	7	0.815	0.50	0.36
10	8	0.78	0.52	0.38
10	9	0.81	0.56	0.42
30	10	0.46	0.34	0.26
30	11	0.42	0.32	0.27
30	12	0.44	0.32	0.28
24.2	13	0.48	0.37	0.28
24.2	14	0.54	0.35	0.29
24.2	15	0.56	----	0.275

^{85}Sr Associated with Vallisneria

^{85}Sr uptake by Vallisneria increased with time during the first few hours. But it started to decrease after four to eight hours, Fig. 4-10. A quasi-equilibrium condition for uptake of ^{85}Sr by Vallisneria seemed to be attained after 30 days. The uptake in all cases has unit of disintegration per minute per gram of dry weight of Vallisneria leaves. Since Vallisneria has no stems and the leaf sizes were about

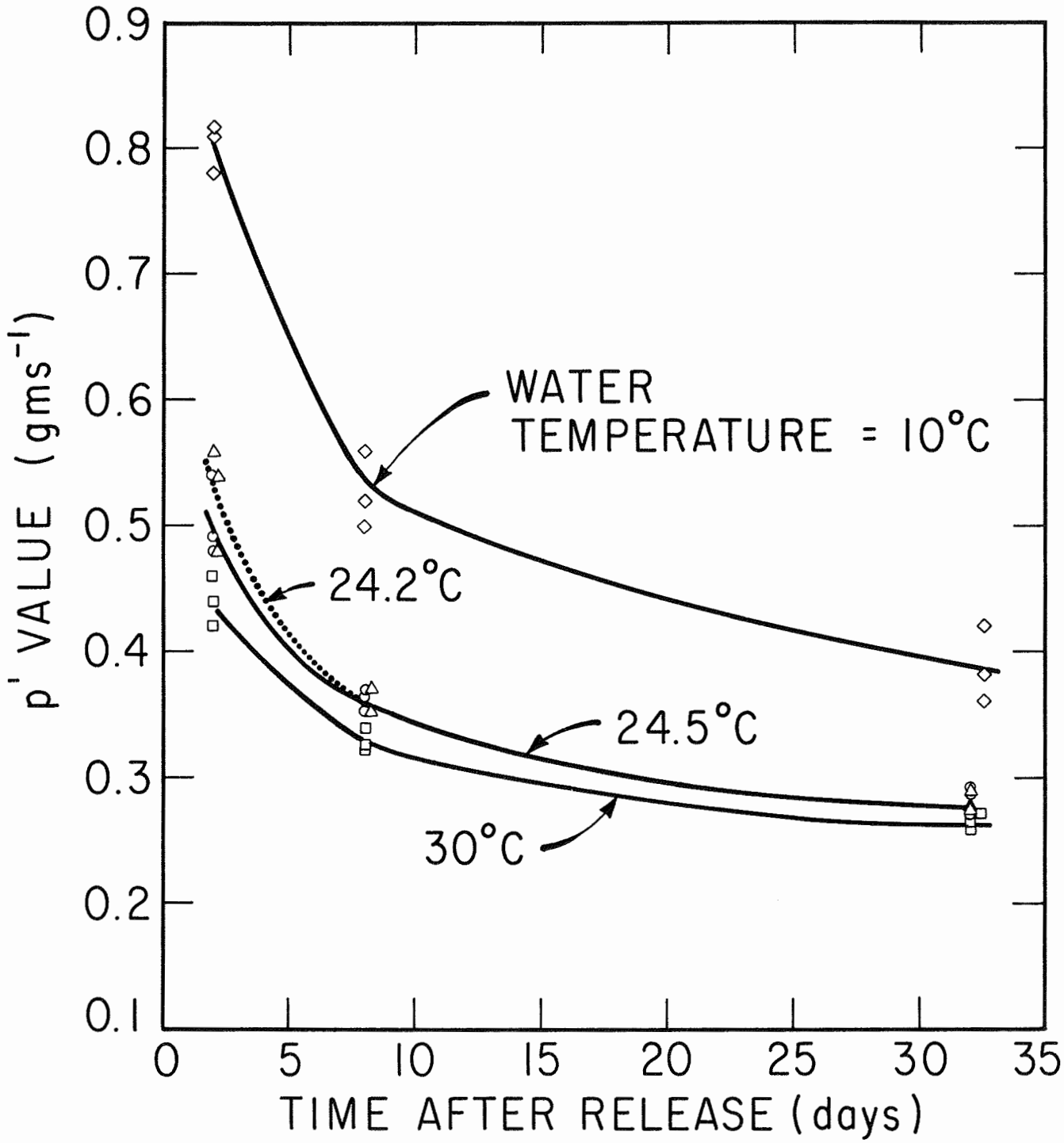

FIG. 4-9. VARIATION OF PENETRATION COEFFICIENT FOR ^{85}Sr IN LAKE AUSTIN SEDIMENTS

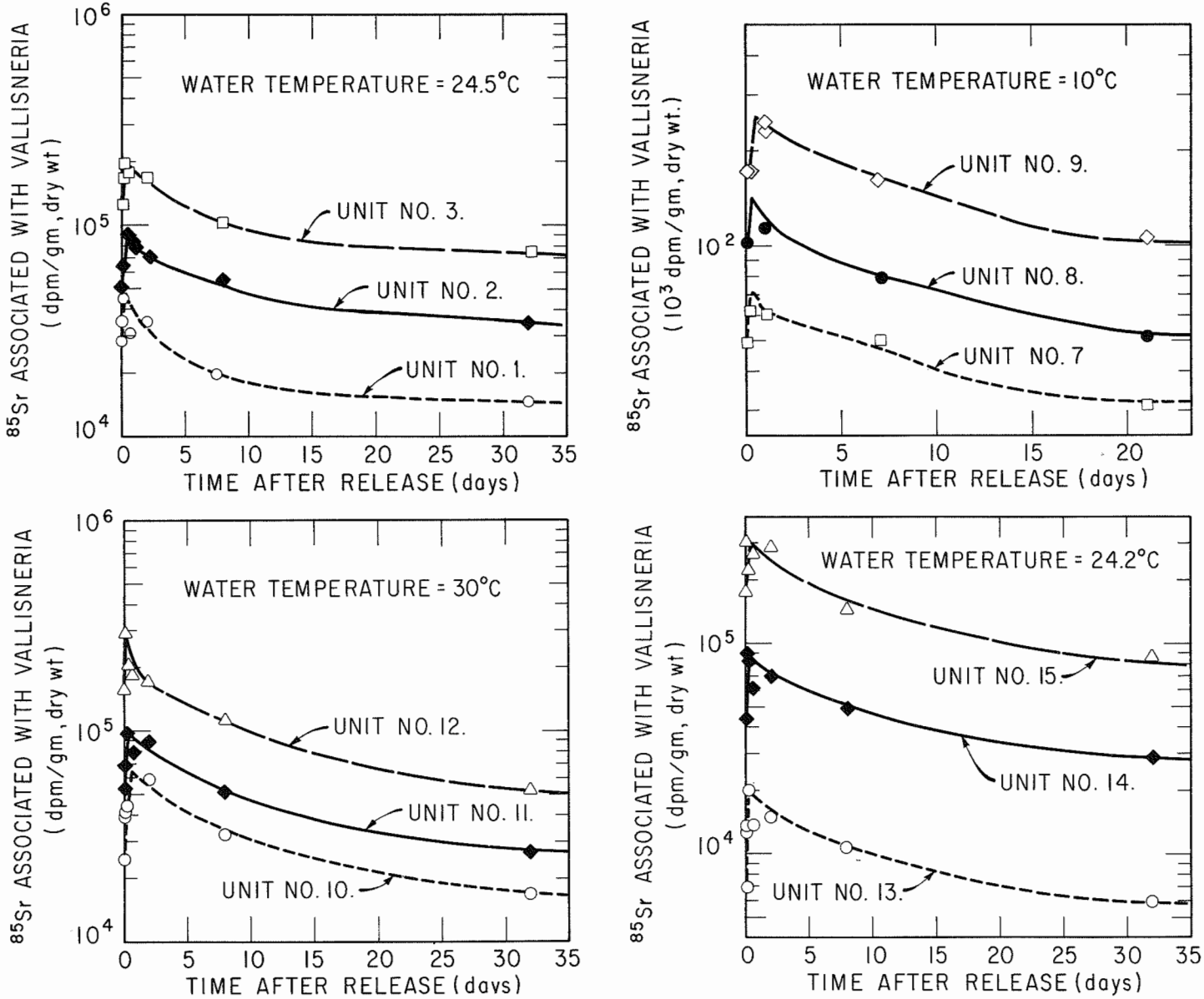

FIG. 4-10. VARIATION OF ^{85}Sr ASSOCIATED WITH VALLISNERIA IN CONTAINED ECOSYSTEM

the same, the surface area per unit weight was fairly constant. It was found to be 0.338 sq. in./gm of dry weight (air dried). Thus, by the insertion of this ratio, the ^{85}Sr uptake by unit surface area can be computed.

Analysis of the Distribution of ^{85}Sr

In order to obtain reproducible results, the uptake of ^{85}Sr by either bottom sediments or Vallisneria was correlated with the concentrations of ^{85}Sr in the liquid phase. The ^{85}Sr associated with Vallisneria or sediments seems to have been predominantly due to sorption. Thus, in the uptake function of ^{85}Sr by sediments, the influence of Vallisneria is a negligible factor. Similarly, the secondary effects due to sediment uptake should be neglected in describing the uptake function of ^{85}Sr by Vallisneria.

Fig. 4-11 presents a plot of ^{85}Sr associated with sediments versus the ^{85}Sr detected in the water. The slope of the line representing the concentration factor was found to increase with time, but the rate of increase decreased, Fig. 4-12.

The uptake function of ^{85}Sr by Vallisneria is given in Fig. 4-13. The concentration factor, the slope of the straight line plot of ^{85}Sr associated with Vallisneria versus that in water, decreased with increasing time. This implies that the rate of decrease of the ^{85}Sr associated with

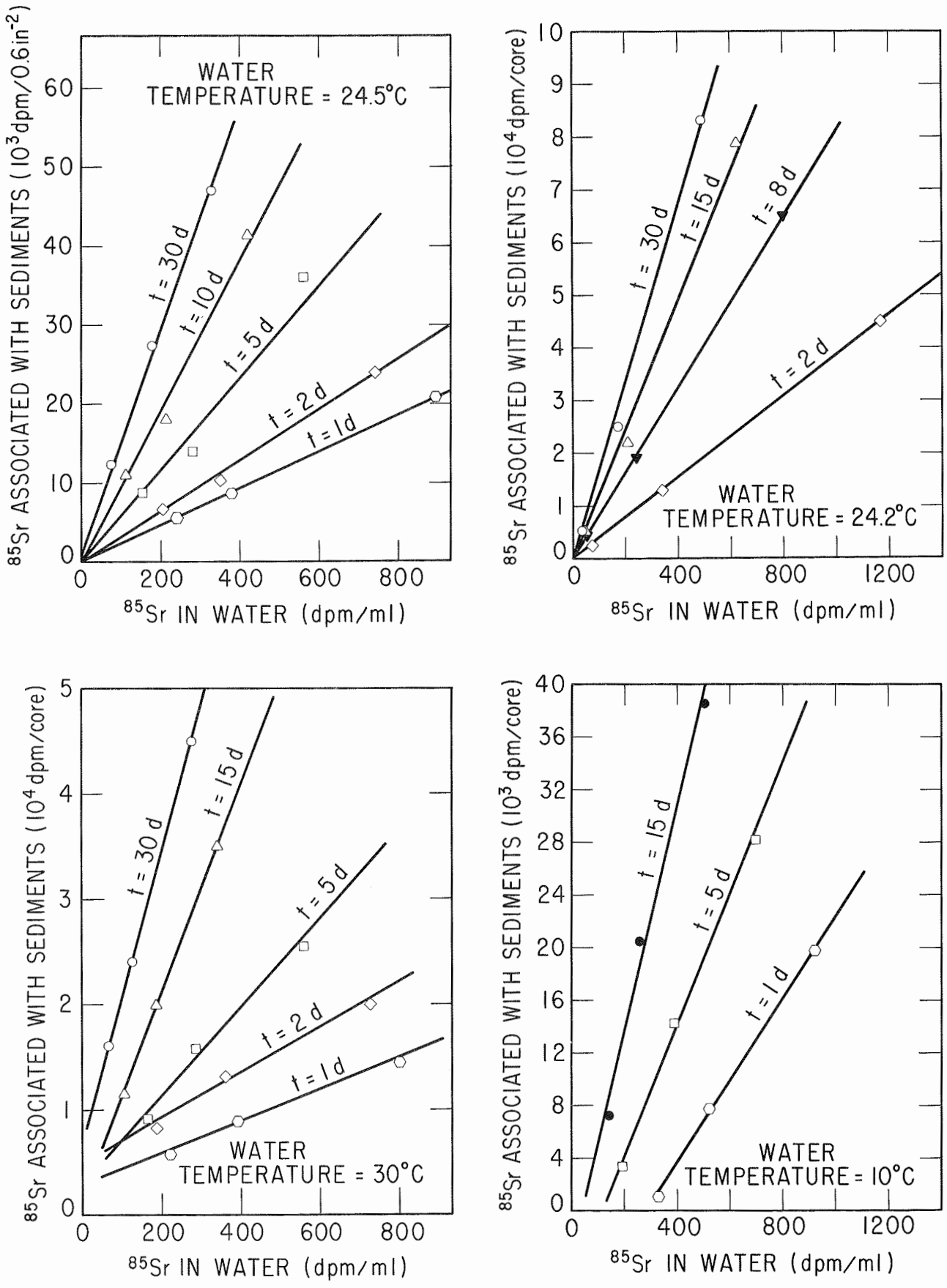

FIG. 4-11. UPTAKE OF ^{85}Sr BY BOTTOM SEDIMENTS

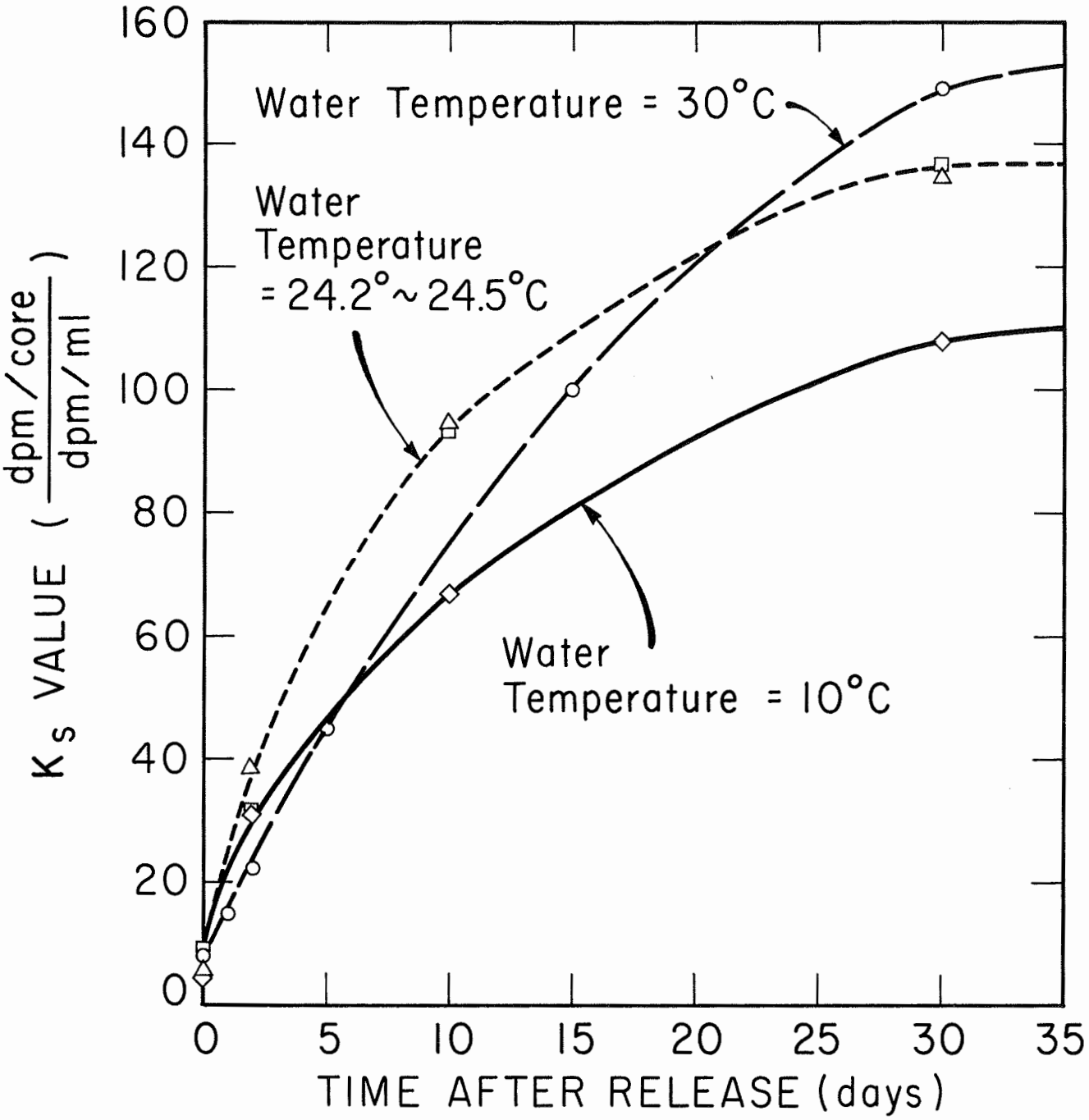

FIG. 4-12. VARIATION OF CONCENTRATION FACTOR, K_S, FOR ^{SR}Sr IN SEDIMENTS

Vallisneria was larger than that in the water phase. As shown in Fig. 4-14, the concentration factor of Vallisneria for ^{85}Sr, K_p, declined with contact time.

The immediate uptake of ^{85}Sr by both bottom sediments and Vallisneria are shown in Fig. 4-15. The immediate concentration factors for ^{85}Sr by sediments and Vallisneria were found to be 5-9 dpm/gm/dpm/ml and 150-175 dpm/gm/dpm/ml, respectively, Table 4-5.

Table 4-5. Concentration Factors for ^{85}Sr in Contained Ecosystem

Water Temperature C°	Time Elapsed (Days)	Bottom Sediments $K_s(t)$ dpm/core / dpm/ml	Vallisneria $K_p(t)$ dpm/gm / dpm/ml
24.5	0	8	170
	2	32	265
	10	93	225
	30	137	205
10	0	4.2	150
	2	31.5	245
	10	67.0	215
	30	86.0	195
30	0	8.8	176
	2	22	275
	10	80	230
	30	140	210
24.2	0	5.3	165
	2	39	255
	10	94	224
	30	135	199

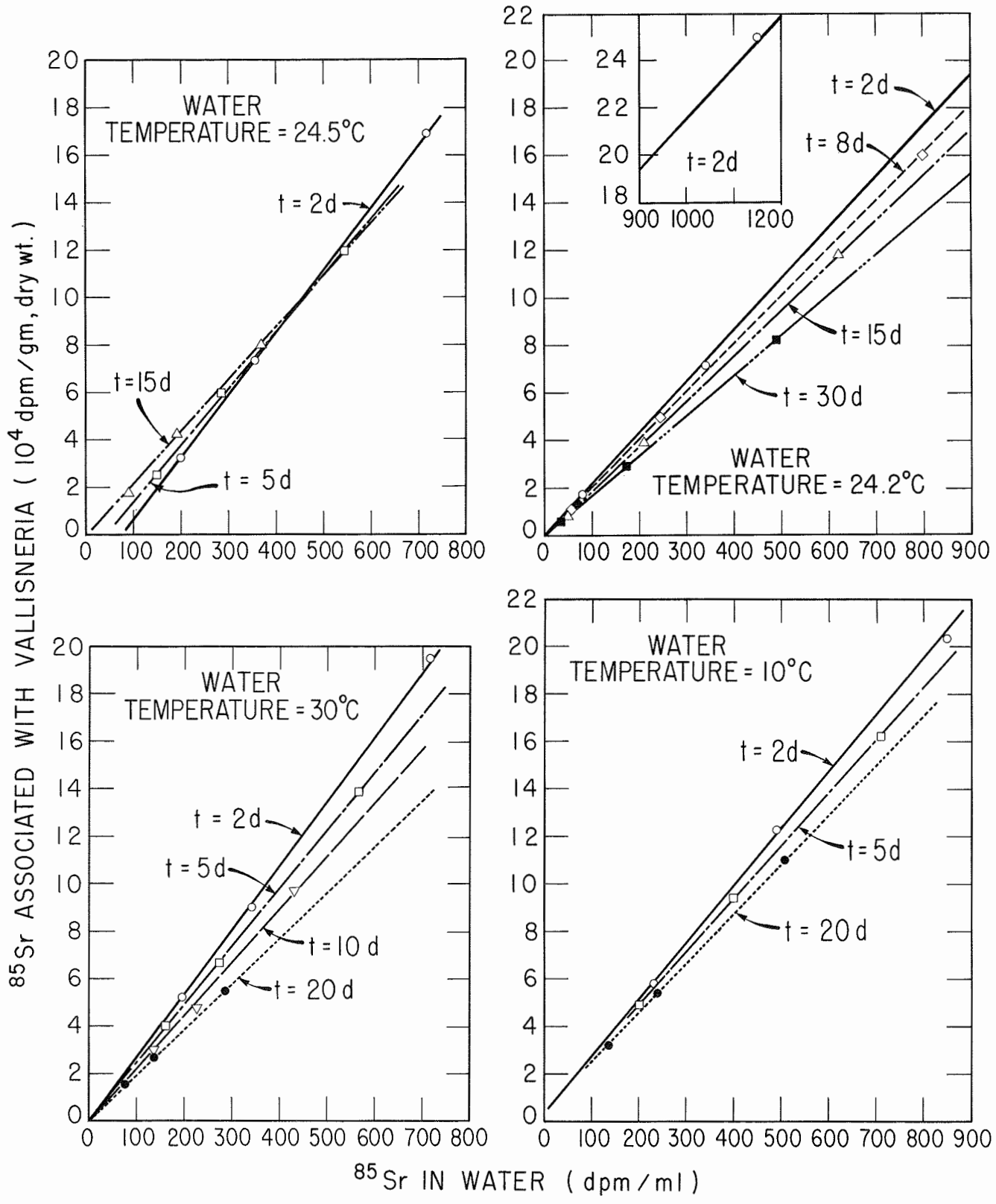

FIG. 4-13. ^{85}Sr UPTAKE BY VALLISNERIA

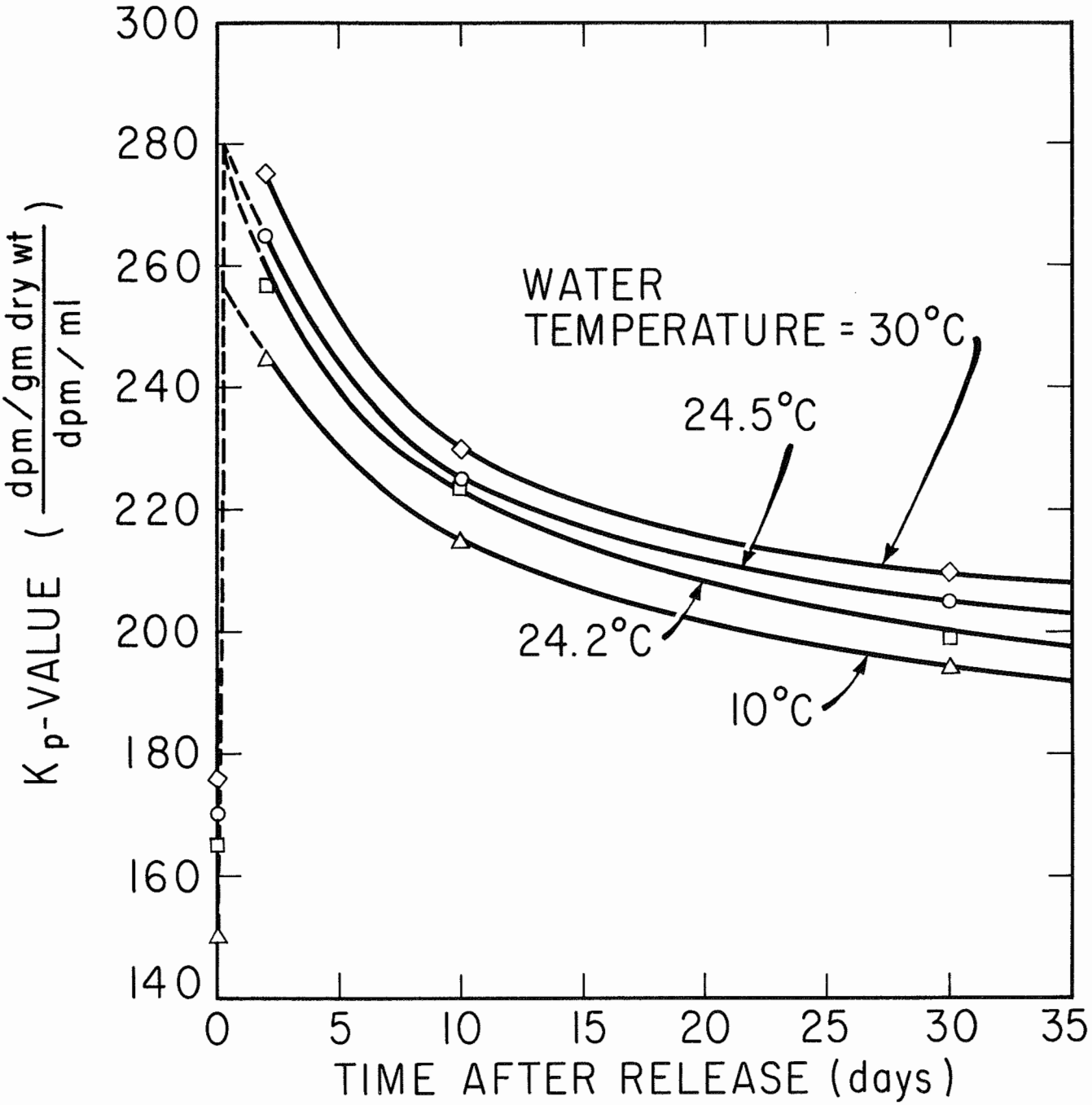

FIG. 4-14. VARIATION OF K_p, CONCENTRATION FACTORS OF ^{85}Sr IN VALLISNERIA

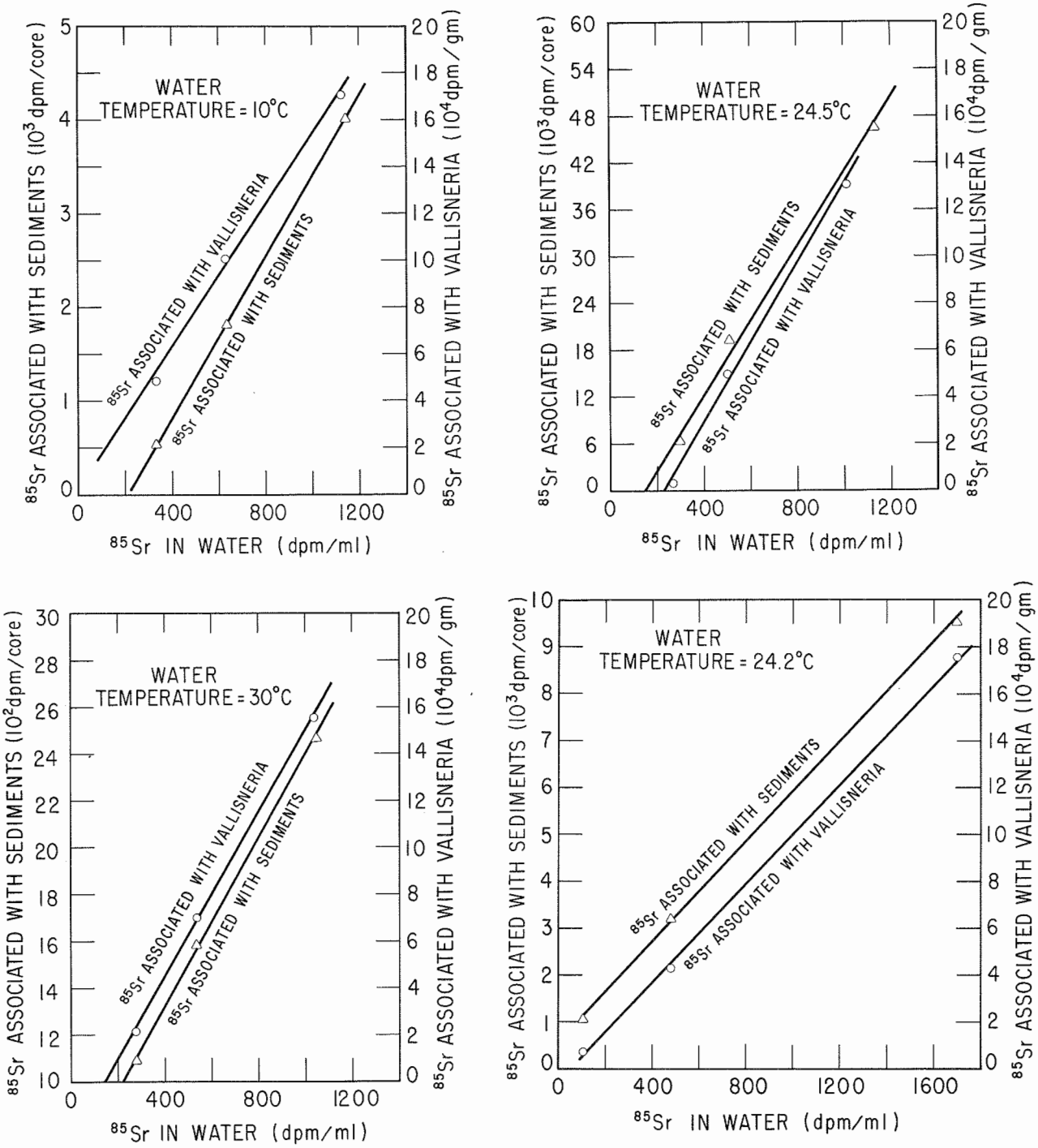

FIG. 4-15. IMMEDIATE UPTAKE OF ^{85}Sr BY BOTTOM SEDIMENTS AND VALLISNERIA

As shown in Figs. 4-12 through 4-16, the overall effect of temperature on the detention of ^{85}Sr by sediments and Vallisneria was not as great as expected. The K_s and K_p values for different temperatures were found to converge within a finite region, Fig. 4-16. A simple correlation between concentration factors and water temperatures was very difficult to evaluate. However, the empirical relation expressing K_p is shown in Eq. 4-4.

$$K_p = K_{p_1} t^{-0.1} \qquad (4\text{-}4)$$

Where

K_p = concentration factor for ^{85}Sr by Vallisneria

t = interaction time in days ≥ 1

$$k_p = 250 + T^{\circ}C \qquad (4\text{-}5)$$

The average K_s-Time relationship for a temperature range of $10^{\circ}C$ to $30^{\circ}C$ may be described by Eq. 4-6.

$$K_s = 21\ t^{0.55} \qquad (4\text{-}6)$$

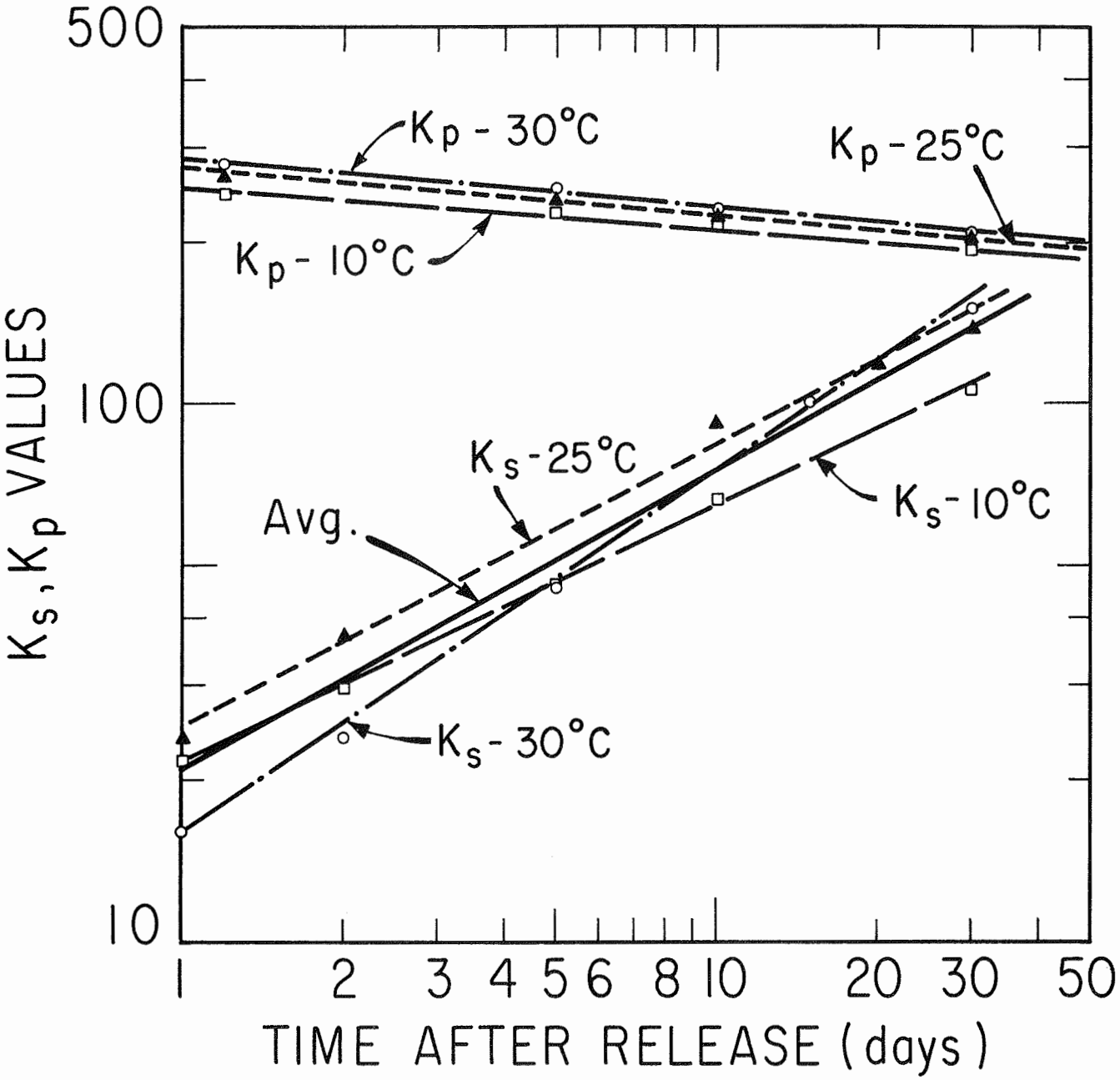

FIG. 4-16. FUNCTIONS OF K_p AND K_s WITH RESPECT TO TIME OF INTERACTION

Chapter V

UPTAKE OF ^{85}Sr IN A MODEL RIVER

This chapter describes the accumulation and release of ^{85}Sr by bottom sediments and Vallisneria in a model river. Included is a study of hydrodynamic mixing. Three dye experiments, two steady state releases, and one instantaneous injection of ^{85}Sr were conducted.

Also, induced environmental stresses were imposed, and the changes in uptake rate were noted. The effect of an organic pollutant will be discussed herein, while other effects will be covered in separate reports (9, 34).

Model River

The model river consisted of a dual-channel metal flume, two circular concrete tanks, a pumping system, a regulating tank, two stilling basins with triangular weirs, and two manometers. Each channel of the rectangular flume was 200 ft. long, 1.25 ft. wide, and 2 ft. deep. The slope of the flume was adjustable in the range of zero to 0.006 ft./ft. through the use of screw jacks. The details of the flume are shown in Figs. 5-1 and 5-2. The two reservoir tanks were 12 ft. deep and each had a capacity of 500,000 gallons. One was used as a supply reservoir, and the other as an effluent monitoring tank.

FIG. 5-1. DUAL-CHANNEL FLOW

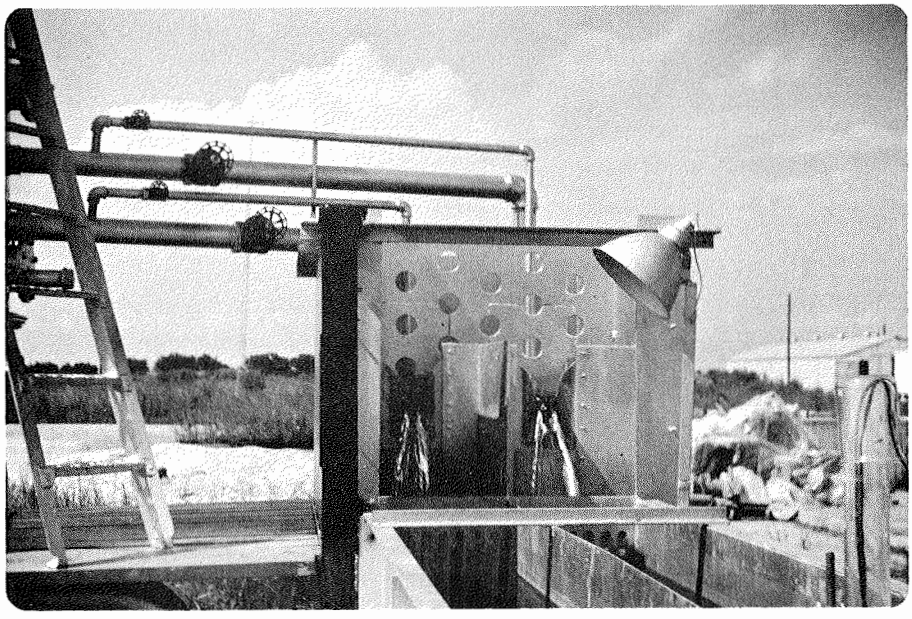

FIG. 5-2. INLET DEVICES ON RESEARCH FLUME

The supply pump was driven by a 10 hp, 860 rpm electric motor and was primed by a "wobble" pump. The capacity of the supply pump was about 1.72 cfs at a 35 ft. head. The regulating tank was a cylindrical steel tank with diameter of 6 ft. and capacity of 1,000 gallons. The water elevation was designed to maintain 8.50 ft. above the bottom of the channel bed. Gate valves were installed for the control of inflow into the stilling basin from the regulating tank. Perforated steel plates were used to dissipate the energy, and brass triangular weirs were installed at the outfall of the stilling basin. The crest of the weir was six inches above the side walls. A manometer was attached to each stilling basin.

Influent Measurement: The relationship between the flow rate and the manometer reading can be expressed by Eq. 5-1.

$$Q = 0.181\ M^{2.587} \qquad (5\text{-}1)$$

Where

Q = flow rate in liters/min

M = manometer reading in cm

Eq. 5-2 gives the flow rate for the triangular weirs.

$$Q = 0.44\ H^{2.30}$$

Where

Q = flow rate in liters/min

H = water head above the crest of weir in cm

Aquatic Environment: The water was a mixture of well water from Balcones Research Center and treated city water. An analysis of the water is shown in Table 5-1.

Table 5-1. Chemical Analysis of Flume Water

	Concentration (mg/l)
Suspended solids	9.8
Alkalinity (T. $CaCO_3$)	225
Hardness ($CaCO_3$)	260
Na	34.9
K	1.0
Ca	44.0
pH	8-9
Conductivity	640 (mho s/cm)

The sediment came from Lake Austin and was placed in the flume at a depth of about 15 cm. X-ray diffraction analysis showed the sediment to consist of the following minerals:

Type of Minerals	Content (%)
Non-clay Minerals (#325 mesh sieve)	
Quartz	40
Calcite	22
Dolomite	8
Clay Minerals (2)	
Montmorillonite	15
Mica	9
Kaolinite	6
Organic Materials	2

The clay fractions contained montmorillonite, kaolinite, and other degraded clays. The cation exchange capacity, as determined by the tagged cesium method, was about 29 meq/100 gm of sediment.

The only macroplant transplanted in the flume was Vallisneria, and it provided approximately 2.2 grams dry weight per square foot of flume surface area. The leaves of the Vallisneria were trimmed during the experiment involving the release of organic pollutants.

Instrumentation: A list of equipment is given in Table 5-2. Details will be covered in a separate report (9).

Waste Treatment: The low-level waste from the flume was filtered through a charcoal filter before released to a holding tank where it was stored for about one month. Finally, after monitoring, the waste was pumped to the Balcones Sewage Treatment Plant. In all cases, the radionuclide levels were much lower than MPC values.

Experimental Procedure

The details of sampling and processing are presented in Appendix II. Additional procedures involved in the ^{85}Sr study are reported in the following sections.

Sampling: Water samples of 100 ml were taken at two different depths in the channel; namely, two and eight inches from the surface. The sampling apparatus is shown in Fig. 5-3.

Table 5-2. Instrumentation of Model River

Equipment and Manufacturer	Location (Distance from Inlet)	No. Used	Measurement
Electronic Thermometer (Research Associates Model F7-2)	5' and 195'	2	Temperature
Galvanic Oxygen Cell	5' and 195'	2	Dissolved Oxygen
Expanded Scale pH Meter (Beckman, Model 76)	5' and 195'	2	pH
Zeromatic pH Meter (Beckman, Model 9600)	100'	1	ORP
Pyroheliometer (Eppley, 180)	100' (One with filter and one without)	2	Light Intensity
Dual Channel Recorder (YSI, Model 81)	5', 100', 195'	3	Continuous record for pH, D. O. and Light Intensity
Conductivity Cell (U-type with self-contained Line Operator Portable Conductivity Bridge)	100'	1	Conductivity
Fluorometer (Turner Model III)	Flume	1	Dye
Scintillation Spectrometer (Nuclear Chicago)	195'	1	Evaluation of Radioactivity
Rectilinear Recorder	195'	1	Continuous Record of the Radioactivity in Solution
512-Channel Gamma Spectrometer (RCL)	Lab	1	Radioactivity - gamma (Gross)
Digital Volt Meter and Paper-Punch Tape Printer	Flume	1	Monitor all Instruments
Autoanalyzer	Lab	1	COD

These samples were refrigerated until the aliquots of 10 ml could be transferred to aluminum planchets for processing and radioactivity analysis. The concentrations of ^{85}Sr associated with the suspended materials were determined by difference measurement, i. e., counts of the liquid before and after filtration through a millipore filter (0.45μ).

The sediment sampler consisted of a lucite tube, an aluminum piston, and a steel sample holder. These are shown in Fig. 5-3. The sediment core was collected by forcing the lucite tube into the sediment. The piston in the tube helped to keep the core intact as the sampler was removed from the flume. After collection, both the sample and the tube were frozen. Then the top three inches of the frozen core were pushed out and cut off for analysis. Following the standard procedure, each of the samples was dried at 110°C for about 24 hours and transferred to an aluminum planchet for counting.

The Vallisneria leaves were collected with steel tongs and rinsed with tap water; selected samples were wiped with filter paper in an attempt to obtain the data for the ^{85}Sr absorbed into the Vallisneria. The leaves were placed in a paper cup, dried under infrared lamps for about 16 hours, and then the dried material was weighed.

Counting Procedures: Since all the samples contained ^{85}Sr, ^{51}Cr, and ^{137}Cs, the multi-channel gamma spectrometer incorporating a four-inch diameter thallium-activated NaI

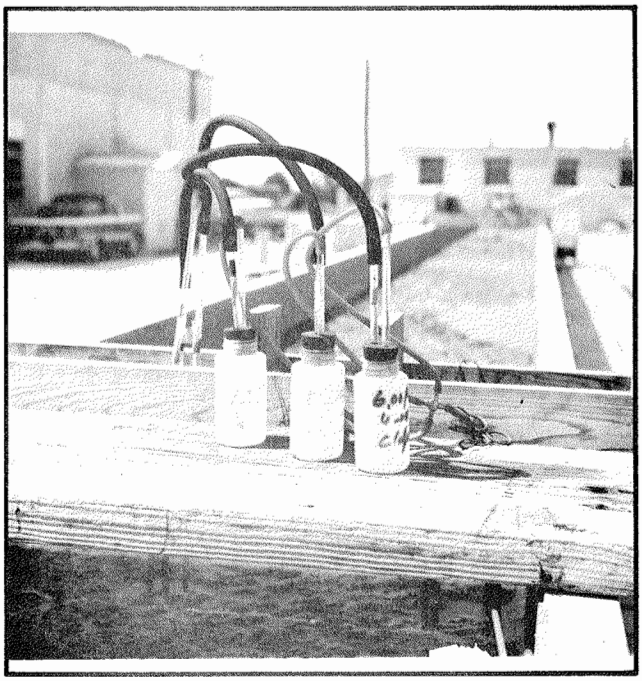

Water Samplers

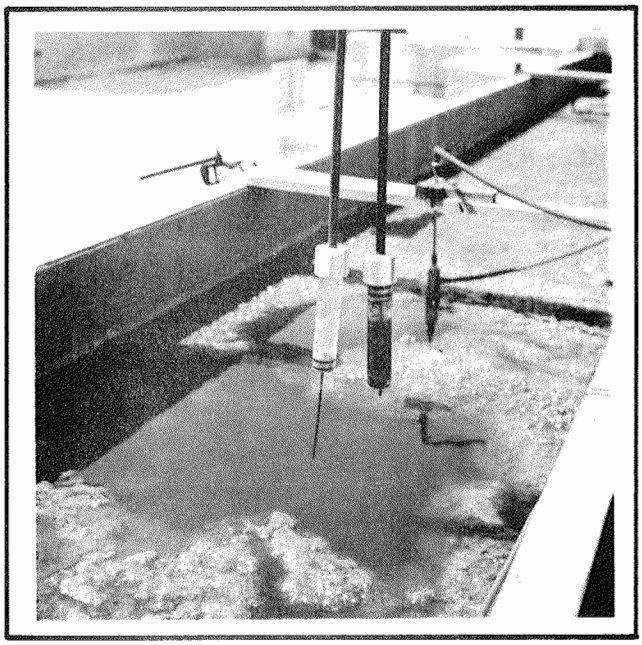

Sediment Samplers

FIG. 5-3. SAMPLERS

crystal in a shielded cabinet was used. The size of the cavity in the shield was 24 x 24 x 27 inches. The cabinet walls, top, and floor consisted of four inches of lead that were interlined with 0.75 inch magnesite, 0.063 inch copper, and 0.125 inch aluminum plates. All data were counted with the same geometrical conditions.

In order to minimize the "drift" of the gamma spectrometer, a calibration test with ^{137}Cs standard was made during each counting period. The selected energy span was 1.0 Mev for the 256-channel group size. ^{137}Cs peak of 0.66 was adjusted to channel 169.

The counting efficiencies for ^{85}Sr, ^{51}Cr, and ^{137}Cs were 17.8, 3.0, and 11.64 percent. Calibration was accomplished by counting ^{85}Sr and ^{51}Cr and ^{137}Cs standards with known concentration of the radionuclides. The contribution coefficients used are cited in Table 5-3. All the data were corrected for counting efficiency, background, absorption, decay, and contribution from other radionuclides. Self-absorption coefficients for ^{85}Sr are given in Fig. 3-4.

Dispersion Studies

The experimental procedures, tracing device, and the data analyses of the dye studies are discussed in this section. The dispersion mechanism, along with convection, is an important factor in radionuclide transport. It has been recognized

Table 5-3. Contribution Coefficients

Contributing Isotopes	Influenced Isotopes		
	^{51}Cr	^{85}Sr	^{137}Cs
^{51}Cr	1.0	0.0	0.0
^{85}Sr	0.1376	1.0	0.0
^{137}Cs	0.168	0.0676	1.0

that the mixing phenomena involved in the transport of radionuclides in a stream system is initiated by the hydrodynamic process (33). Though the dispersion coefficient could be computed by using one of the analytical equations, dye studies are probably more reliable and accurate for this small-scale model river. Various flow conditions have been investigated due to the fact that the dispersion coefficient is a function of the discharge and the shear stress of the fluids. In this dual-channel model river, the cross section through the entire length and the flow rate for each experimental period was kept constant. Therefore, the correlation between the average velocity in the channel and the dispersion coefficient was emphasized.

Experiments: All releases were instantaneous and rapid mixing occurred in both lateral and vertical directions. Rhodamine BMG manufactured by Du Pont was selected as the tracer. A Turner fluorometer was used with a special set of

filters (#110-832 as primary, #110-833 as secondary). These filters partially correct for the interference from the micro-algal suspensions.

The calibration for the fluorometer is shown in Fig. 5-4. The linearity of Rhodamine B with the fluorometer readings was established, especially in the lower range of the Rhodamine B concentrations.

Three dye experiments were made at different velocities; namely, 5.03×10^{-2}, 2.82×10^{-2}, 1.02×10^{-2} ft./sec. The first dye study was made to evaluate the duality of the dual-channel flume. These data are shown in Fig. 5-5. An average velocity was maintained at 5.03×10^{-2} ft./sec with a discharge at 150 liters/min. About 1000 mgs of Rhodamine B were released in each channel. The second and third dye experiments were made with an average velocity of 2.82×10^{-2} ft./sec and 1.02×10^{-2} ft./sec, respectively. About 800 mgs of Rhodamine B were released for these two experiments. The average time-concentration relationships are shown in Figs. 5-6 and 5-7.

Analyses: The Fortran program DISPRSN, as presented in Appendix I, was designed to analyze the data. Based on Eqs. 5-3 and 5-4, it is possible to calculate readily the mean flow through time and the variance.

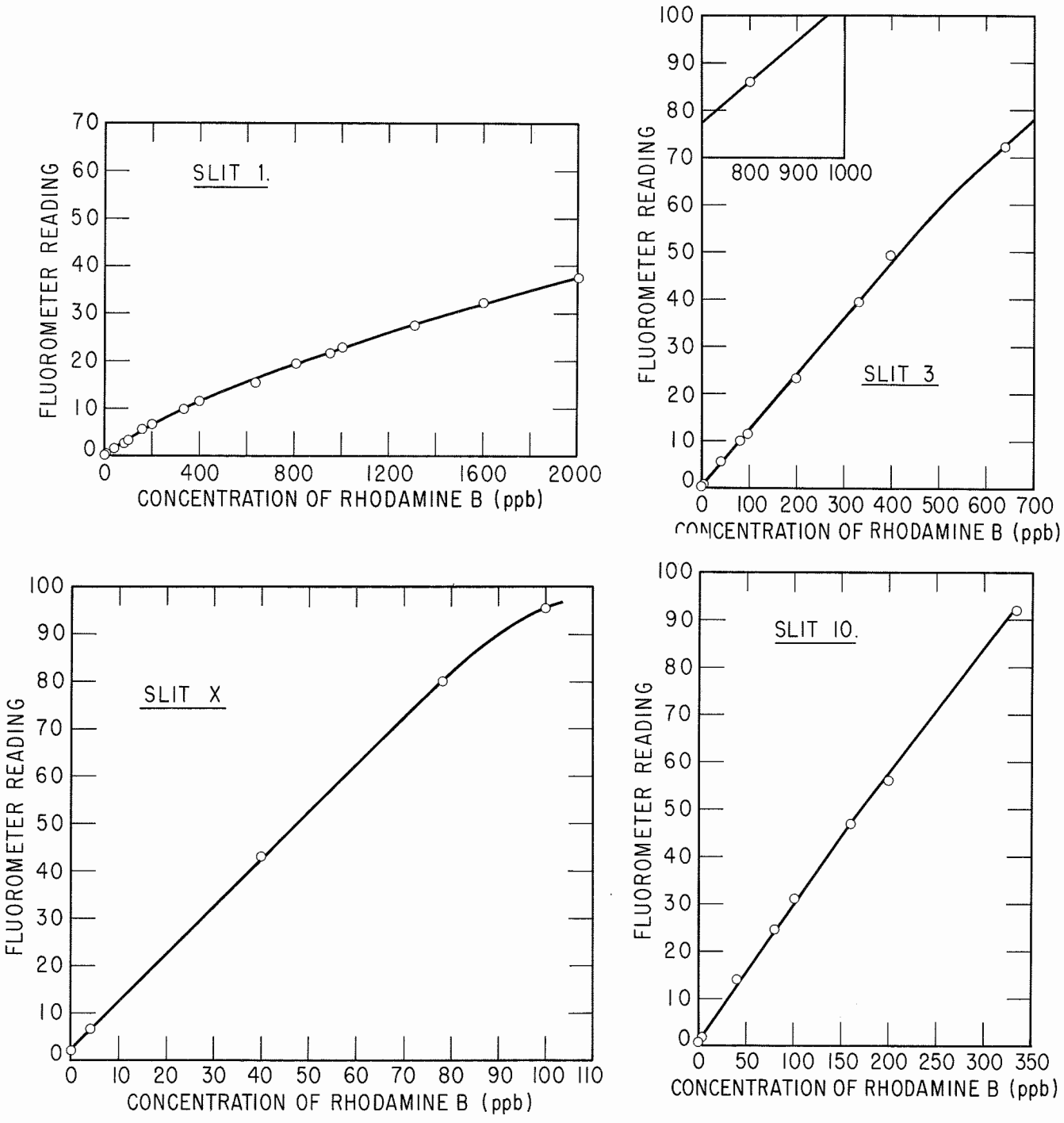

FIG. 5-4. CALIBRATION OF FLUOROMETER

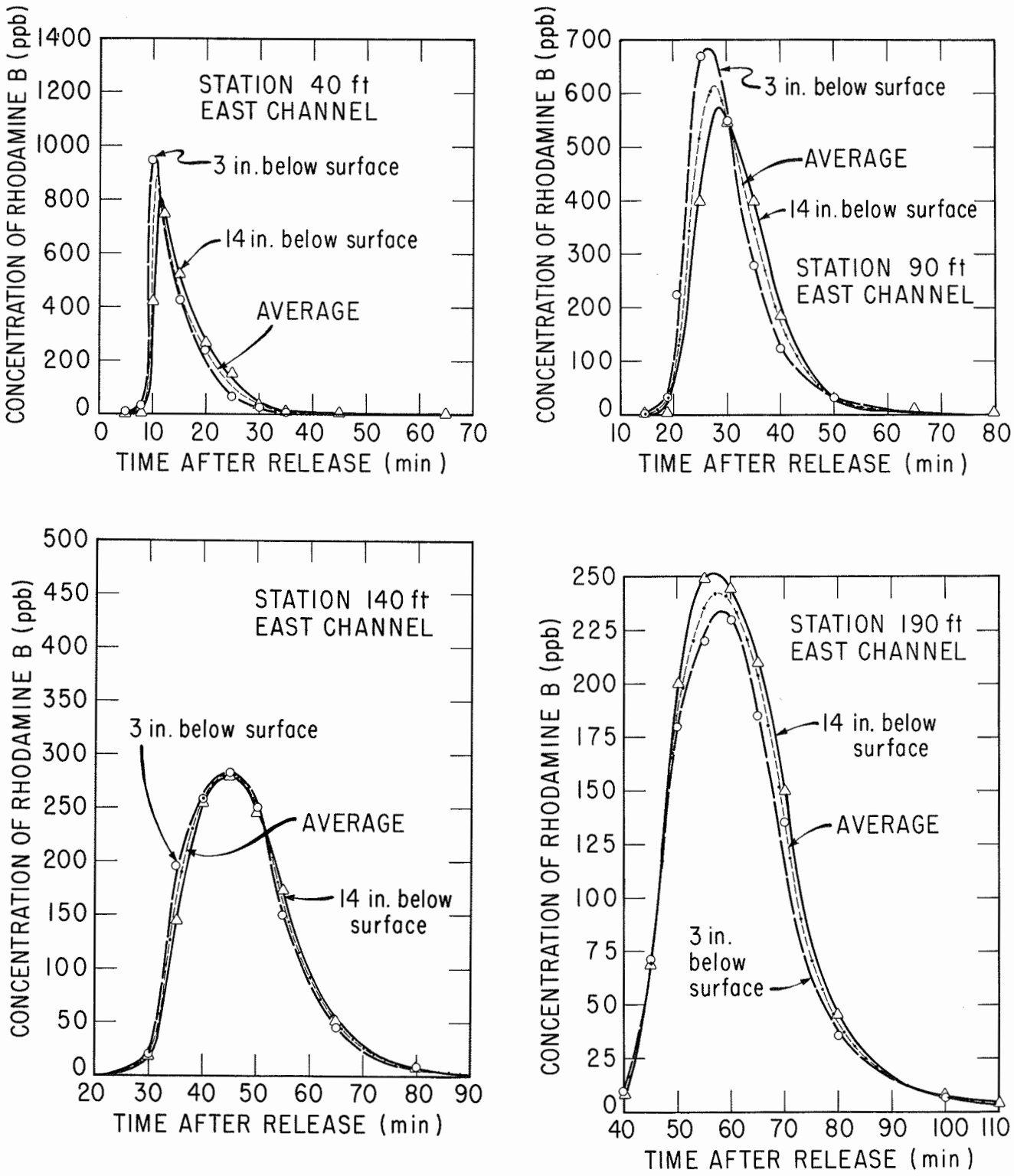

FIG. 5-5. LONGITUDINAL DISTRIBUTION OF RHODAMINE B IN EAST CHANNEL OF DYE STUDY I

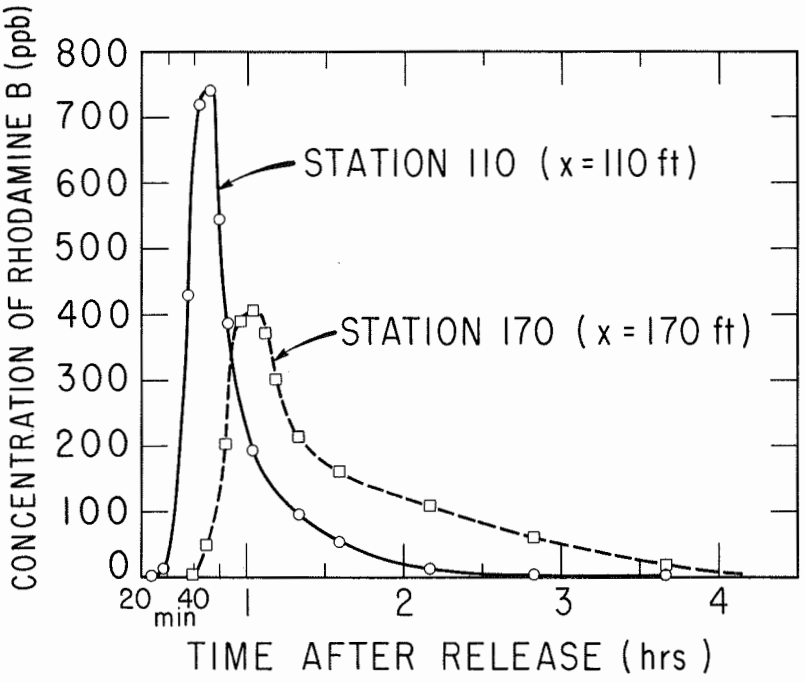

FIG. 5-6. LONGITUDINAL DISTRIBUTION OF RHODAMINE B FROM DYE STUDY II

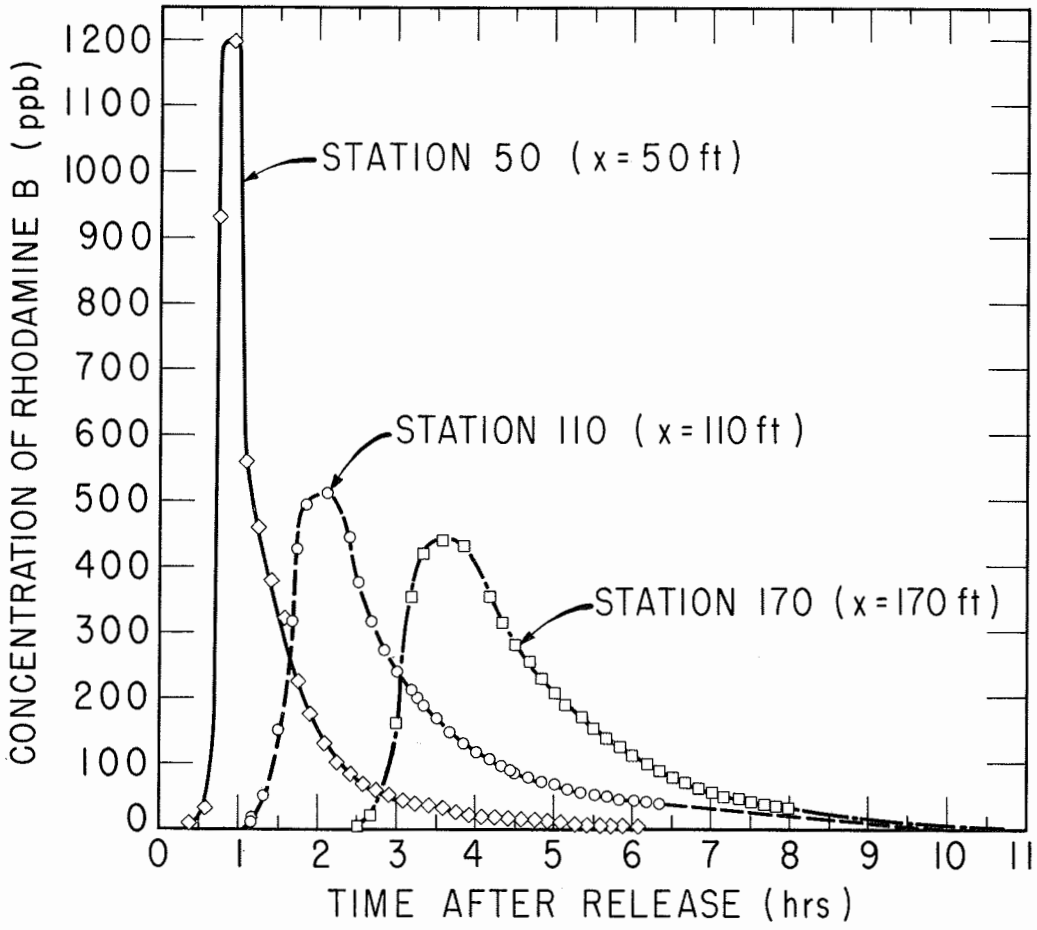

FIG. 5-7. LONGITUDINAL DISTRIBUTION OF RHODAMINE B FROM DYE STUDY III

$$\bar{t} = \frac{\sum_{i=1}^{n} C_i \, t_i}{\sum_{i=1}^{n} C_i} \qquad (5\text{-}4)$$

$$\sigma_t^2 = \frac{\sum_{i=1}^{n} (t_i - \bar{t})^2 \, C_i}{\sum_{i=1}^{n} C_i} \qquad (5\text{-}4)$$

Where

C_i = the average concentration for i^{th} small rectangular section under the time-concentration curve corresponding to the time t_i

$\bar{t}$ = mean flow through time

σ_t^2 = variance in time

For the convenience of the read-in process, the time t_i was transformed into the function of initial time, t_o, and the time increment, Δt, as expressed in Eqs. 5-5 through 5-7.

$$t_i = t_o + i\,\Delta t \qquad (5\text{-}5)$$

$$\bar{t} = \frac{\sum_{i=1}^{n} C_i (t_o + i\,\Delta t)}{\sum_{i=1}^{n} C_i} \qquad (5\text{-}6)$$

and

$$t^2 = \frac{\sum_{i=1}^{n} (t_o - \bar{t} + i\,\Delta t)^2}{\sum_{i=1}^{n} C_i} \qquad (5\text{-}7)$$

Then, by Eq. 2-12 and $\sigma_x^2 = U^2 \sigma_t^2$, the dispersion coefficient, D_x, can be calculated by Eq. 5-8.

$$D_x = \frac{1}{2} U^2 \frac{\sigma_{t_1}^2 - \sigma_{t_2}^2}{t_1 - t_2} \qquad (5\text{-}8)$$

Where

$U = \frac{Q}{A}$

$\sigma_{t_j}^2$ = the variance in time unit of the time-concentration relationship with mean flow through time $\bar{t}_j$

The arguments used in the program DISPRSN were as follows:

TIME (I) - time value corresponding to each concentration value (In Eq. 5-3 this term was designated by t_i.)

CONC (I) - value designated by C_i in Eq. 5-3

DISPR (J)- D_x computed from j_{th} measurement of a dye study

VARNS (J)- σ_t^2 in Eq. 5-4

VARNX (J)- σ_x^2 in Eq. 5-8

TMEAN (J)- $\bar{t}$ in Eq. 5-3

UNITM (J)- $\int_0^\infty C dt$ in Eq. 2-10

TMASS (J)- $\int_0^\infty tC dt$ in Eq. 2-10

X (J) - distance between the sampling point and the release point

Results: The dispersion coefficients, D_x, for different velocities were calculated using data generated by these dye experiments and data from the literature (4, 40, 53).

The mean flow through time, T, the longitudinal variance in length, σ_x^2, and the longitudinal dispersion coefficients, D_x, are cited in Table 5-4. The relationship between mean velocities and calculated dispersion coefficients are given in Fig. 5-8. It may be noted that the dispersion coefficients increase with increasing velocities.

The biota in a channel may cause increased dispersion coefficients because of the increased intensity of turbulence and decreased scale of turbulence. This might explain why Rowe's data (40) provided a larger dispersion coefficient. His experiment was conducted when the amount of biomass in the model river was about ten times that used in tests reported herein.

Continuous Release of ^{85}Sr

Continuous release of ^{85}Sr was made to evaluate the river system under conditions approaching equilibrium. Two experiments were conducted for two different discharges in the channel. In the first experiment, two initial concentrations of ^{85}Sr were introduced. The west and east side, respectively, of the dual-channel system received 0.0523 MPC (117 dpm/ml) and 0.0265 MPC (60 dpm/ml). The time period and flow conditions were the same, i. e., Q = 15 liters/min/channel, and $\bar{V}$ = 0.512 ft./min. In the second experiment, ^{85}Sr was released only in the west channel of the research

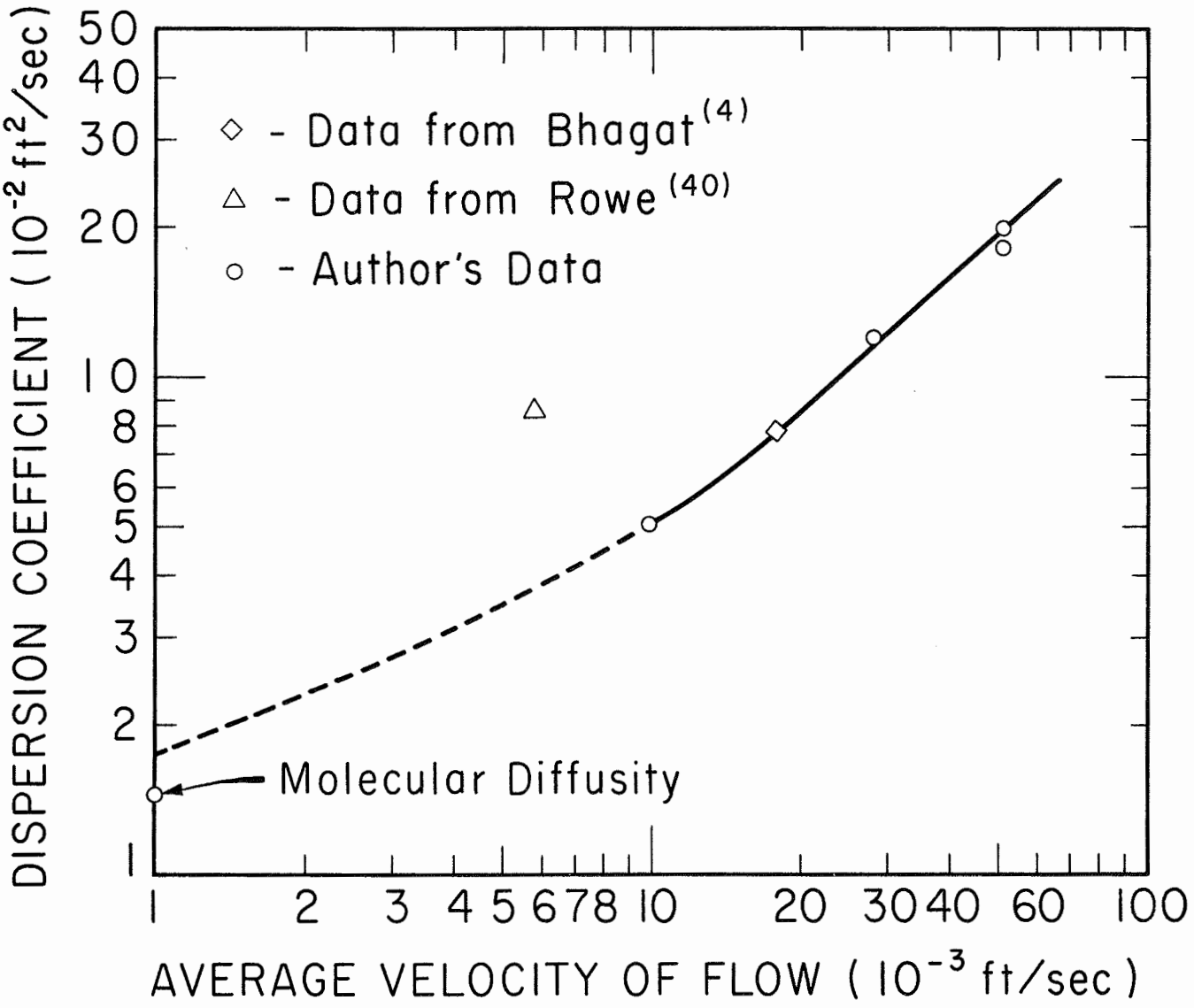

FIG. 5-8. CORRELATION OF DISPERSION COEFFICIENT WITH VELOCITY IN MODEL RIVER

Table 5-4. Dispersion Coefficient [a]

	$\bar{U}$ (ft/sec)	x (ft)	T (min)	σ_x^2 (ft^2)	D_x (ft^2/sec)
*	0.0057	100	350	886.8	0.0860
*	0.0057	200	820	5743.4	
**	0.018	95	90	467.2	0.077
**	0.018	145	141	704.0	
	0.0505	90.0	29.5	417.6	0.18
	0.0505	140.0	47.6	832.5	0.20
	0.0505	190.0	62.4	1106.4	
	0.028	110.0	68.0	1661.1	0.12
	0.028	170.0	126.7	2623.8	
	0.0098	110.0	189.9	2813.8	0.0505
	0.0098	170.0	286.4	3399.7	

(a) Note:

T = mean flow through time

D_x = longitudinal dispersion coefficient

σ_x^2 = longitudinal variance in length

$\bar{U}$ = average velocity of flow in channel

x = distance from release point

(b) * data from the dye studies of Rowe, et al

** data from the dye studies of Bhagat

flume. The initial concentration of ^{85}Sr was 0.052 MPC and the discharge was 50 liters/min. The Vallisneria was trimmed before the start of the second experiment to remove an aquatic side effect. However, a continuous release of ^{85}Sr in the aquaria has been made at first for the designing information of the experiments described above.

Aquaria Study: Two aquaria, unit Nos. 5 and 6, were used for the preliminary studies of continuous release of ^{85}Sr in the model river. Exposed to the outdoor environment, both aquaria were allowed to develop ecological stability before beginning the study. The flow rate was approximately 50 ml/min and the mean flow through time was computed to be about 12 hours. A stirrer was used to maintain complete mixing and in this respect, the aquaria could be considered as a cell in the model river. The time-concentration relationships and ^{85}Sr uptake are shown in Fig. 5-9.

It was noted that the equilibrium was attained sooner in the water than in either the sediment or the Vallisneria. Based on the results shown in Fig. 5-9, the total release period in the model river was determined to be eight mean flow through times.

^{85}Sr in Water: The concentration of ^{85}Sr in the aqueous phase increased with time very rapidly before the steady state concentration was reached. More frequent sampling was undertaken during the early stages of the tests. The

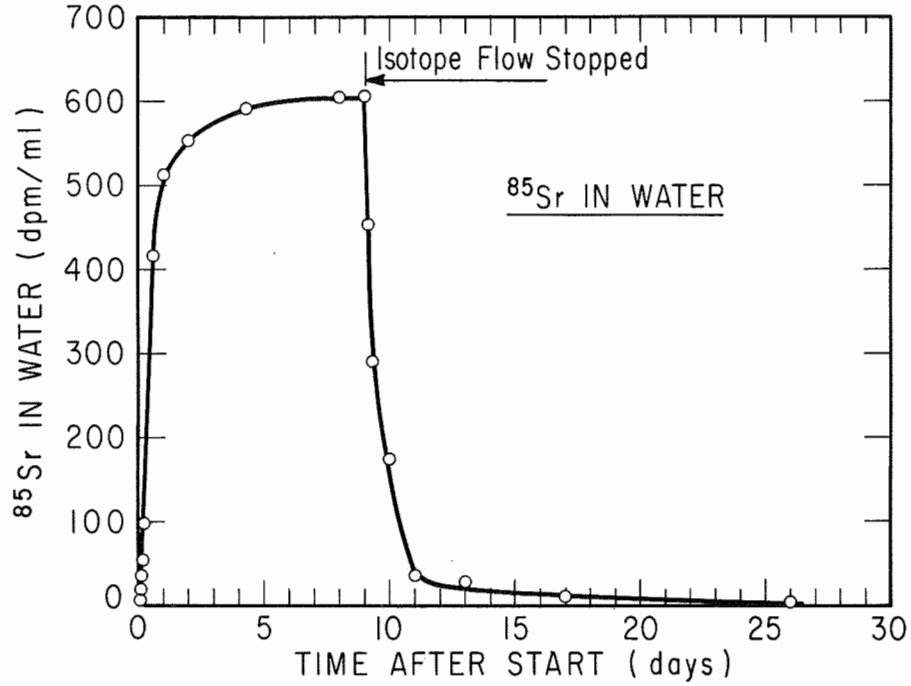

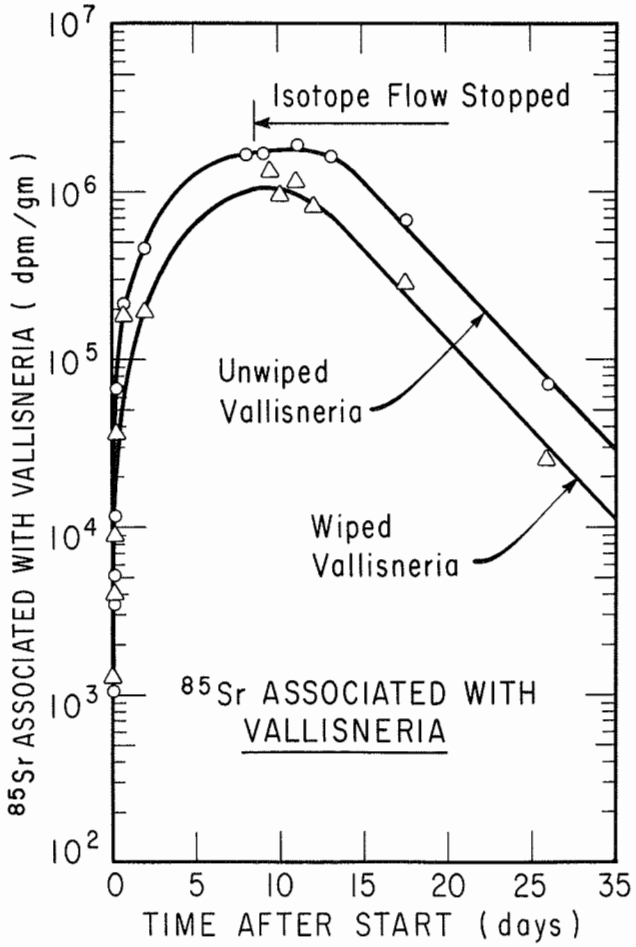

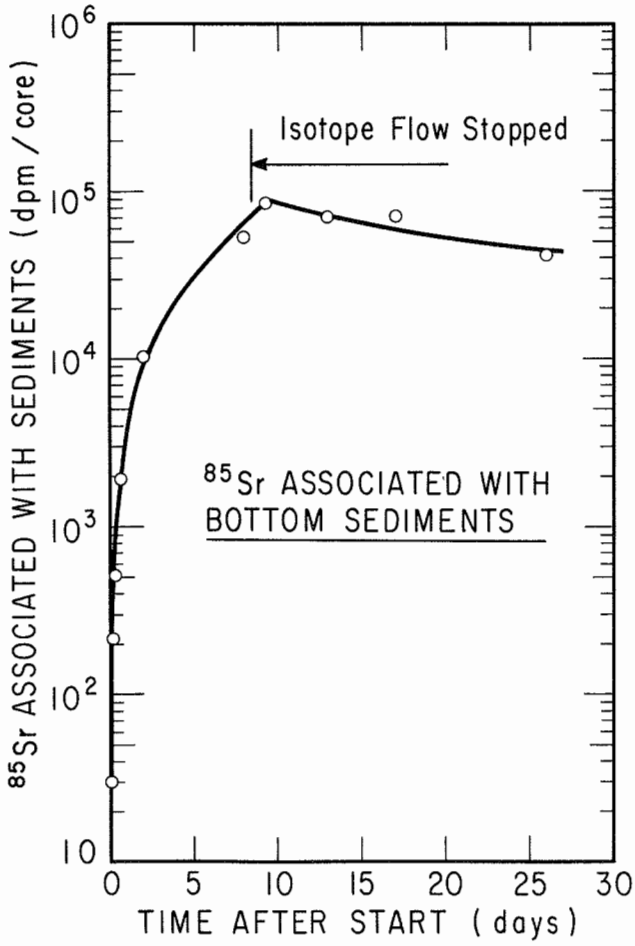

FIG. 5-9. TIME-CONCENTRATION RELATIONSHIP OF ^{85}Sr IN FLOWING AQUATIC UNIT

variation of ^{85}Sr in water is shown in Figs. 5-10 and 5-11. To establish equilibrium it was necessary to release ^{85}Sr continuously for more than four mean flow-through times. The steady state concentration of ^{85}Sr for all sampling stations was found to be a constant value of about 110 dpm/ml (west channel) and about 55 dpm/ml (east channel). These concentrations were slightly less than the initial concentrations. Therefore, there was uptake of ^{85}Sr by sediments and Vallisneria. The delayed ^{85}Sr was shown in Fig. 5-12. It was believed that the delayed ^{85}Sr was originally retained in sediments and Vallisneria through uptake.

Notably, complete mixing was not achieved within the first 20 ft. during the first four hours of continuous release, Fig. 5-10. In addition, it may be noticed that the delayed ^{85}Sr concentrations in all samples from downstream stations were higher than those from upstream stations. This indicates that both sediments and Vallisneria tended to release ^{85}Sr to the water after the influx was stopped.

The variation in ^{85}Sr concentration for higher velocities was similar to that for lower velocities. In the second experiment, the average velocity was about 1.71 ft./min, which provided transition flow. The flow was about 50 liters/min. As shown in Fig. 5-13, the steady state concentration of ^{85}Sr in water was about 118, 110, and 106 dpm/ml, respectively, for stations 10, 30, and 70 feet from the release point, while

the initial concentration was calculated to be about 120 dpm/ml. The difference between the initial concentration and the steady state concentration in the water is assumed to be due to the uptake by sediments and Vallisneria.

^{85}Sr in Sediments: The uptake of ^{85}Sr by bottom sediments was dependent on turbulence and contact time. In other words, ^{85}Sr uptake by sediments might be the result of the diffusion into sediments through the interstitial water and the subsequent sorption of radionuclides by sediment particles. Diffusion is recognized to be a function of turbulence, whereas sorption is dependent on contact time.

The total ^{85}Sr in each sediment was used as a basis for the ^{85}Sr associated with sediments. The variations of ^{85}Sr in sediments for the first and second experiments are presented in Figs. 5-14 and 5-15, respectively. It appears that ^{85}Sr in sediments varied with the ^{85}Sr concentration in water.

The mass transfer coefficient for ^{85}Sr in sediments was defined by the non-equilibrium differential equation, Eq. 5-8.

$$\frac{aD}{\forall_s} \frac{\partial M_s}{\partial t} = K_1 \frac{A_s}{\forall_s} (M_o - M) = \frac{K_1}{D} (M_o - M) \qquad (5\text{-}8)$$

Where

M_s = total mass of radionuclides transferred into the sediments in unit compartment of channel

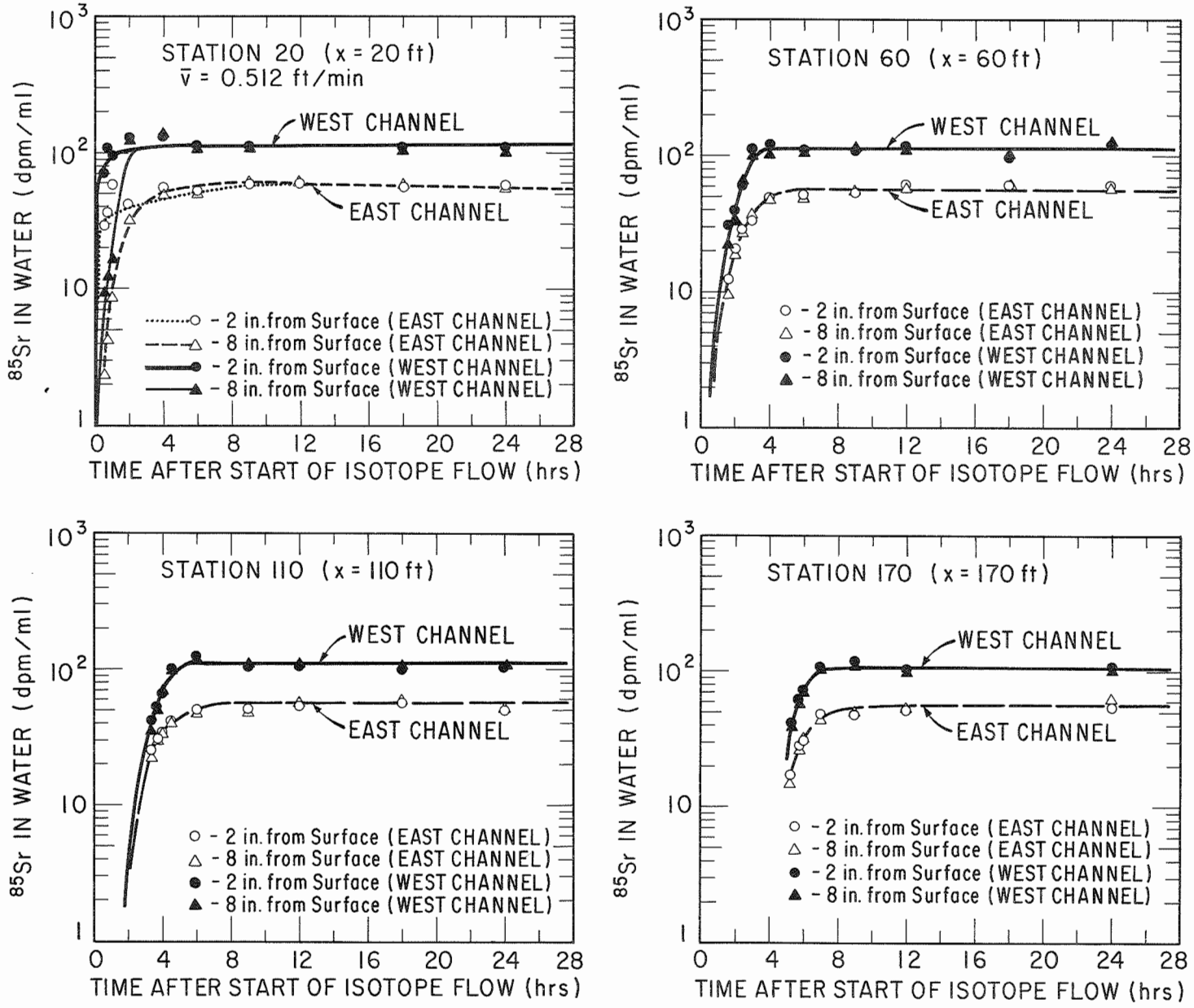

FIG. 5-10. ACCUMULATION OF ^{85}Sr IN WATER

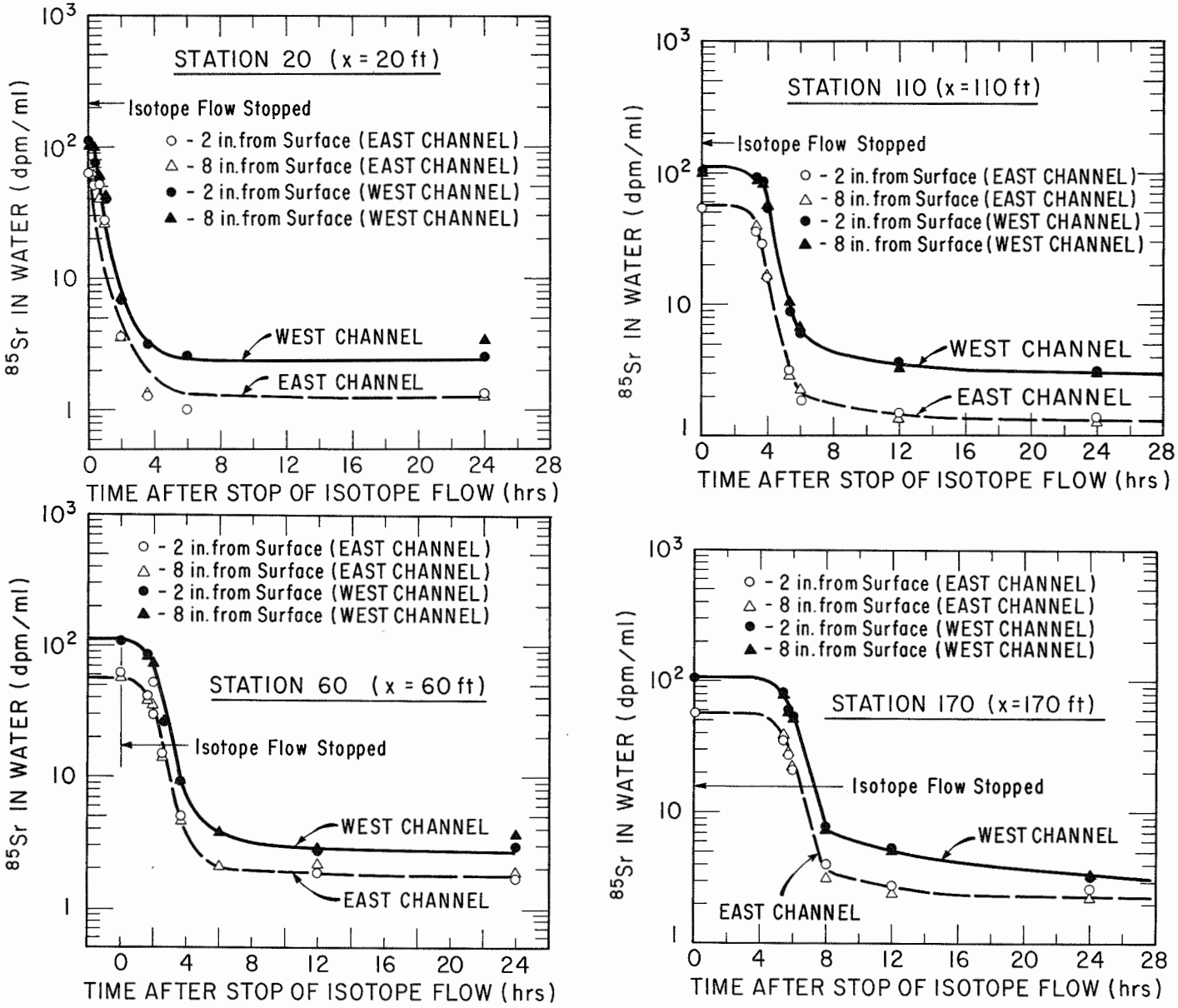

FIG. 5-11. DILUTION OF ^{85}Sr IN WATER

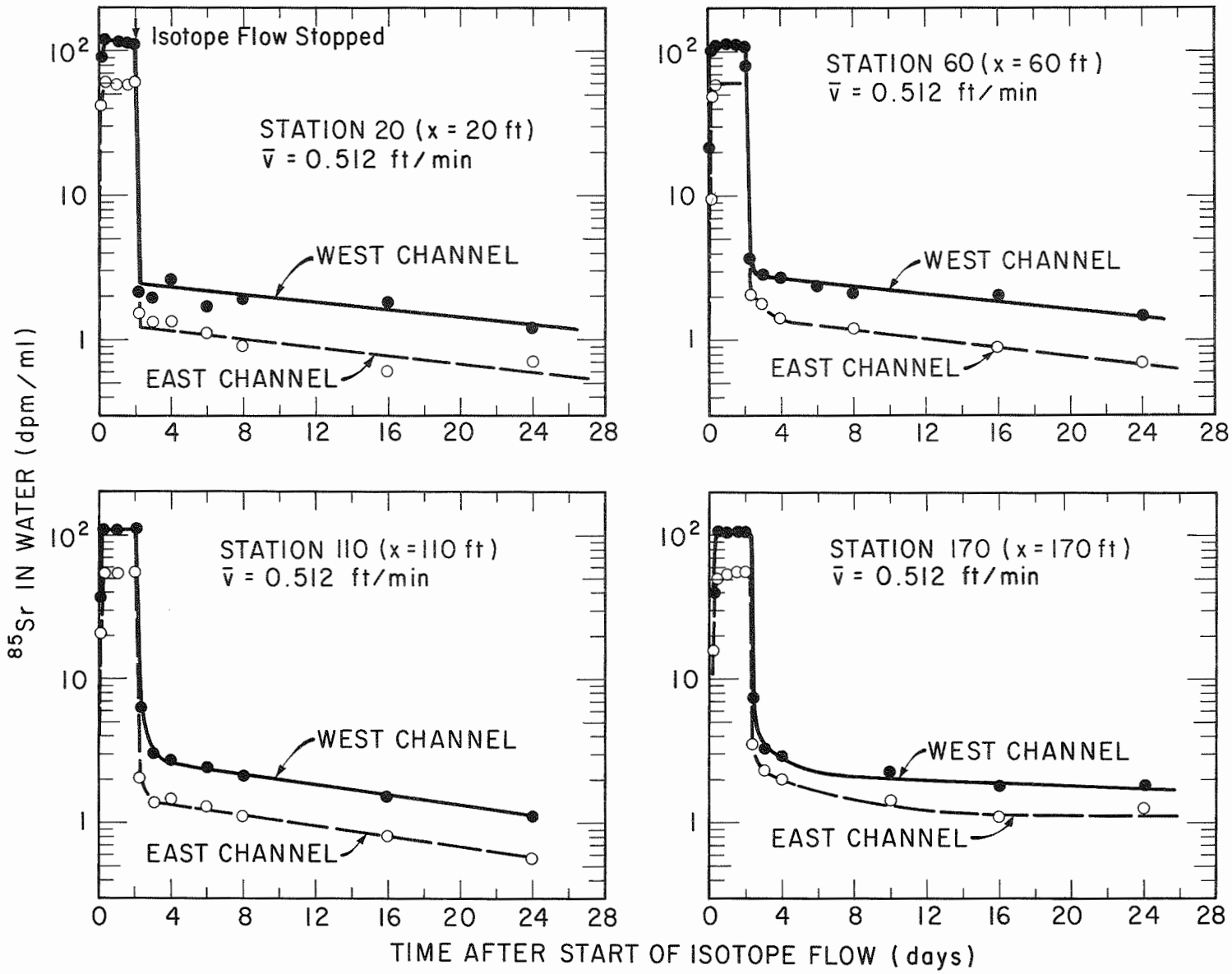

FIG. 5-12. LONGITUDINAL DISTRIBUTION OF ^{85}Sr IN LAMINAR FLOW

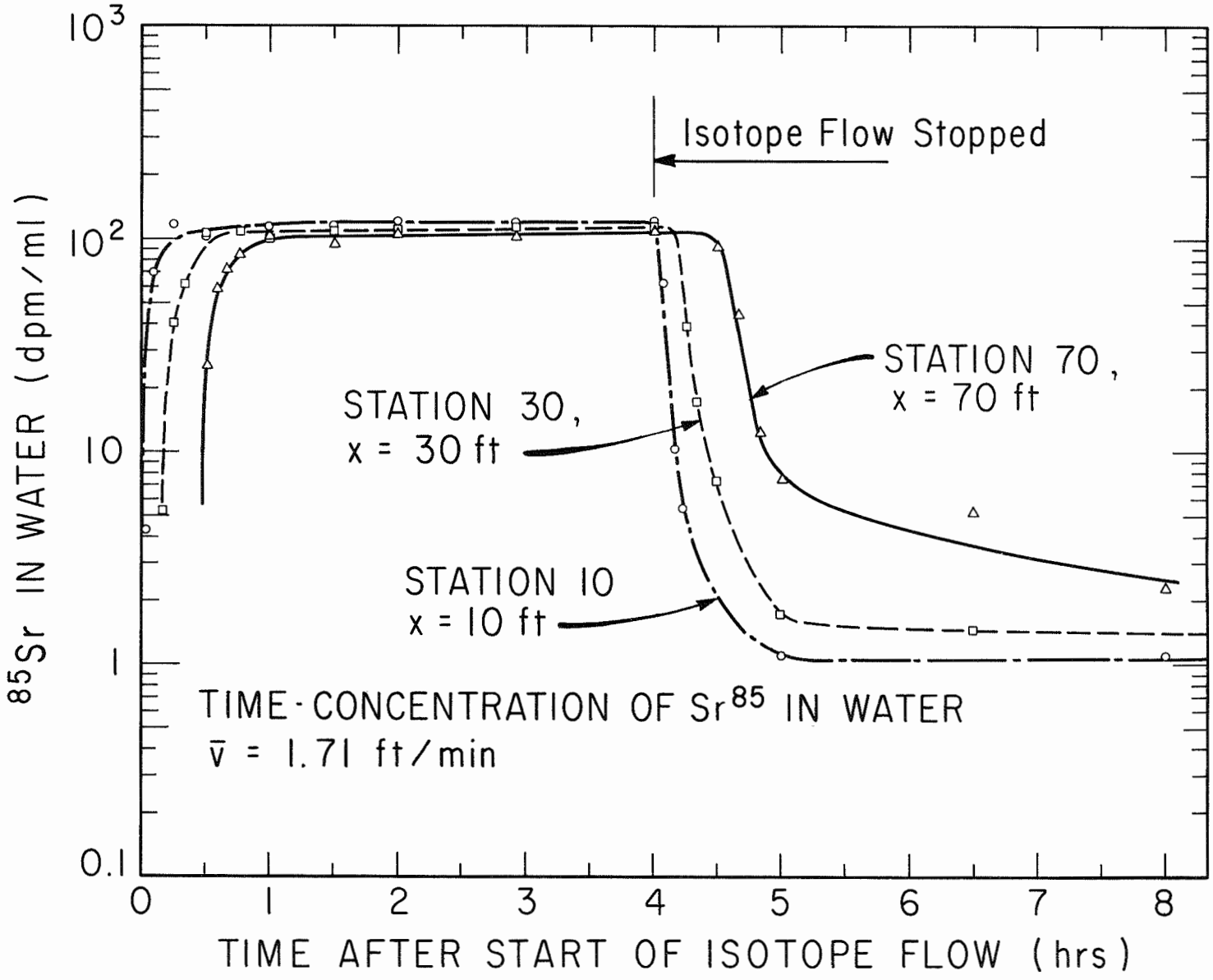

FIG. 5-13. LONGITUDINAL DISTRIBUTION OF ^{85}Sr IN TRANSITION FLOW

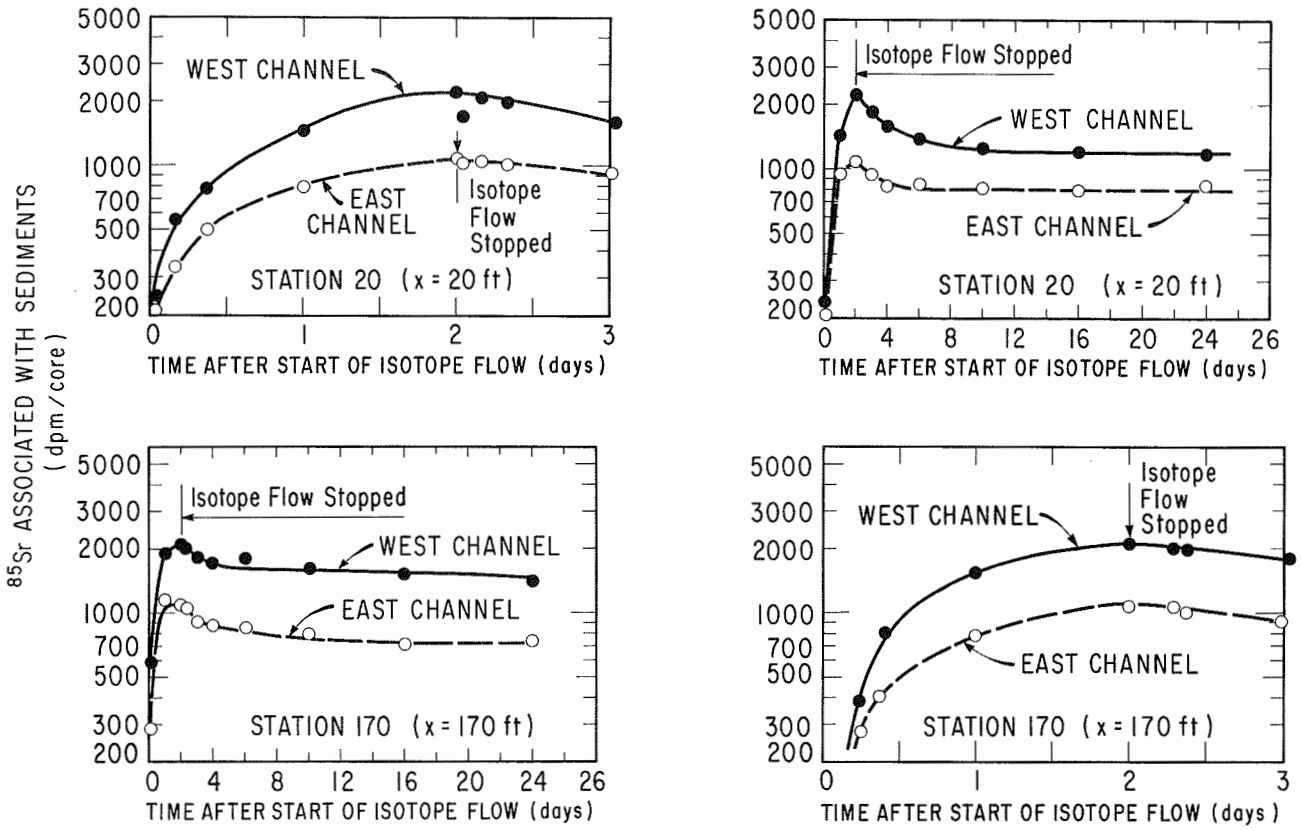

FIG. 5-14. ^{85}Sr UPTAKE BY BOTTOM SEDIMENTS IN LAMINAR FLOW

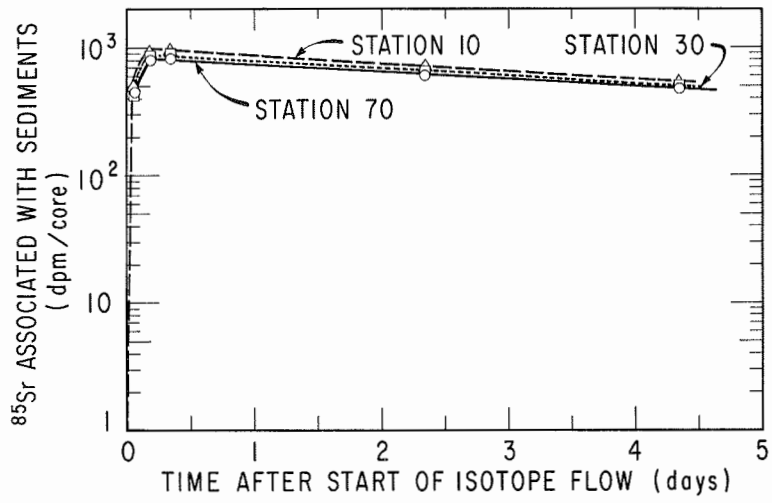

FIG. 5-15. ^{85}Sr UPTAKE BY BOTTOM SEDIMENTS IN TRANSITION FLOW

M = total radionuclides in a sediment core

a = cross-section of sample core, 0.6 $in.^2$

t = time of reaction

$\forall_s$ = volume of sediments in each unit compartment

A_s = surface area of each unit compartment

D = depth of sediments in the channel

M_o = saturation value for M

K_1 = mass transfer coefficient

From aquaria study, $M_o = K_s C_w$ (5-9)

Where

K_s = the equilibrium distribution coefficient of radionuclides in bottom sediments

C_w = concentration of radionuclides in water; constant value for continuous release

By definition

$$M = \frac{M_s}{\forall_s} aD \quad ; \quad \text{and let } k_1 = \frac{K_1}{D} \tag{5-10}$$

thus

$$\frac{\partial M}{\partial t} = k_1 (K_s C_w - M) \quad ; \quad M=0 \text{ if } t=0$$

Then

$$M = K_s C_w (1-e^{-k_1 t}) \tag{5-11}$$

and

$$k_1 = -\frac{1}{t} \ln \frac{K_s C_w - M}{K_s C_w} \tag{5-12}$$

Based on the average water temperature, 25°C, the equilibrium distribution coefficient, K_s, was estimated to be 140 (dpm/core/cpm/ml). The k_1 value is represented by the slope of the plot of $\ln \frac{140\ C_w - M}{140\ C_w}$ versus time, t. The k_1 values for ^{85}Sr uptake by sediments were found to be 0.0045 hr^{-1} and 0.011 hr^{-1} for the velocity of 0.512 ft./min and 1.71 ft./min. The k_1 values for ^{85}Sr release from sediments were 0.04 day^{-1} and 0.020 day^{-1}, Figs. 5-16 and 5-17. Thus, different mass transfer coefficients for uptake and release were obtained. This was probably due to the fact that part of ^{85}Sr in sediments was bonded chemically with sediment particles.

Penetration of ^{85}Sr in Sediments: The penetration of ^{85}Sr into the bottom sediments of the model river was studied in the first experiment, and the results are reported in Fig. 5-18. The penetration coefficients are cited in Table 5-5. Notably, the vertical distribution of ^{85}Sr in sediments decreased exponentially with depth only in case of continuous uptake.

Table 5-5. Penetration Coefficients in the First Continuous Release Experiment

Time After Release	Penetration Coefficient Distance from the Release Point (20 ft.)	(170 ft.)
4 hrs	0.345	0.384
2 days	0.280	0.317

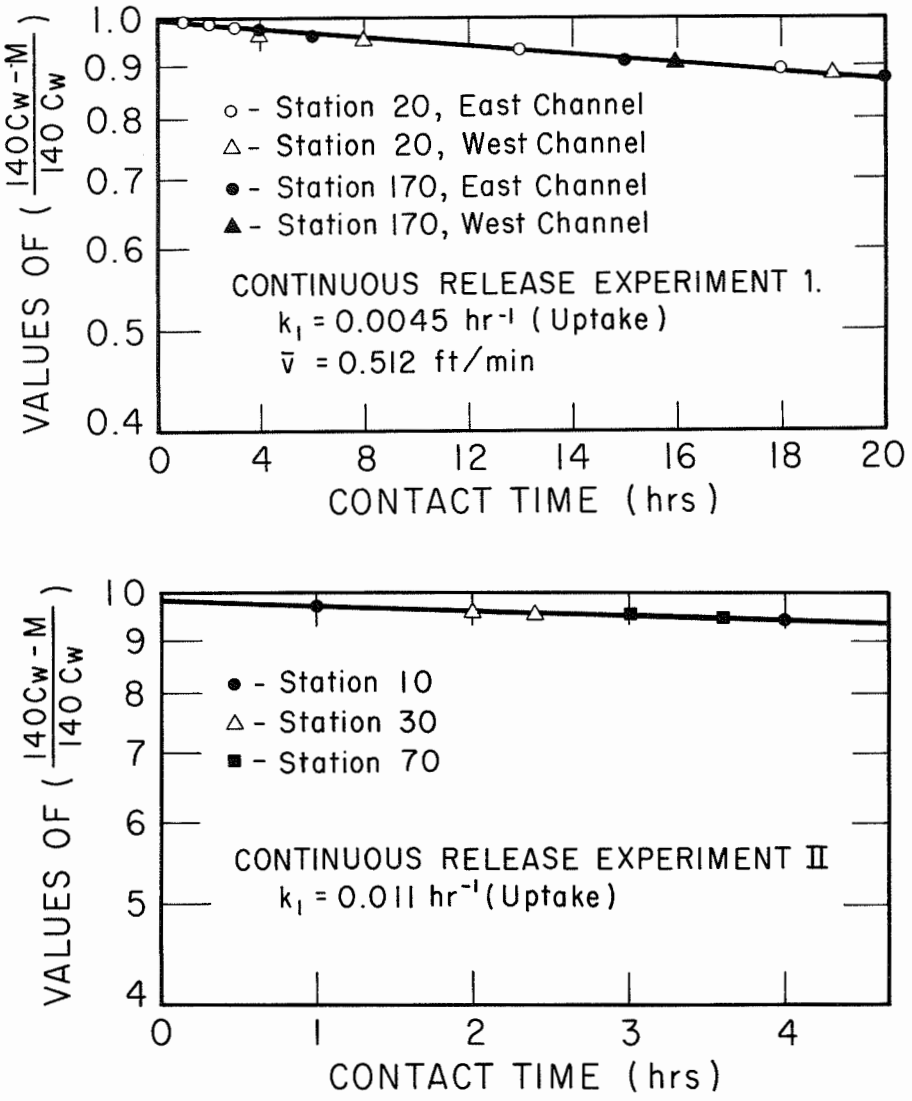

FIG. 5-16. MASS TRANSFER COEFFICIENT FOR ^{85}Sr UPTAKE BY SEDIMENTS

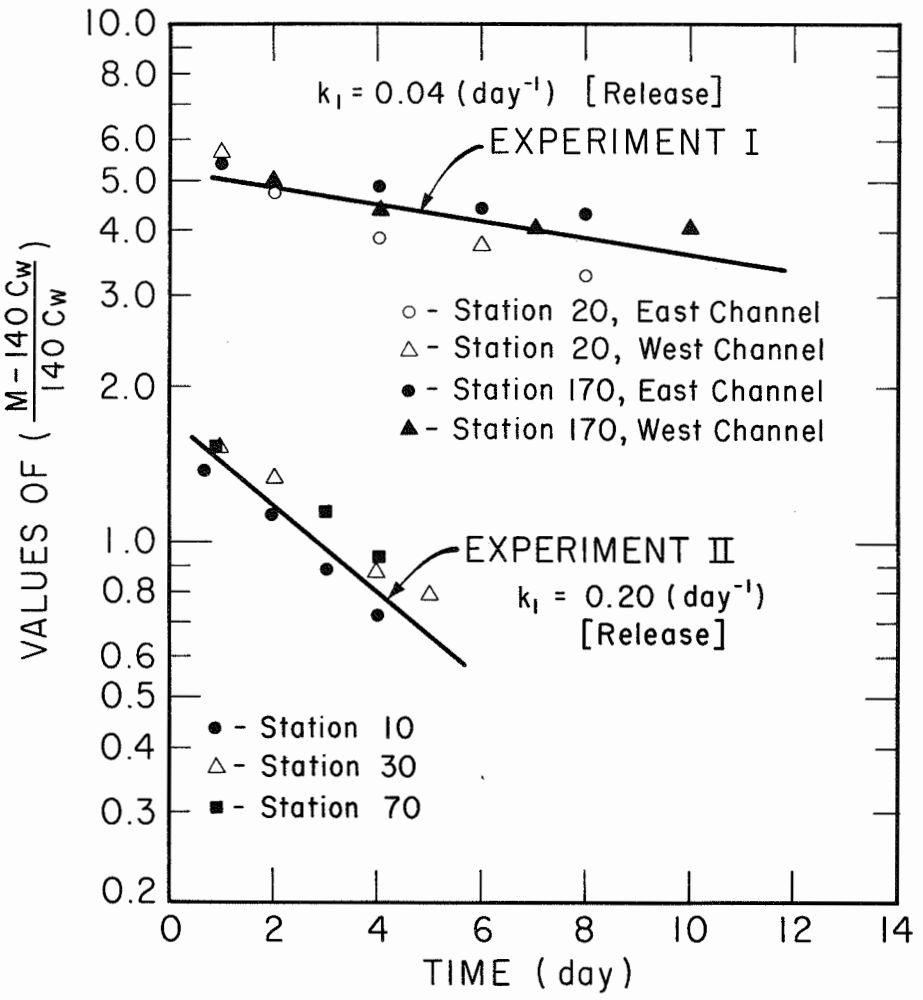

FIG. 5-17. MASS TRANSFER COEFFICIENT FOR ^{85}Sr RELEASE FROM SEDIMENTS

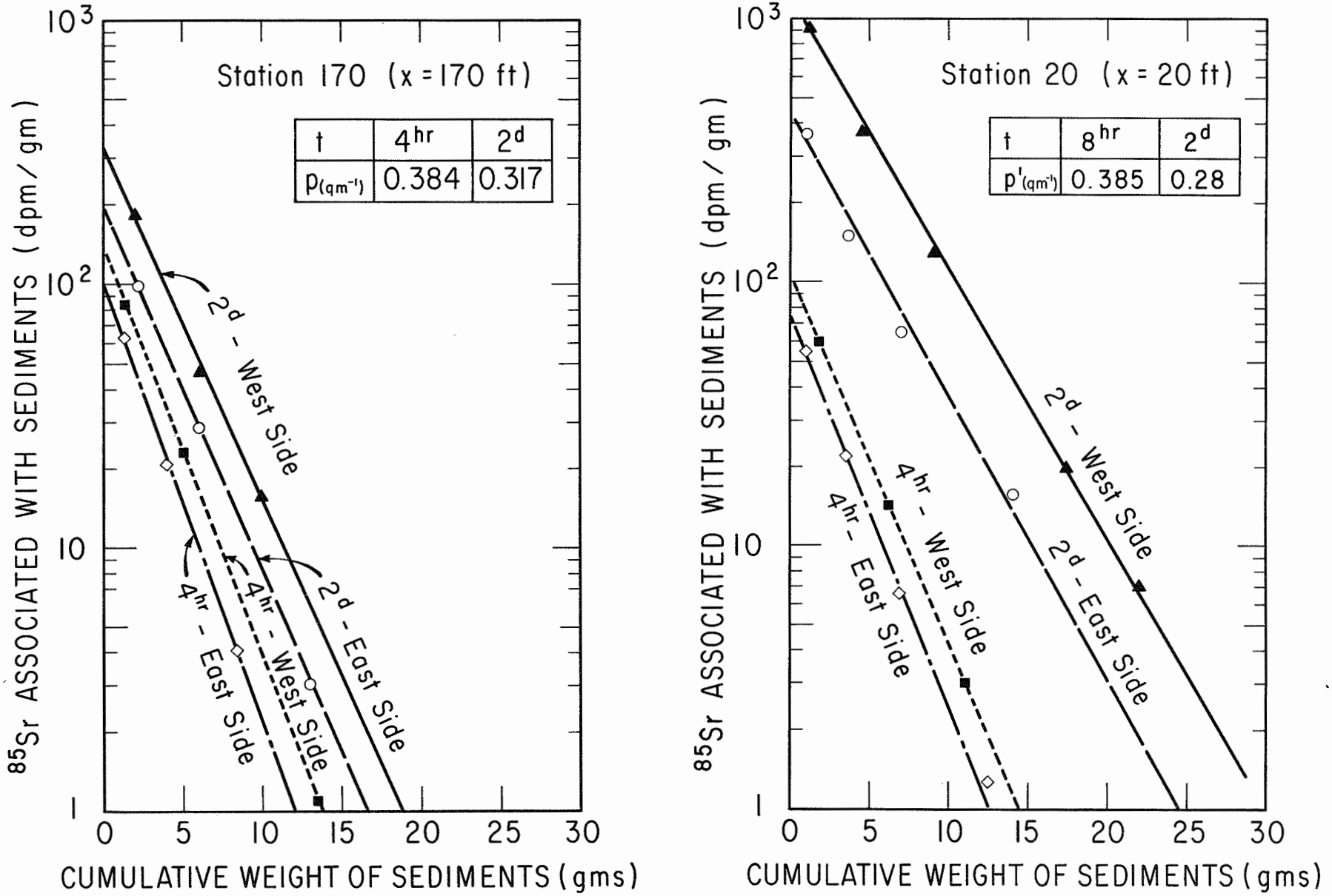

FIG. 5-18. PENETRATION OF ^{85}Sr INTO THE SEDIMENTS

^{85}Sr on Vallisneria: Variations of ^{85}Sr associated with Vallisneria are presented in Fig. 5-19. It was found that the ^{85}Sr on Vallisneria was very sensitive to changes of ^{85}Sr concentration in water. The equilibrium concentration of ^{85}Sr on Vallisneria was attained very rapidly, but after ^{85}Sr isotope flow was stopped, the ^{85}Sr on Vallisneria dropped to a minimum value abruptly. The concentration factor, K_p, of ^{85}Sr by Vallisneria was calculated to be about 720 dpm/gm/dpm/ml. The minimum ^{85}Sr on Vallisneria was found to be about 50,000 dpm/gm of dry weight. Since the biomass was maintained to be only 2.2 gms/sq. ft., the total ^{85}Sr associated with Vallisneria in the model river was negligible.

Immediate Concentration Factor: Immediate ^{85}Sr uptake by either sediments or Vallisneria was qualified by the immediate concentration factor. The immediate uptake concentration factors were 2.25 dpm/core/cpm/ml and 90 dpm/gm/dpm/ml, respectively, for sediments and Vallisneria, Fig. 5-20.

Instantaneous Release of ^{85}Sr

To test the applicability of the mathematical model developed in Chapter 6, dual-experiments with instantaneous release of ^{85}Sr were conducted in the model river. A solution containing 0.504 mc of $^{85}Sr\ Cl_2$ was injected in each channel at a point 20 ft. from the inlet of the research flume. A total of five sampling stations, one upstream and four downstream from the release point, were used. At each of the

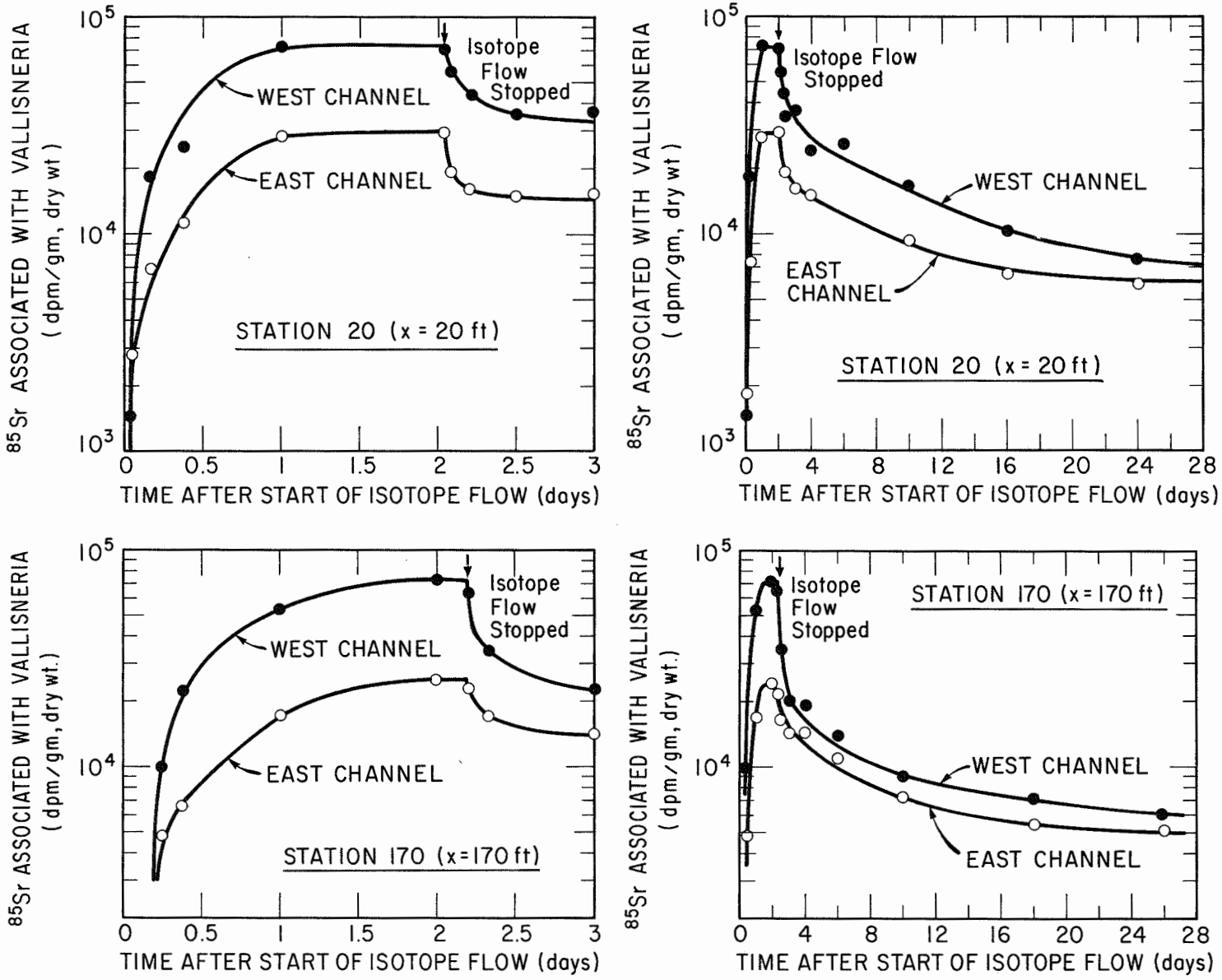

FIG. 5-19. ^{85}Sr ASSOCIATED WITH VALLISNERIA IN THE FIRST CONTINUOUS RELEASE EXPERIMENT

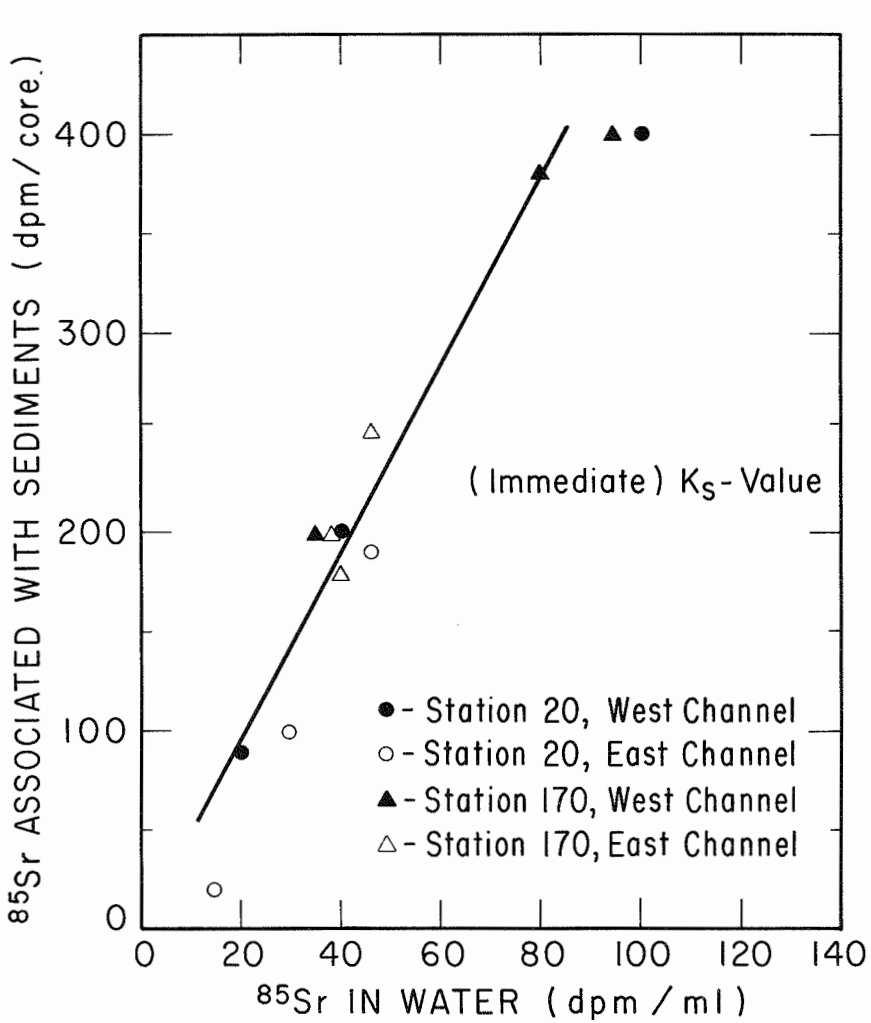

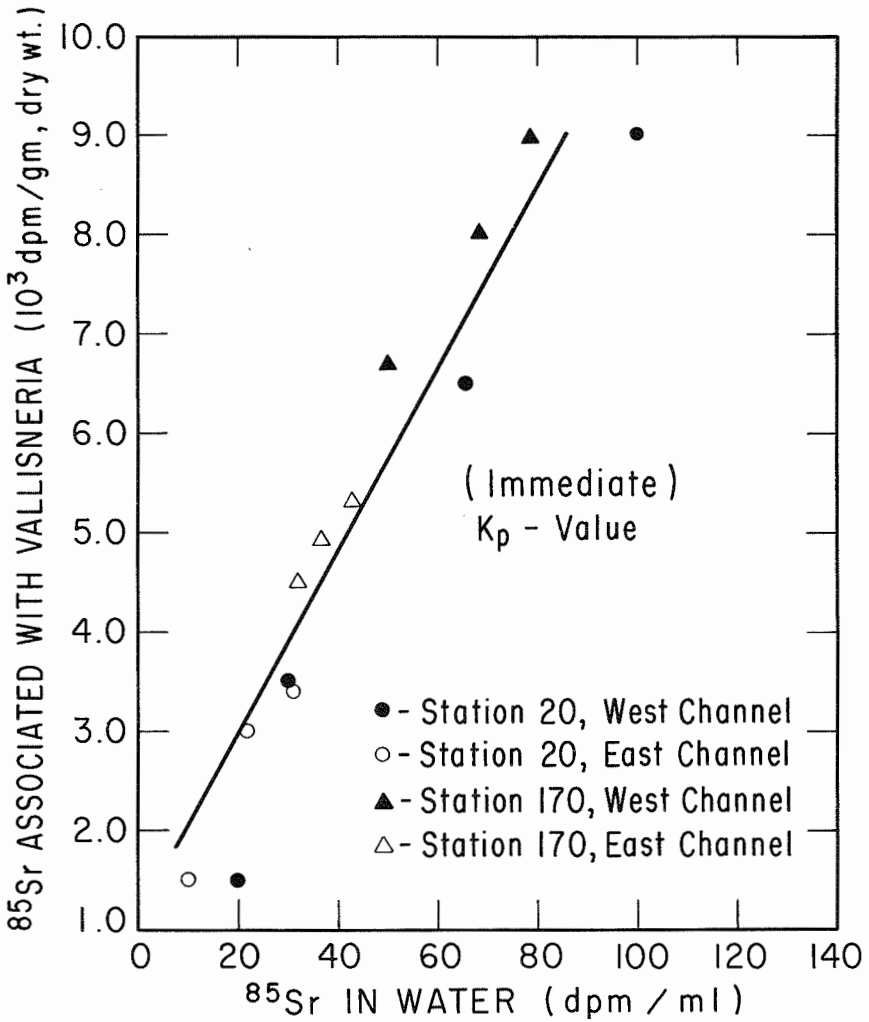

FIG. 5-20. IMMEDIATE UPTAKE OF ^{85}Sr BY SEDIMENTS AND VALLISNERIA

downstream sampling stations, 20, 50, 90, and 170 ft. from release point, samples for water, bottom sediments, and Vallisneria were collected. At the upstream station, 10 ft. from the release point, only selected water samples were monitored. The flow in each channel was adjusted to 50 liters/min. With a ~10 in. water depth throughout each channel, the average velocity over the cross section was about 1.71 ft./min.

A schedule with 5-10 minutes sampling interval was applied to each sampling point during the period when the plume of the radionuclides passed by. Total monitoring time for this experiment was 24 days. Since the same amount of ^{85}Sr was injected in each channel, this dual-experiment would be considered as a duplicated experiment.

^{85}Sr in Water: Time-concentration relationships of ^{85}Sr in water are presented in Figs. 5-21 and 5-22. Complete mixing through the entire depth was observed, especially at the stations located further downstream from the release point.

The retention of ^{85}Sr is exhibited in Figs. 5-23. Notably, ^{85}Sr concentration in the prolonged tail of the curve was about the same for both channels. This indicates that a similar aquatic environment had been established in the dual-channel system.

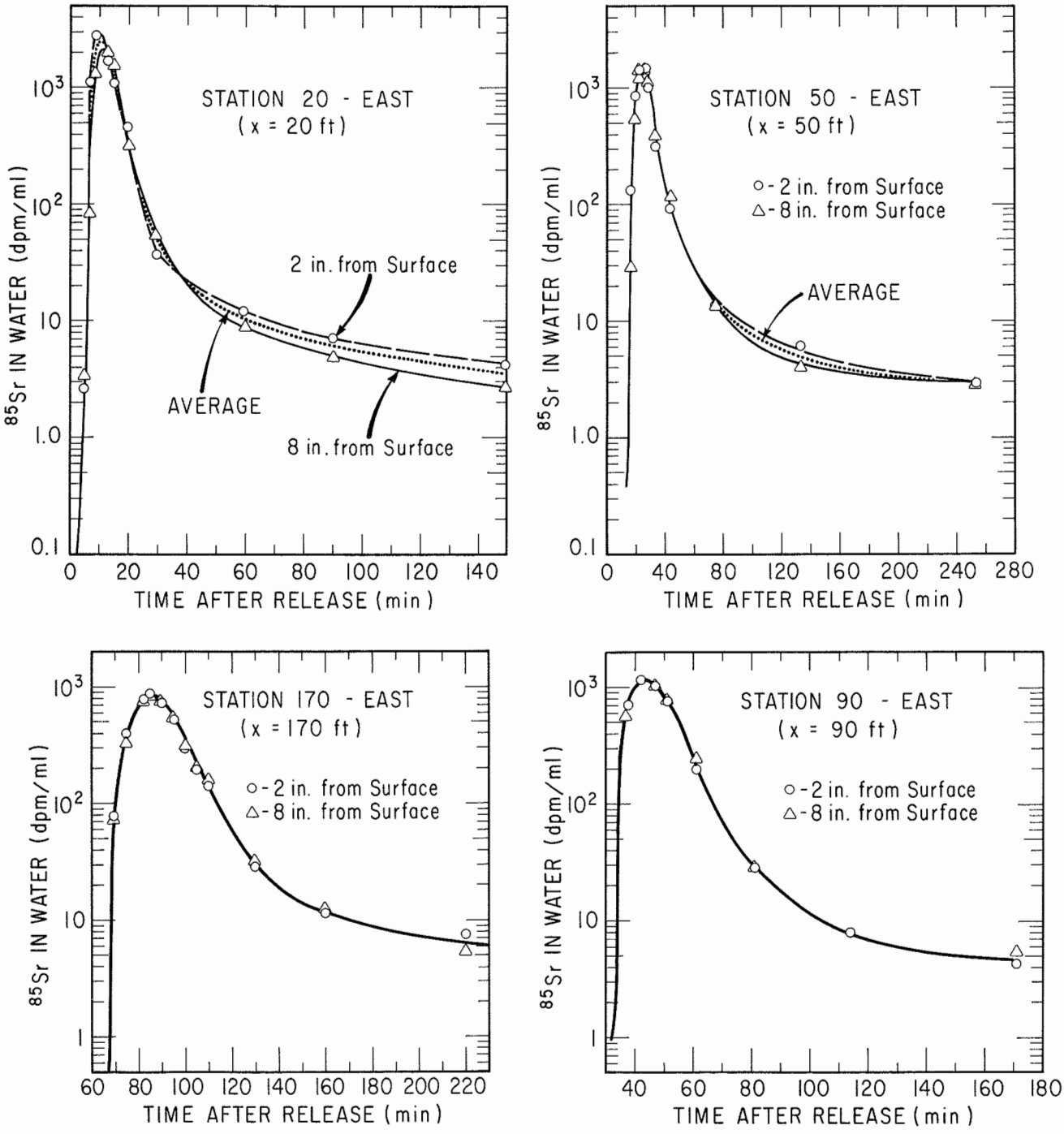

FIG. 5-21. TIME-CONCENTRATION OF ^{85}Sr IN EAST CHANNEL

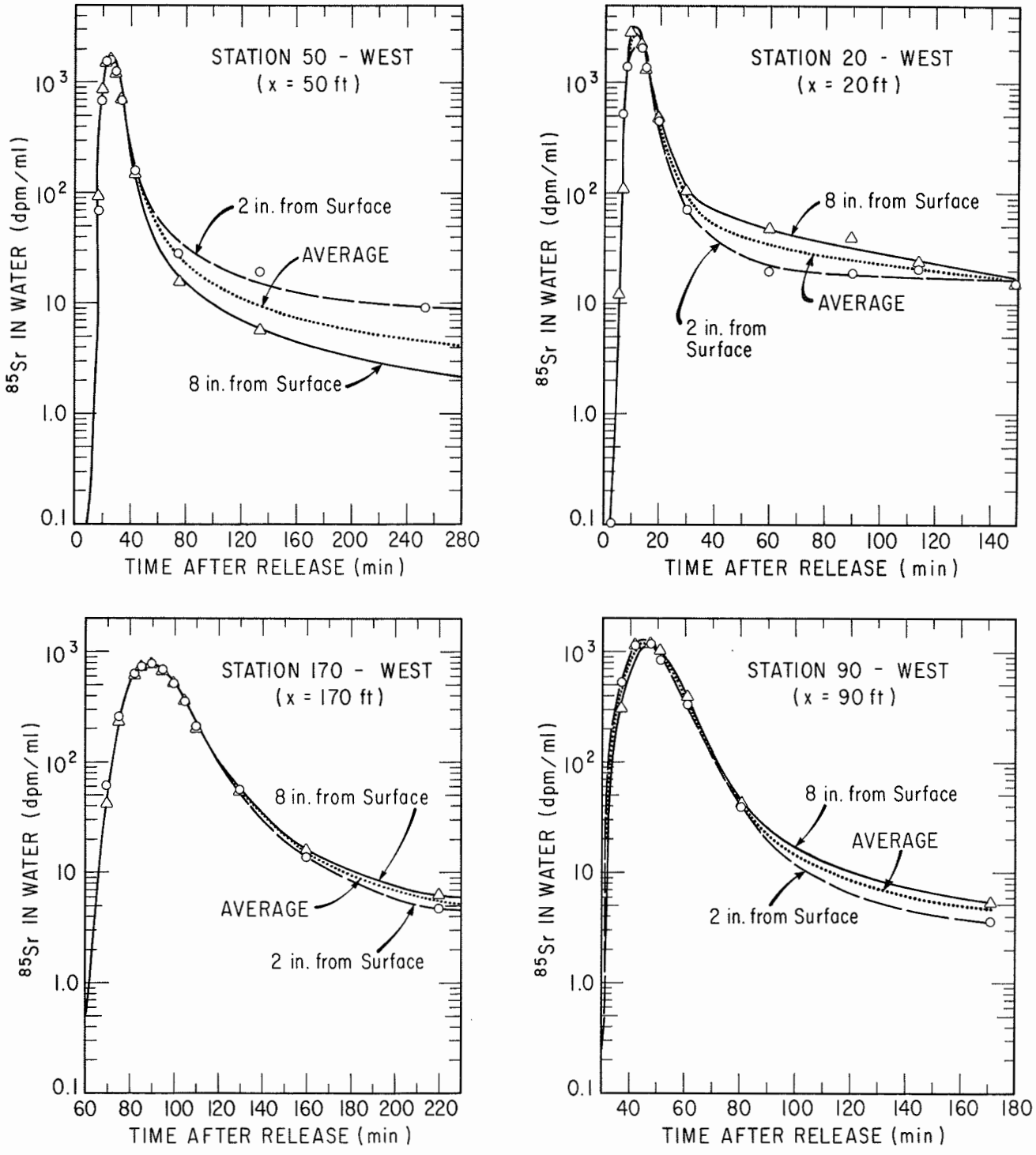

FIG. 5-22. TIME-CONCENTRATION OF ^{85}Sr IN WEST CHANNEL

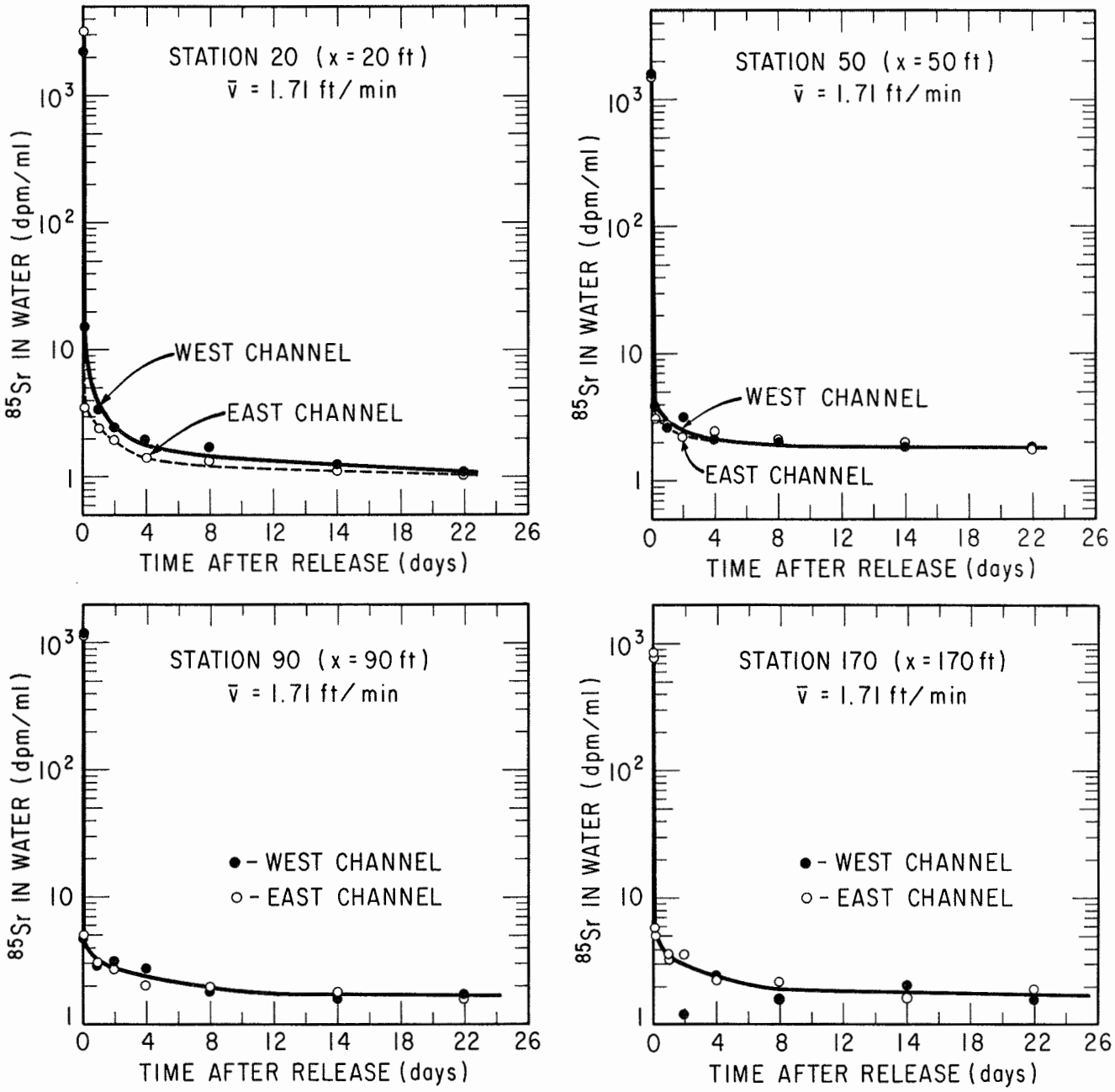

FIG. 5-23. DELAYED ^{85}Sr IN AQUEOUS PHASE

^{85}Sr in Sediments: The ^{85}Sr associated with bottom sediments was measured with regard to the longitudinal distribution, the retaining effect, and the immediate uptake. The time-concentration effect of ^{85}Sr in sediments followed the same variations as that in water. However, the release of ^{85}Sr from sediments was slow, Fig. 5-24.

In the long-term measurement of the ^{85}Sr in bottom sediments, it was observed that there was a certain amount of ^{85}Sr retained in the sediments over protracted periods. The retained ^{85}Sr in the sediments was about 230 dpm/core, Fig. 5-25. Based on the minimum ^{85}Sr in water, 1.7 dpm/ml, as shown in Fig. 5-23, the equilibrium distribution coefficient for ^{85}Sr in the sediments was calculated to be 136 dpm/core/cpm/ml. This value is approximately equal to that predicted on the basis of the stagnant aquaria study.

The immediate uptake of the ^{85}Sr by sediments was studied and correlated with the corresponding ^{85}Sr in aqueous phase, Fig. 5-28. The immediate concentration factor, K_{so}, was calculated to be 1.3 dpm/core/dpm/ml.

^{85}Sr on Vallisneria: The longitudinal variation of ^{85}Sr on Vallisneria and the retaining effects contributed from Vallisneria were studied. The time-concentration of ^{85}Sr on Vallisneria indicated that most of the ^{85}Sr was released back into the water immediately after the plume passed, Fig. 5-26. More than 90% of the ^{85}Sr initially

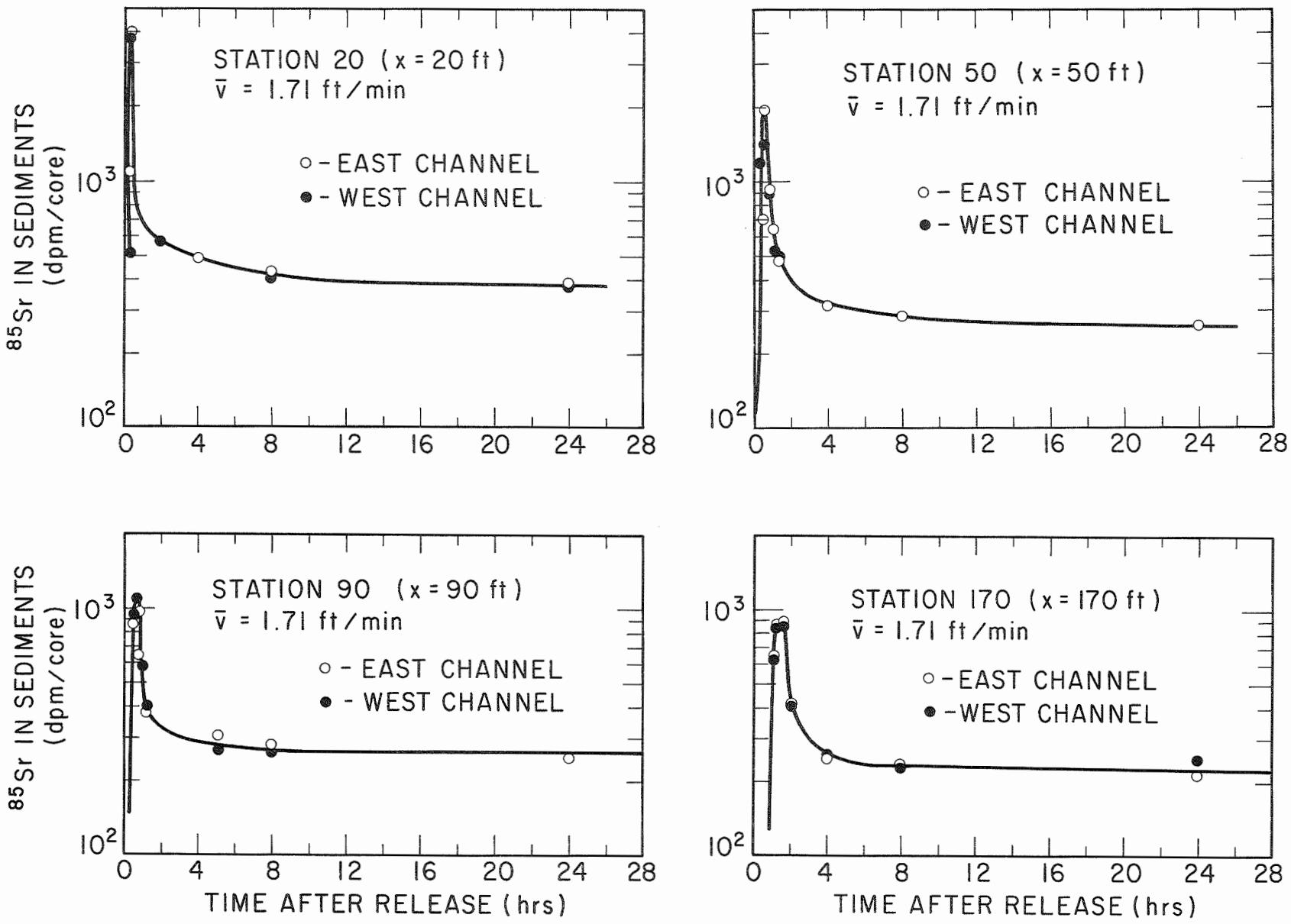

FIG. 5-24. TIME-CONCENTRATION OF ^{85}Sr ASSOCIATED WITH SEDIMENTS

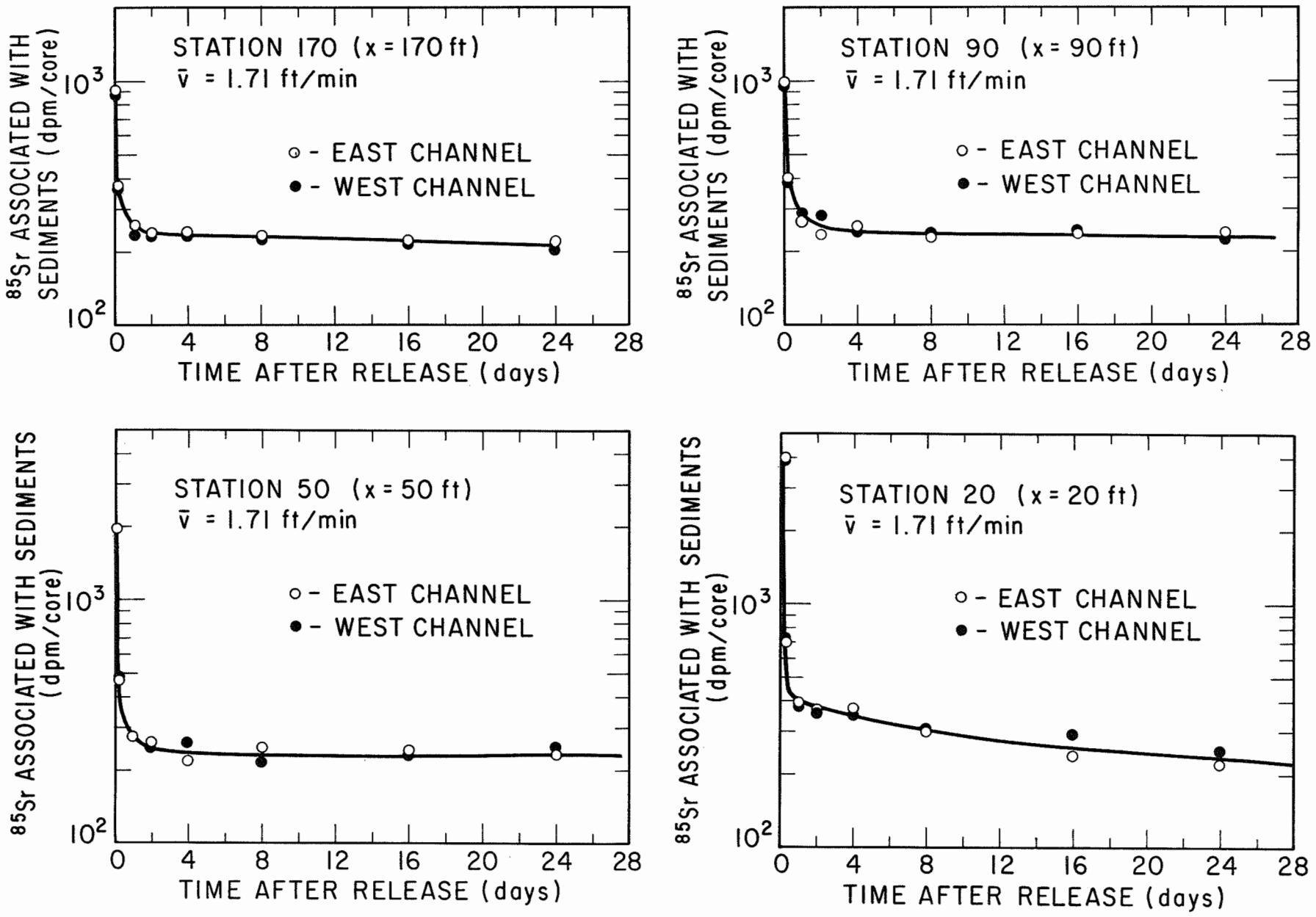

FIG. 5-25. DELAYED ^{85}Sr IN THE BOTTOM SEDIMENTS

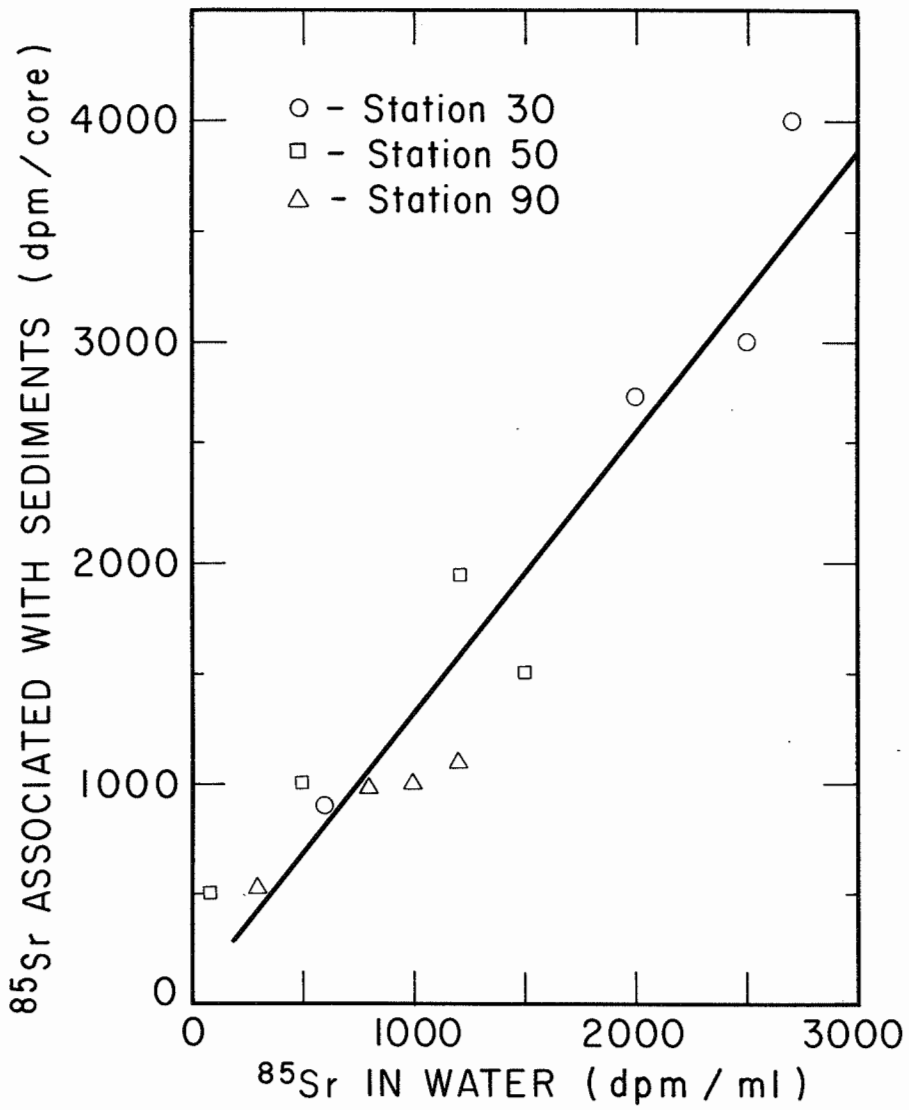

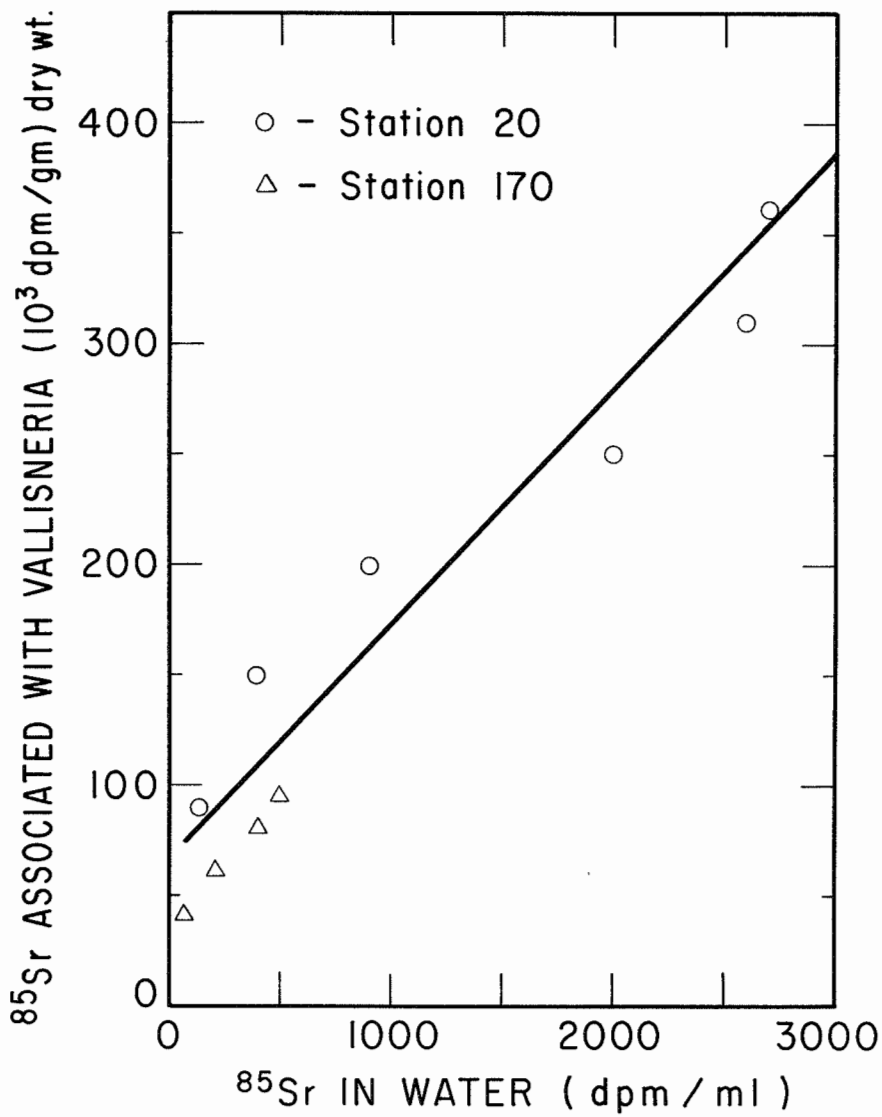

FIG. 5-28. IMMEDIATE UPTAKE OF ^{85}Sr BY SEDIMENTS AND VALLISNERIA

sorbed was released back within 8 hours after the plume passed. The retention of ^{85}Sr by Vallisneria was insignificant, Fig. 5-27. The ^{86}Sr on Vallisneria at all stations was found to be about 200-300 dpm/gm four weeks after injection of ^{85}Sr. The immediate uptake of ^{85}Sr by Vallisneria was fairly significant, Fig. 5-28. The immediate uptake by Vallisneria, K_{p_o}, was found to be 110 dpm/gm/dpm/ml.

Effect of Organic Pollutants on ^{85}Sr Transport

With the continuous release of dextrose and raw sewage, the organic polluted stream was simulated in the west channel of the model river. The raw sewage flow was 50 ml/min. and the dextrose was about 12 ml/min. Continuous release of 0.05 MPC ^{85}Sr with 5 liters/min. of freshwater flow was used for each of the dual-channels. Initial COD in the polluted channel was 190 mg/l, Table 5-6. The D. O. profile was measured and the sag part was observed between the point of 150 ft. and the point of 190 ft. from release point, Table 5-7.

Table 5-6. Chemical Oxygen Demand in Model River Water

Distance from Release Point (ft)	COD	
	Polluted Channel (mg/l)	Unpolluted Channel (mg/l)
30	190	18
80	100	20
160	100	10

Table 5-7. Dissolved Oxygen

Date	Time	Stations of Measurement, Distance from Inlet in Ft. Polluted Water Channel 20	40	60	80	100	120	140	160	180	198	Fresh Water Channel 198
10/21/66	0945	16.20	16.25	16.25	16.65	16.63	16.45	16.56	16.82	16.51	16.36	0.
10/21/66	1500	12.31	12.87	12.95	12.52	12.59	12.39	12.26	12.00	11.93	12.04	0.
10/21/66	1925	8.64	8.29	8.33	8.28	8.47	8.33	8.37	8.26	8.07	8.07	0.
10/22/66	0805	8.41	8.63	8.62	8.55	8.68	8.53	8.59	8.37	8.34	8.30	0.
10/22/66	1035	10.89	10.91	10.80	10.59	10.80	10.82	10.61	10.73	11.12	11.12	0.
10/22/66	1530	14.49	15.40	15.28	15.28	14.29	14.66	14.29	14.05	13.74	13.24	0.
10/22/66	1925	10.27	10.81	10.82	10.72	10.20	9.94	10.03	9.24	10.44	10.44	0.
10/23/66	1130	9.44	9.53	9.44	9.22	8.80	8.72	8.72	8.69	8.52	8.36	12.29
10/23/66	1645	13.68	14.24	14.24	13.90	13.37	13.18	12.67	12.53	12.33	12.34	15.46
10/24/66	0815	7.51	8.29	9.34	9.30	9.30	9.74	9.63	9.46	9.13	8.79	9.98
10/24/66	1200	9.78	9.69	9.64	9.69	9.79	9.79	9.79	9.69	9.62	9.59	11.06
10/24/66	2015	7.67	7.75	7.50	7.41	7.45	7.35	7.16	7.16	7.25	7.28	8.37
10/26/66	0830	.66	.57	.49	.40	.41	.60	.99	2.18	4.45	4.58	9.43
10/26/66	1200	4.04	3.10	2.69	2.56	2.67	3.70	3.93	4.16	4.12	3.81	13.51
10/26/66	1705	5.19	4.21	3.83	3.38	2.93	2.93	3.21	3.33	3.54	3.71	11.84
10/26/66	2200	2.93	2.13	2.13	1.95	1.82	1.95	2.08	2.08	1.72	0.	8.92
10/27/66	0935	5.57	6.13	6.24	6.35	5.33	4.47	3.65	2.40	1.73	1.21	9.95
10/27/66	1200	5.50	5.94	7.05	7.15	7.17	6.85	6.16	5.78	5.32	4.67	11.53
10/27/66	1530	7.94	7.59	7.52	8.07	8.92	9.55	9.58	9.26	9.36	9.03	13.31
10/27/66	1730	5.98	5.42	5.22	5.09	5.60	6.64	6.93	6.93	7.20	7.37	10.27
10/27/66	2100	4.97	3.98	3.20	2.91	3.03	3.60	3.60	4.47	4.84	4.84	7.89
10/28/66	0020	7.41	5.22	2.09	1.19	1.81	2.09	2.09	2.25	2.68	3.28	8.20
10/28/66	0430	7.26	7.34	6.76	4.35	1.20	.80	2.01	2.01	2.41	2.98	9.33
10/28/66	0650	5.12	5.45	5.59	4.86	3.47	1.56	.70	1.40	2.08	2.13	7.47
10/28/66	0915	5.85	5.91	5.89	5.57	4.53	3.81	2.93	1.82	1.05	.71	8.62
10/28/66	1130	5.57	5.90	5.78	5.82	5.87	5.57	5.02	4.37	3.86	3.20	10.58
10/28/66	1600	7.10	7.37	7.47	8.15	8.82	9.40	9.40	9.25	8.82	8.60	13.24
10/28/66	2130	5.43	4.38	3.53	3.04	3.11	3.11	3.11	3.76	4.40	4.51	7.96
10/28/66	2400	6.74	4.27	2.82	2.17	2.28	2.89	2.75	2.28	3.16	3.22	6.75
10/29/66	0630	4.26	4.78	4.34	3.22	2.66	1.86	1.43	1.43	1.70	1.68	5.88
10/29/66	1500	6.71	5.54	5.64	5.87	6.48	6.91	6.48	6.36	6.13	6.36	12.60
10/29/66	2245	5.55	2.71	2.64	2.17	2.17	1.70	1.97	2.44	2.78	2.99	11.33
10/30/66	0315	6.30	5.67	4.53	1.61	1.20	1.67	1.42	1.42	1.57	1.89	9.45
10/30/66	0930	7.21	5.08	5.08	5.29	5.93	5.08	3.73	3.05	2.71	2.71	8.53
10/30/66	1755	7.42	6.59	5.03	5.13	5.79	6.32	6.92	6.95	6.51	6.04	12.65
10/31/66	0910	5.92	5.51	4.91	3.63	2.77	2.41	1.93	1.61	2.41	1.93	9.53

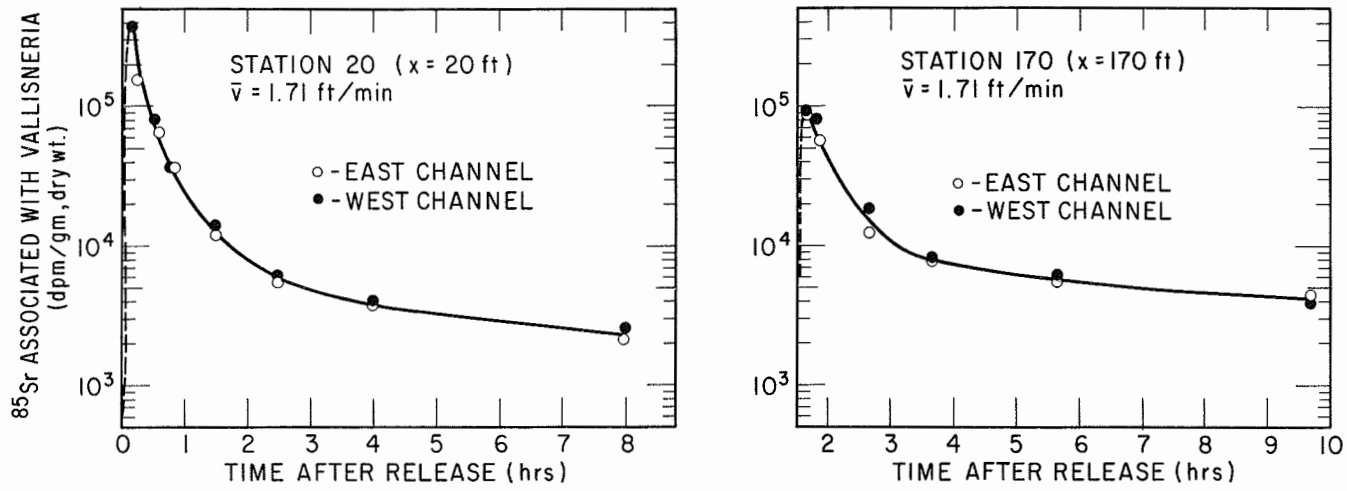

FIG. 5-26. TIME-CONCENTRATIONS OF ^{85}Sr ASSOCIATED WITH VALLISNERIA

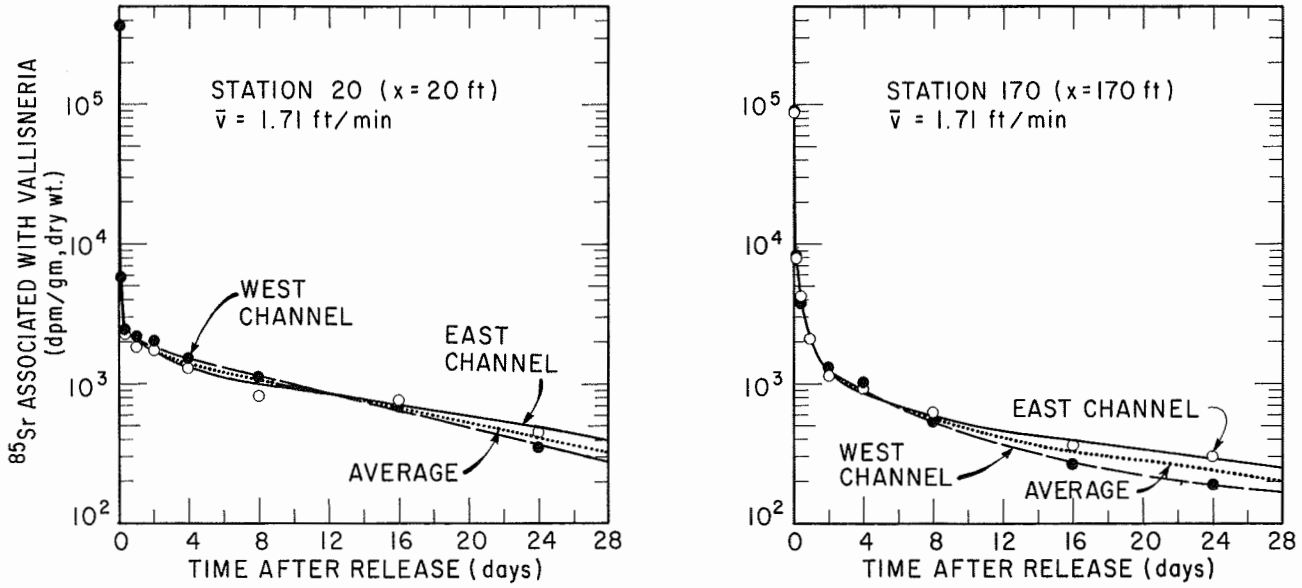

FIG. 5-27. DELAYED ^{85}Sr ASSOCIATED WITH VALLISNERIA

^{85}Sr in Water: Time-concentration of ^{85}Sr in polluted aqueous phase is shown in Fig. 5-29. ^{85}Sr in the polluted channel was found to be higher than that in the unpolluted channel during the entire period having ^{85}Sr inflow, but it became reversed after the stop of ^{85}Sr influx. These relations were probably due to the presence of organic suspensions in the polluted water.

^{85}Sr in Sediments: The time variation and the vertical distribution of ^{85}Sr in the bottom sediments of the polluted environment were studied and compared with that of the unpolluted environment. It was found that the ^{85}Sr in polluted sediments was higher than that in the unpolluted sediments, Fig. 5-29. The increase of ^{85}Sr uptake might be caused by the deposit of the organic suspension with ^{85}Sr sorbed on and the biological activity in the polluted sediments.

A significant increase in ^{85}Sr penetration was observed in the polluted sediments, Fig. 5-31 and Table 5-8. The decreased penetration coefficient suggested that the biological activity in the sediments was probably a very important factor in controlling the migration of ^{85}Sr in the sediments.

Table 5-8. Penetration Coefficient-Based on Polluted Environment

Time After Start (Hrs)	Penetration Coefficient	
	Freshwater Channel (gm^{-1})	Polluted Water Channel (gm^{-1})
18	0.44	0.167
36	0.35	0.160
48	0.34	0.155

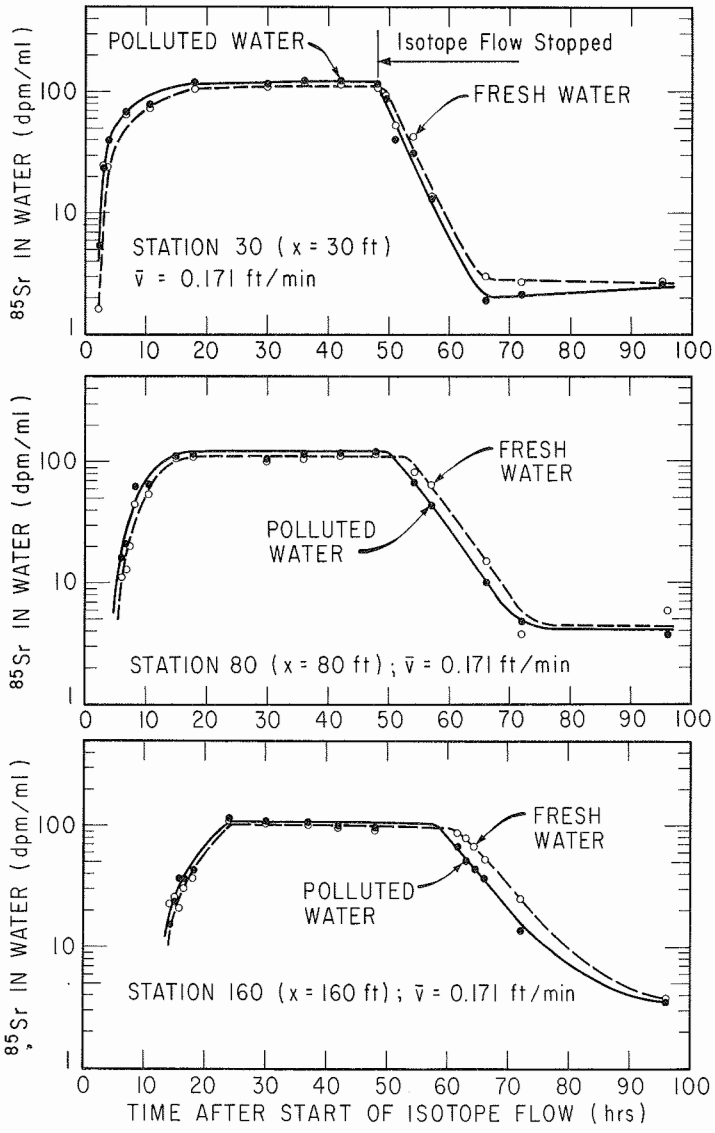

FIG. 5-29. LONGITUDINAL DISTRIBUTION OF ^{85}Sr IN POLLUTED CHANNEL

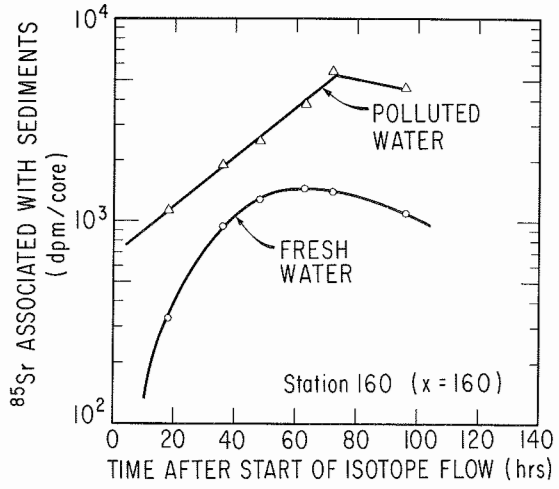

FIG. 5-30. ^{85}Sr ASSOCIATED WITH SEDIMENTS IN POLLUTED ENVIRONMENT

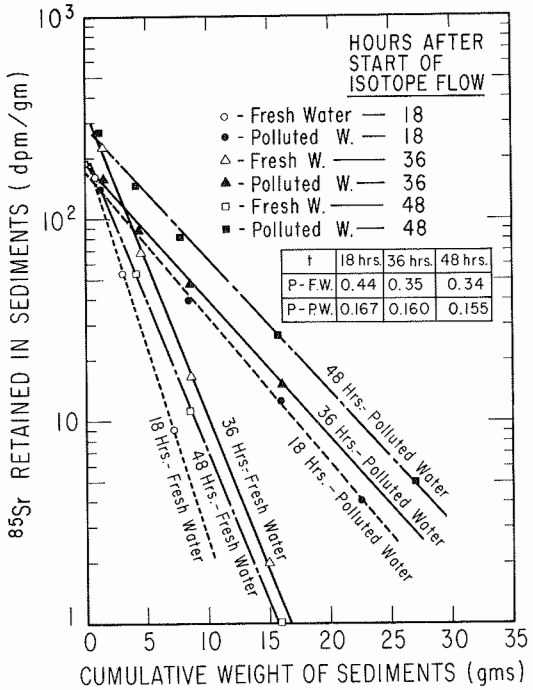

FIG. 5-31. ^{85}Sr PENETRATION INTO THE SEDIMENTS IN POLLUTED ENVIRONMENT

Chapter VI

MATHEMATICAL DEVELOPMENT

The analytical process for modeling the transport function of radionuclides in a stream system can now be approximated. For the case under discussion, the physical, chemical, biological sorption mechanism, as well as the desorption mechanism are expressed in mathematical form. Boundary values are described for these special cases. Also, the numerical analysis and the Fortran programming routines are developed for the engineering application of the model.

The Sorption-Desorption Concept

The limitations in accurately evaluating the transport of radionuclides in streams seem to occur as a result of: (a) the inability to describe correctly the time-concentration effect, and (b) the difficulty in obtaining an accurate balance between mass influx and efflux. A logical formulation has to include the non-equilibrium interactions between radionuclides in the aqueous phase and in the solid phases.

Gloyna, *et al* (54, 40, 42, 4) have indicated that the discrepancies between the dispersed flow and observed data might have been due to sorption of radionuclides on bottom sediments and aquatic plants. Furthermore, it was shown that most of the sorbed fraction of radionuclides would be desorbed

by fresh water inflow and consequently discharged. Based on studies reported herein, it was found that the retention of radionuclides by Vallisneria was insignificant.

The mass transfer of radionuclides in the sediments is derived by the concentration gradient. For the non-equilibrium sorption, the gradient is based on the difference between the equilibrium concentration and the existing concentration in the sorbent. The equilibrium sorption function is unique for each type of sorbent. Thus, the mass exchange rate is different from one sorbent to another for certain radionuclides.

Development of the Mathematical Equations

Simultaneous partial differential equations describing the transport function of radionuclides in the stream system are derived by applying the sorption and desorption concepts to the mass balance principle. Homogeneous distribution of various solid media and constant inflow of freshwater are assumed.

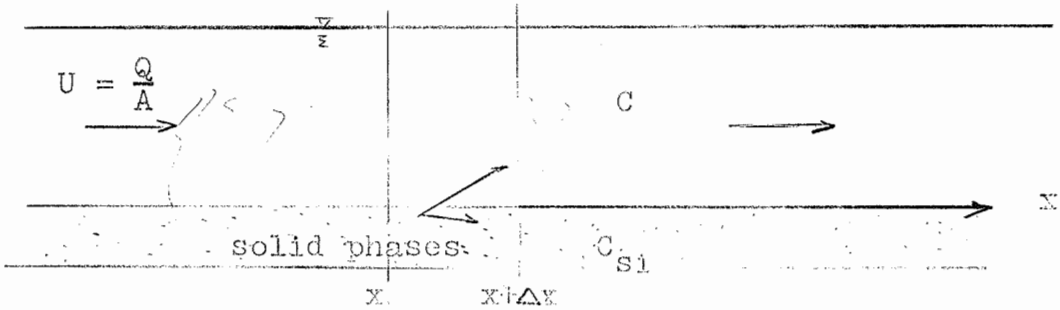

Referring to the above diagram and Eq. 6-1, a mass balance is made across the section x to x+Δx for a certain radionuclide in the stream:

$$\frac{\partial (CA\Delta x)}{\partial t} = AN\Big|_x - AN\Big|_{x+\Delta x} + QC\Big|_x - QC\Big|_{x+\Delta x} + \sum_{i=1}^{n} A_{s_i} N_{s_i} \quad (6\text{-}1)$$

Where

C = concentration of radionuclide in water, $C(x, t)$

x = longitudinal distance from origin (the origin in most cases was the injection point of radionculides)

A = the cross section for the water inflow

A_{s_i} = the contact area between the water and the i^{th} solid sorbent

AN = the rate of mass transfer by longitudinal dispersion

Q = water inflow in the stream

$A_{s_i} N_{s_i}$ = the rate of mass transfer into the water phase from i^{th} solid sorbent

Based on Fick's diffusion theory and the non-eqiulibrium sorption mechanism, the terms for N and N_{si} are expressed as:

$$N = - D_x \frac{\partial C}{\partial x} \quad (6\text{-}2)$$

$$N_{s_i} = K_i (C_{s_i} - C_{s_i}^{0}) \quad ; \quad i=1, 2, \ldots, n \quad (6\text{-}3)$$

Where

D_x = longitudinal dispersion coefficient

K_i = mass transfer constant between water and i^{th} sorbent

$C_{s_i}^0$ = equilibrium concentration of radionuclides associated with i^{th} sorbent

C_{s_i} = concentration of radionuclide in i^{th} sorbent
= $C_{s_i}(x, t)$

In order to simplify the terms of $\sum_{i=1}^{n} A_{s_i} N_{s_i}$ in Eq. 6-1, the wetted soils and aquatic plants are considered separately, and the contact areas can be correlated with x and A as follows:

$A_s = (W + 2H)\Delta x$

$A_{p_i} = a_i M_i A \Delta x$

$A = W \times H$

Where

A_s = total contact area for soils

A_{p_i} = the contact area for i^{th} aquatic plant

M_i = the biomass per unit volume of aqueous environment for i^{th} aquatic plant

W = width of channel bottom

H = wetted perimeter of the bank portion of the channel cross section

a_i = surface area per unit biomass

Therefore

$$\sum_{i=1}^{n} A_{s_i} N_{s_i} = W\Delta x\, N_{s_1} + 2H\,\Delta x\, N_{s_2} + \sum_{i=3}^{n} a_i M_i A\,\Delta x\, N_{s_i} \qquad (6\text{-}4)$$

Where

i = 1 used for the bottom sediments designation

i = 2 used for the bank soils designation

Then, dividing Eq. 6-4 by ($A\Delta x$) and taking limits as $\Delta x \to 0$, the partial differential equation describing the radionuclide transport function can be expressed as:

$$\frac{\partial C}{\partial t} = D_x \frac{\partial^2 C}{\partial x^2} - U\frac{\partial C}{\partial x} + \frac{1}{H} N_{s_1} + \frac{2}{W} N_{s_2} + \sum_{i=3}^{n} a_{p_i} M_i N_{s_i} \quad (6\text{-}5)$$

However, the $C_{s_i}^0$ is usually expressed in terms of the function of C, $g_i(C)$, hence,

$$\frac{\partial C}{\partial t} = D_x \frac{\partial^2 C}{\partial x^2} - U\frac{\partial C}{\partial x} + \frac{k_1}{H}\left[C_{s_1} - g_1(C)\right] + \frac{2k_2}{W}\left[C_{s_2} - g_2(C)\right] + \sum_{i=3}^{n} a_i M_i K_i \left[C_{s_i} - g_i(C)\right] \quad (6\text{-}6)$$

The partial differential equations describing the non-equilibrium radionuclide sorption reactions in the sorbent are derived as,

$$\frac{\partial C_{s_1}}{\partial t} = \frac{k_1}{D_1}\left[g_1(C) - C_{s_1}\right] \quad (6\text{-}7)$$

$$\frac{\partial C_{s_2}}{\partial t} = \frac{k_2}{D_2}\left[g_2(C) - C_{s_2}\right] \quad (6\text{-}8)$$

$$\frac{\partial C_{s_i}}{\partial t} = a_i K_i \left[g_i(C) - C_{s_i}\right] \quad ; \quad i=3, 4, \ldots, n \quad (6\text{-}9)$$

The terms D_1 and D_2 are the effective depths of soil in the bottom and along the bank. The effective depth may be defined as the depth where the concentration of radionuclides is equal to or less than .001% of that at the interface. There are (n+1)variables,

C_{s_i} (i=1,...., n) and C, and (n+1) simultaneous equations. Moreover, for a solution of the above model (n+2) boundary conditions are required. For the case of instantaneous injection at x=0 and at t=0, the following boundary values can be assumed:

$$C(x, 0) = 0 \quad ; \quad x>0 \tag{6-10}$$

$$\lim_{x \to \infty} C(x, t) \to 0 \tag{6-11}$$

$$\lim_{t \to \infty} C(x, t) \to C_{\infty} \text{ (finite value)} \tag{6-12}$$

$$C_{s_i}(x, 0) = 0 \quad ; \quad x>0 \quad ; \quad i=1, 2, \ldots, n \tag{6-13}$$

Equation 6-14 describes the initial condition,

$$C(0, 0) = \frac{M}{AU} \delta(t-0) \tag{6-14}$$

Therefore, (n+2) boundary conditions and one initial condition are provided.

Transport of Radionuclides in Ordinary Stream

The transport formula for the radionuclides in stream systems with dominant sorption by bottom sediments is presented. Notably, this prediction equation developed herein may be adapted to the transport function of any other sorptive compound to the beds of the stream. The simultaneous partial differential equations describing such a typical system are presented in Eqs. 6-15 and 6-16.

$$\frac{\partial C}{\partial t} = D_x \frac{\partial^2 C}{\partial x^2} - U\frac{\partial C}{\partial x} - \frac{k_1}{H}\left[g_1(C)-C\right] \qquad (6\text{-}15)$$

$$\frac{\partial C_s}{\partial t} = \frac{k_1}{D_1}\left[g_1(C)-C\right] \qquad (6\text{-}16)$$

Within the range of maximum permissible concentration (MPC) of each radionuclide, the $g_i(C)$ could generally be assumed a linear function, i. e.,

$$g_1(C) = K_s C$$

Where

K_s = equilibrium distribution coefficient

The concentration of radionuclide associated with sediments can be expressed in terms of the total amount found in a uniform sample. Then, Eqs. 6-14 and 6-15 become

$$\frac{\partial C}{\partial t} = D_x \frac{\partial^2 C}{\partial x^2} - U\frac{\partial C}{\partial x} - \frac{k_1}{Ha}\left(K_s C-M\right) \qquad (6\text{-}17)$$

and

$$\frac{\partial M}{\partial t} = k_1\left(K_s C-M\right) \qquad (6\text{-}18)$$

Where

M = the total radionuclides in a constant sampling area, a

$k_1=\frac{K_1}{D}$ = mass transfer coefficient for the radionuclide between water phase and solid phase

The boundary conditions are:

$$C(x,\ 0) = 0 \quad ; \quad x>0 \qquad (6\text{-}19)$$

$$\lim_{t \to \infty} C(x, t) = C \quad \text{(finite value)} \tag{6-20}$$

$$\lim_{x \to \infty} C(x, t) \to 0 \tag{6-21}$$

$$M(x, 0) = 0 \quad ; \quad x > 0 \tag{6-22}$$

and the initial condition for the instantaneous release is:

$$C(0, 0) = \frac{M}{AU} \delta(t-0) \tag{6-23}$$

Where

$\delta(t-0)$ = the Dirac delta function

By using the Laplace transform technique, the transformed equations are:

$$C(x, s) = \frac{M}{AU} e^{\frac{Ux}{2D_x}} e^{-x\sqrt{\frac{U^2}{4D_x^2} + \frac{1}{D_x}\left[dK_s - s + \frac{dk_1 K_s}{s+k_1}\right]}} \tag{6-24}$$

Where

s = the transformed variable from t

$d = \frac{k_1}{Ha}$

With the aid of the operational (55) Eq. 6-25,

$$L^{-1}\left\{\int_0^t J_o\left[2\sqrt{\tau(t-\tau)}\right] F(\tau)d\tau = \frac{1}{s} f(s+\frac{1}{s})\right. \tag{6-25}$$

the inversion of Eq. 6-24 can be obtained:

$$C(x, t) = \frac{Mx}{2AU\sqrt{\pi D_x}} e^{\left(\frac{Ux}{2D_x} - k_1 t\right)} \int_0^t I_1\left[2\sqrt{dk_1 K_s (t-\tau)\tau}\right] \sqrt{\frac{dk_1 K_s}{t-\tau}} \frac{1}{\tau}$$

$$e^{-\left(\frac{x^2}{4D_x \tau} + B\tau\right)} d\tau \tag{6-26}$$

Where

I_1 = the first order of the modified Bessel function of the first kind

τ = dummy variable

$B = \frac{U^2}{4D_x} + dK_s - k_1$ (6-27)

Based on Eqs. 6-18 and 6-26, the function of M(x, t) can be developed:

$$M(x, t) = k_1 K_s \int_0^t e^{-k_1(t-\lambda)} C(x, \lambda)\, d\lambda \quad (6\text{-}28)$$

Where

λ = dummy variable

The details involved in the solutions of the simultaneous equations are presented in Appendix III.

Computation Technique

The numerical analysis and mathematical methods used to apply Eq. 6-26 have been studied. The Fortran program is based on the modified Simpson's formula and the recurrence relations in Bessel functions.

Numerical Integration: Since the integrand in Eq. 6-26 cannot be integrated analytically, the numerical integration method was used. Simpson's formula with end corrections as suggested by Fröberg (17) was used. The usual Simpson's rule is:

$$\int_a^b f(x)\, dx = \frac{h}{3}\left[f_0 + 4f_1 + 2f_2 + 4f_3 + \cdots + 4f_{2n-1} + f_{2n}\right] + O(h^4) \quad (6\text{-}29)$$

Where

h = $\frac{b-a}{2n}$ (width for each trapezoid)

$2n$ = number of total intervals

f_i = $f\ (a+ih)$; $i=0, 1, \ldots, 2n$

$O(h^4)$ = the possible error in the order of h^4

The modified Simpson's formula is based on the equality of error corrections for different numerical increments. Let J_1 be the integrated value as stated in Eq. 6-29. Then assign J_2 to the value calculated from Eq. 6-30.

$$J_2 = \frac{k}{3}\left[g_0+4g_1+2g_2+ \text{---} +4g_{2m-1}+g_{2m}\right] + O(k^4) \qquad (6\text{-}30)$$

Where

k = $\frac{h}{2}$

g_i = $f\ (a+ik)$, $i=1; 2, \ldots, 2m$

$O(k^4)$ = the possible error in the order of k^4

Since $O(k^4) \approx (\frac{h}{2})^4$ and $O(h^4) \approx h^4$, then $16\ O(k^4) \approx O(h^4)$.

Thus, Eq. 6-31 can be established

$$16(J_2-J) = J_1-J \qquad (6\text{-}31)$$

Where

J = true value for the integral $\int_a^b f(x)\,dx$

Therefore, a more accurate value for the integral can be obtained by Eq. 6-32.

$$J = \frac{16\ J_2-J_1}{15} \qquad (6\text{-}32)$$

The possible error in Eq. 6-32 was established to be about $O(h^6)$.

Calculation of Bessel Function: The subroutine program BESSEL is called for the computation of the modified Bessel function in the integrand of Eq. 6-26. The method utilized is to set $e^{-X} I_M(X)$ to the small number α. Then, all the Bessel functions in lower orders are generated according to Eq. 6-33.

$$I_m(X) = \frac{2(m+1)}{X} I_{m+1}(X) + I_{m+2}(X) \qquad (6\text{-}33)$$

Where

$m = 0, 1, 2, \ldots M$

With the aid of Eq. 6-34, the normalizing constant is calculated for $I_1(X)$ values.

$$I_0(X) + 2 \sum_{m=1}^{M} I_m(X) = e^X \qquad (6\text{-}34)$$

The accuracy of the results computed by this subroutine BESSEL was found to be well satisfied with possible error of $\pm$ 1.0 x 10^{-9}.

Program TRNSPRT: The TRNSPRT written in Fortran -63 was developed for this study. The details are as follows:

(a) For a time value t, the increment value h was set at h=t/400.0 (6-35)

(b) The value for the argument of Bessel function was computed by

$$\zeta_i = 2\sqrt{dk_1 K_s \tau_i (t-\tau_i)} \qquad (6\text{-}36)$$

Where

τ_i = i·h; i=1, 2, ..., 399

ζ_i = the argument for the time of i·h minutes from release time.

(c) The first order modified Bessel function with argument ζ_i was calculated by use of the subroutine BESSEL and then assigned to be Bl_i.

(d) The functional value of integrand was then calculated for each Bl_i value and the given x value.

$$f_i = Bl_i \left(\frac{dk_1K_s}{t-t_i}\right)^{\frac{1}{2}} \frac{1}{\tau_i} \exp\left(-\left(\frac{x^2}{4D_x t_i} + Bt_i\right)\right) \qquad (6\text{-}37)$$

(e) Based on the order of the time increment, the f_i values were categorized into three groups and summed as:

$$S_1 = f_2 + f_6 + f_{10} + f_{14} + \cdots\cdots\cdots f_{398}$$
$$S_2 = f_4 + f_8 + f_{12} + f_{16} + \cdots\cdots\cdots f_{396} \qquad (6\text{-}38)$$
$$S_3 = f_1 + f_3 + f_5 + f_7 + \cdots\cdots\cdots f_{399}$$

(f) The numerical integrated value, J, was computed with the use of the modified Simpson's formula.

$$J_1 = (4S_1 + 2S_2) \qquad (6\text{-}39)$$

$$J_2 = (4S_3 + 2S_2 + 2S_1) \qquad (6\text{-}40)$$

$$J = (16J_2 - J_1)/15.0 \qquad (6\text{-}41)$$

(g) Finally, the concentration of radionuclides in water for a given time t and distance x was calculated by,

$$C(x, t) = \frac{M}{2AU\sqrt{\pi D_x}} (J) \exp \left(\frac{Ux}{2D_x} - k_1 t\right) \qquad (6\text{-}42)$$

The arguments used in TRNSPRT are as follows:

X - distance from the release point for the location of predicting station, x

NP - total number of predicting stations

MN - total number of concentration values presented for a station

TIME - time value in minutes for the prediction, t

DELTA - time increment

TAU - time variables between 0 ~ t, t_i

H - function of integrand

S1 - summation value of S_1

S2 - summation value of S_2

S3 - summation value of S_3

H1 - summation value of J_1

H2 - summation value of J_2

CONC - concentration value of C (x, t)

The program TRNSPRT is listed in Appendix I.

Chapter VII

DISCUSSION

In this chapter the validity of the mathematical model is examined by comparing the predicted ^{85}Sr concentrations with the results of the experimental work. An empirical approach is proposed, and dispersion coefficients are calculated.

The Fortran program developed for this transport model and the mathematical derivations of the formula are presented in Appendices I and II.

Validity of Formulation

A comparison was developed as based on the dispersed flow model and the sorption-desorption model. According to the dispersed flow model, the transport of ^{85}Sr, after instantaneous injection, may be described by Eq. 7-1.

$$C(x, t) = \frac{M}{A\sqrt{4\pi D_x t}} e^{-\left(\frac{x-Ut}{4D_x t}\right)^2} \qquad (7\text{-}1)$$

Where

$C(x, t)$ = concentration of tracer in water (mass per unit volume)

M = total mass of tracer released in test

A = area of stream cross section

D_x = longitudinal dispersion coefficient

U = average velocity of water

x = distance from the release point

The transport function as based on the sorption-desorption model is given in Eq. 7-2.

$$C(x, t) = \frac{Mx}{2AU\sqrt{\pi D_x}} \; e^{\left(\frac{Ux}{2D_x} - k_1 t\right)} \; N(x, t) \qquad (7\text{-}2)$$

Where

$$N(x, t) = \int_0^t I_1 \left[2\sqrt{dk_1 K_s (t-\tau)\tau}\right] \sqrt{\frac{dk_1 K_s}{t-\tau}\,\frac{1}{\tau}} \; e^{-\left(\frac{x^2}{4D_x \tau} + B\tau\right)} \, d\tau \qquad (7\text{-}3)$$

$d = \dfrac{k_1}{H \cdot a}$

H = depth of water

a = sampling area of sediments in each sediments core, 0.6 in.^{2}

$B = \dfrac{U^2}{4D_x} + d\,K_s - k_1$

k_1 = mass transfer constant for the radionuclide exchanged through the interface of the flowing water and the bottom sediments

K_s = equilibrium distribution coefficient involving bottom sediments and radionuclide

I_1 = the modified Bessel function of first order of first kind

τ = the variable for time varying between zero to t

Values for k_1 and K_s were computed on the basis of aquaria and continuous release experiments. These data will be shown in Table 7-3.

For purposes of explanation, it is desirable to use the data developed in Chapter 5 for the instantaneous release case. The following values were assigned to both prediction equations.

$M = 0.55 \text{ mc} = 1.20 \times 10^{9} \text{ dpm/channel}$

$A = 1.04 \text{ ft.}^2$

$D_x = 0.11 \text{ ft.}^2/\text{sec} = 6.6 \text{ ft.}^2/\text{min}$

$U = 0.031 \text{ ft./sec} = 1.85 \text{ ft./min}$

$H = 0.835 \text{ ft.}$

$a = 0.416 \times 10^{-2} \text{ ft.}^2$

$k_1 = 0.011 \text{ hr}^{-1} = 0.183 \times 10^{-3} \text{ min}^{-1}$

$K_s = 140 \text{ dpm/core/dpm/ml}$

Then, given values of x and t, it is possible to compute C(x, t) through the use of Eqs. 7-1 and 7-2. The comparisons between these two prediction equations and the experimental data are shown in Figs. 7-1 and 7-2.

It was realized that the function for the distribution of radionuclides in the stream could not be adequately expressed by dispersed flow models. In fact, the deviations are significant. However, similar experimental discrepancies have also been reported by investigators who concerned themselves with longitudinal mixing. Taylor (49) attributed the discrepancies to a significant laminar layer which was not considered in his theory, and Elder (14) made some quantitative attempts to explain the problem with his postulation of a

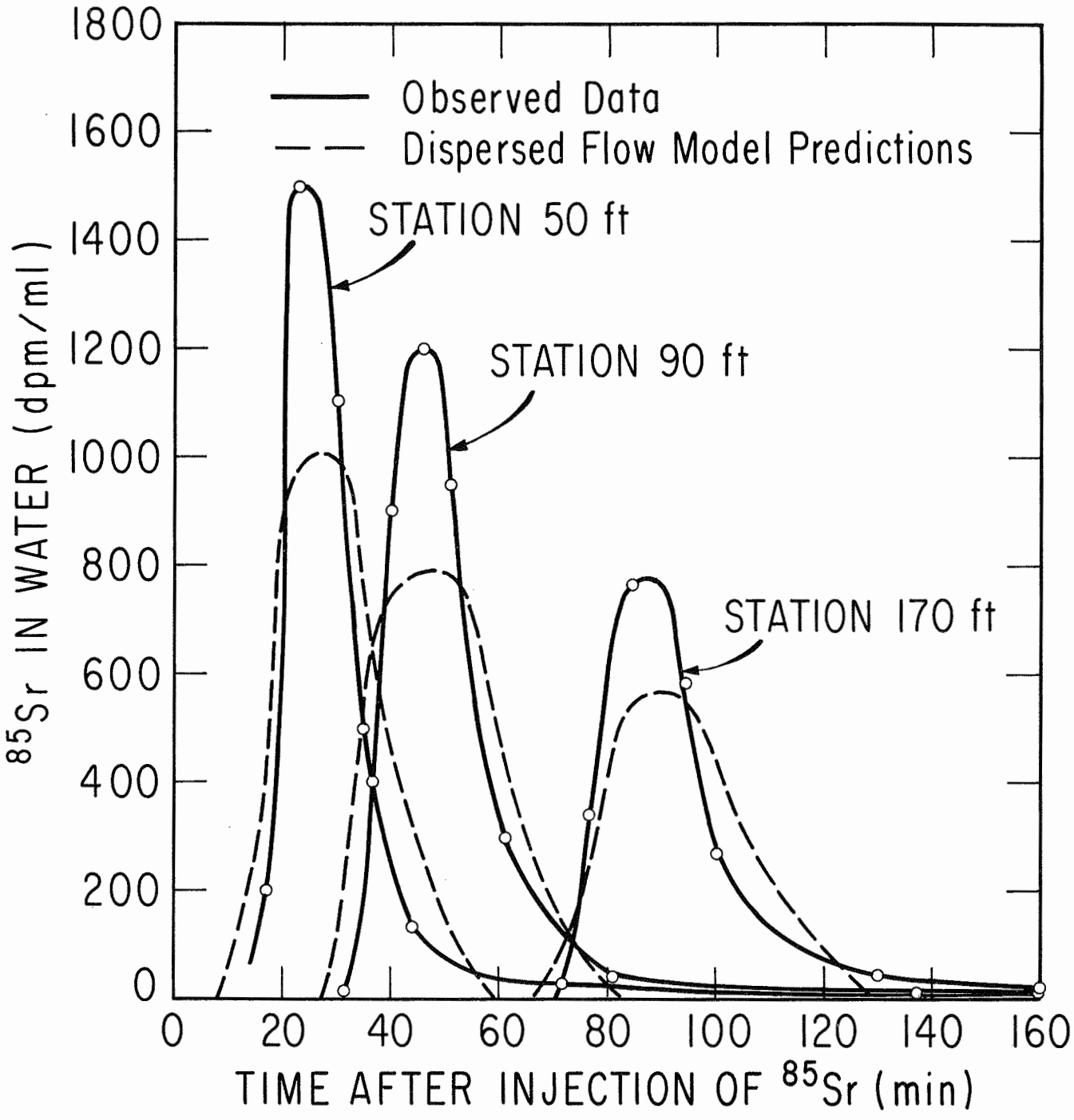

FIG. 7-1. EXPERIMENTAL DATA AND DISPERSED FLOW MODEL

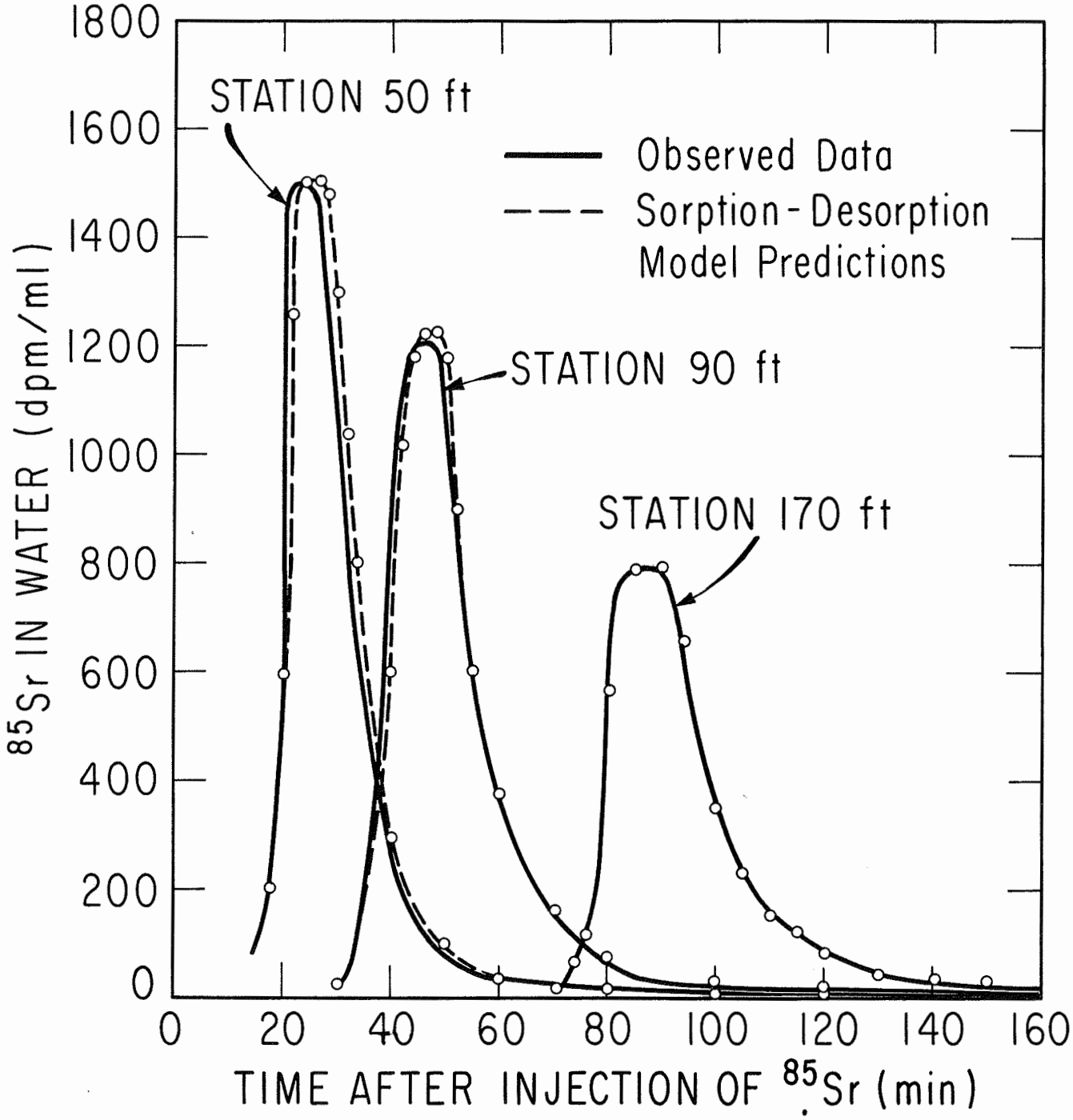

FIG. 7-2. EXPERIMENTAL DATA AND SORPTION - DESORPTION MODEL

laminar sublayer. Hays and Krenkel (22) suggested the dead-zone concept for the explanation of the skewed time-concentration relationship. The detention effect caused by sorption of radionuclides was greater than that postulated by the laminar sublayer hypothesis. Therefore, it must be concluded that the dispersed flow model is not completely satisfactory with the prediction of radionuclides in the stream.

In contrast, predictions based on the sorption-desorption model were found to be comparable with experimental data derived from the model river studies. The deviation between values decreased with increased distance from the release point. This could be explained by Fischer's statement (15) --there exists an initial period during which the mechanism of convective diffusion produces a diffusant cloud differing markedly from that described by the one-dimensional dispersion equation. Equation 6-17 describes the radionuclide influx and efflux in the water phase, and it is based on the one-dimensional dispersion condition. Thus, it appears that Eq. 7-2 can be used to describe the transport of radionuclides in a river system with high sorption capacity in the sediments, especially where the one-dimensional dispersion condition can be satisfied.

Notably, the sorption-desorption model can also be applied to the prediction of radionuclide transport as influenced by plants rather than sediments. The modifications required

can be made by changing Eqs. 6-14 and 6-15 to Eqs. 7-4 and 7-5.

$$\frac{\partial C}{\partial t} = D_x \frac{\partial^2 D}{\partial x^2} - U\frac{\partial C}{\partial x} - m_b K_2 (C_p - K_c C) \qquad (7\text{-}4)$$

$$\frac{\partial C_p}{\partial t} = K_2 (C_p - K_c C) \qquad (7\text{-}5)$$

Where

m_b = biomass in unit volume

K_2 = mass transfer coefficient

C_p = the concentration of radionuclides in unit weight of biomass

K_c = concentration factor for the aquatic plant

Using the same boundary conditions established for Eq. 6-15, the solution is found in Eq. 7-6.

$$C(x, t) = \frac{Mx}{2AU\sqrt{\pi D_x}} \; e^{\left(\frac{Ux}{2D_x} - K_2 t\right)} \; N'(x, t) \qquad (7\text{-}6)$$

Where

$$N'(x, t) = \int_0^t I_1 \left[2\sqrt{m_b K_2^2 K_c (t-\tau)\,\tau}\right] \sqrt{\frac{m_b K_2^2 K_c}{t-\tau}} \; \frac{1}{\tau} \; e^{-\left(\frac{x^2}{4D_x \tau} + B'\tau\right)} \, d\tau \qquad (7\text{-}7)$$

$$B' = \frac{U^2}{4D_x} + m_b K_2 K_c - K_2 \qquad (7\text{-}8)$$

Extension of the Sorption-Desorption Model

The mathematical model can be expanded and can describe the more complex interactions. For example, where the

mixture of radionuclides is assumed to be the diffusant, each type of radionuclide can be considered separately. Also, the detention caused by dead zone is included.

$$\frac{\partial C_j}{\partial t} = D_x \frac{\partial^2 C_j}{\partial x^2} - U \frac{\partial C_j}{\partial x} + \sum_{i=1}^{n} \alpha_i \, k_{ij} \left[C_{ij} - g_j(C_j) \right]$$

$$+ k_{d_j} \frac{P}{A} (C_{d_j} - C) \qquad (7\text{-}9)$$

$$\frac{\partial C_{d_j}}{\partial t} = k_{d_j} \frac{P}{A_{d_j}} (C - C_{d_j}) \qquad (7\text{-}10)$$

$$\frac{\partial C_{ij}}{\partial t} = k_{ij} \left[g_j(C_j) - C_{ij} \right] \qquad (7\text{-}11)$$

Where

C_j = concentration of j^{th} radionuclide in water

α_i = total weight of i^{th} sorbent in unit volume

C_{ij} = the concentration of j^{th} radionuclide in i^{th} sorbent

$g_j(C_j)$ = equilibrium concentration function

k_{ij} = mass transfer function for j^{th} radionuclide associated with i^{th} sorbent

C_{d_j} = concentration of j^{th} radionuclide in the dead zone

i = index for sorbent = 1, 2, 3, ..., n

j = index for radionuclide = 1, 2, 3, ..., m

P = wetted contact length

A_{d_j} = dead zone area

k_{d_j} = mass transfer coefficient for j^{th} radionuclide in the dead zone

The term k_{ij} is the most complex function to be determined. It is the dependent variable of radionuclides concentration and various chemical, physical, and biological complexities. However, k_{ij} can be determined in various laboratory studies.

The solutions for the model represented by Eqs. 7-9, 7-10, and 7-11 may be obtained by use of numerical explicit methods. It is important to note that the one-dimensional flow conditions have to be satisfied; otherwise Eq. 7-12 must be used instead of Eq. 7-9.

$$\frac{\partial C_j}{\partial t} = \frac{\partial}{\partial x}\left(E_x \frac{\partial C_j}{\partial x}\right) + \frac{\partial}{\partial y}\left(E_y \frac{\partial C_j}{\partial y}\right) + \frac{\partial}{\partial z}\left(E_z \frac{\partial C_j}{\partial z}\right) + D_m \nabla^2 C_j - U\frac{\partial C_j}{\partial x} + \sum_{i=1}^{n} \alpha_i k_{ij}\left[C_{ij} - g_j(C_j)\right] + k_{d_j}\frac{P}{A}\left(C_{d_j} - C_j\right) \quad (7\text{-}12)$$

Where

D_m = molecular diffusivity

E_x = turbulent diffusivity along x direction

E_y = turbulent diffusivity along y direction

E_z = turbulent diffusivity along z direction

and $V = W = 0$

Dispersion Coefficients for the Model River

An empirical formula was developed for the calculation of dispersion coefficients in the model river. Since the slope of the channel and the cross section along the channel are constant in the model river, the only variable is the average velocity. Fig. 7-3 shows the correlation between the dispersion coefficient and the average velocity in the channel. Reynold's number and Sherwood's number were calculated from data obtained from dye releases. Generally, Sherwood's number decreased with an increasing Reynold's number. This rate of decrease approaches zero for higher turbulence, whereas the rate of decrease increases very rapidly where laminar conditions exist. Based on the best fit in Fig. 7-3, it was possible to write the empirical expression describing the correlation between Sherwood's number and Reynold's number as follows:

$$S_h = 3.78\ (R_e)^{-0.08}$$

Where

S_h = Sherwood's number = $\frac{D_x}{UR}$

R_e = Reynold's number = $\frac{UR}{\nu}$

R = hydraulic radius

Another empirical formula for the dispersion coefficient is derived from Fig. 5-11.

$$D_x = 29\ (U)^{0.9}$$

Where

D_x = dispersion coefficient in ft.^{2}/sec

U = average velocity in ft./sec

Distribution of the Radionuclides in the Sediments

The uptake rate of ^{85}Sr by the bottom sediments can be quantified in terms of various coefficients. As cited in Table 7-1, the penetration coefficient is related to the contact time and temperature. The empirical relationship, as based on Fig. 7-4, can be expressed as follows:

$$P'(t) = mt^{-n} \tag{7-12}$$

Where

$$n = 0.167\ (1.002)^{(T-25)} \tag{7-13}$$

$$m = 0.60\ (1.03)^{(T-25)} \tag{7-14}$$

T = temperature in ^oC

The equation for the migration of ^{85}Sr in the bottom sediments can be represented by Eq. 7-15.

$$C_s(w, t) = C_{s_o}\ e^{-p(t)w} \tag{7-15}$$

Where

$C_s(w, t)$ = the radionuclide concentration at depth w and time t

w = total cumulative weight from interface

t = the contact time t

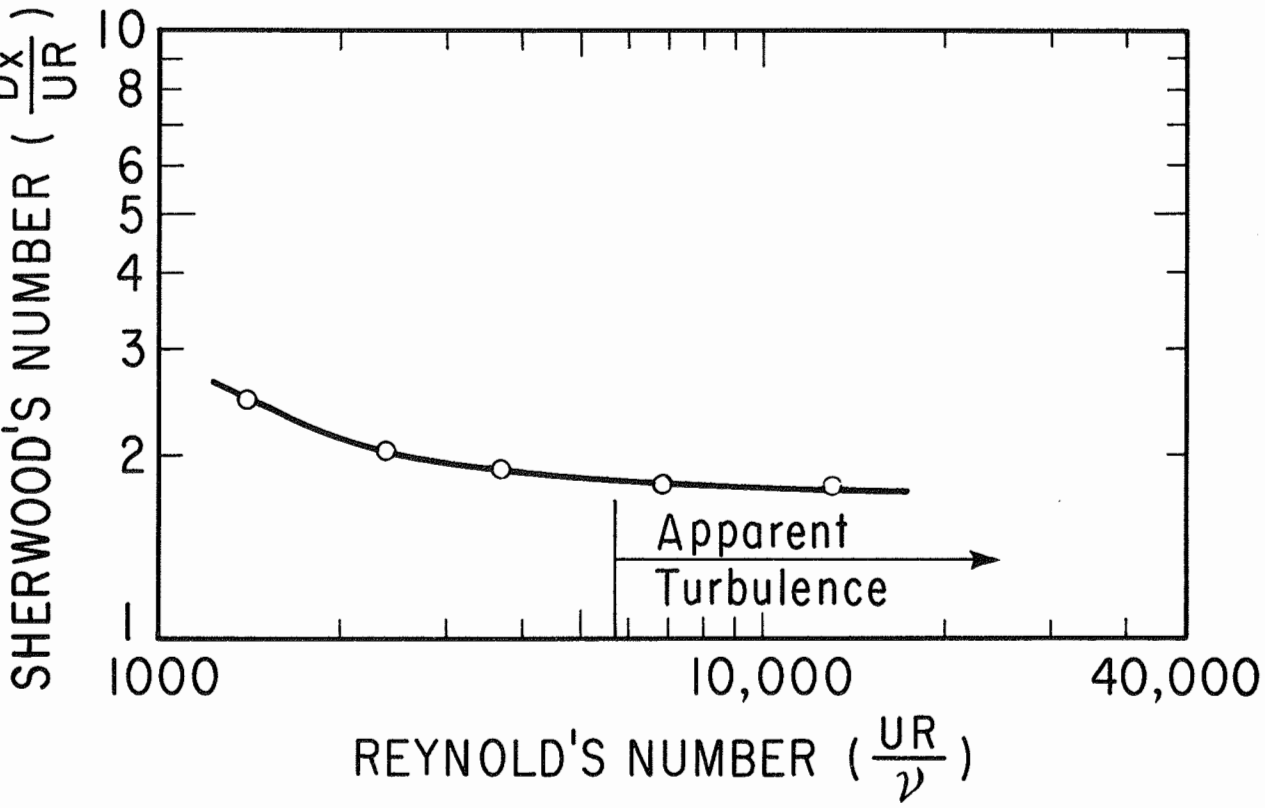

FIG. 7-3. DISPERSION COEFFICIENT FUNCTION IN THE MODEL ROOM

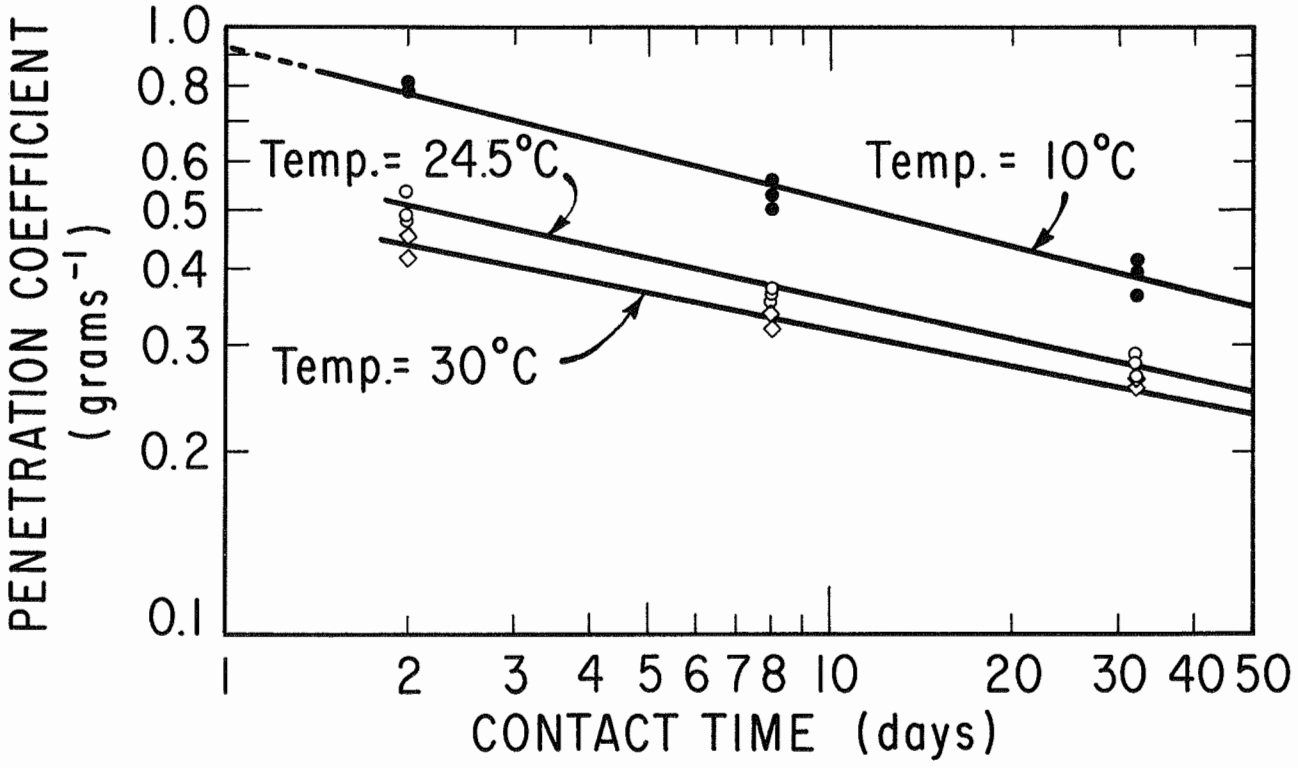

FIG. 7-4. PENETRATION COEFFICIENT OF ^{85}Sr INTO THE BOTTOM SEDIMENTS

C_{s_o} = the saturated interface concentration

$p'(t)$ = the penetration coefficient, a function of contact time t

Eq. 7-15 may be applicable to the prediction of radionuclides in deeper sediments, such as found in holding ponds.

The concentration factor of ^{85}Sr, K_s, for sediments increases with contact time as shown in Fig. 4-12 and Table 7-2. Also, the temperature may cause an increase in the K_s value, but this effect was not very significant for the temperature range involved. Based on Fig. 4-16, the average K_s value can be represented by Eq. 7-16.

$$K_s = 21.0\ t^{0.55} \qquad (7\text{-}16)$$

It is important to note that none of the functions presented in this section considered the common ion effect nor any other chemical complexities.

Table 7-1. Average Penetration Coefficients of ^{85}Sr (gm^{-1})

Temperature °C	Penetration Coefficient Contact Time (Days) 2	8	32
10	0.81	0.53	0.39
24.5	0.52	0.36	0.29
30	0.44	0.33	0.27

Table 7-2. Concentration Factor of ^{85}Sr in Sediments

K_s $\frac{(dpm/core)}{dpm/ml}$

Temperature °C	Concentration Factor Contact Time (Days) 0	2	10	30
10	4.2	31.5	67.0	86.0
24.5	7	36	94	136
30	8.8	22	80	140

Mass Transfer Coefficient for ^{85}Sr into the Sediments

Based on the non-equilibrium sorption reaction, the mass transfer function of radionuclides into the sediments can be written as Eq. 7-17.

$$k_1 = -\frac{1}{t} \ln \frac{K_s C_w - M}{K_s C_w} \qquad (7\text{-}17)$$

Where

k_1 = mass transfer coefficient

t = time of reaction

K_s = equilibrium state distribution coefficient

M = total radionuclides in the sediment core of sample

C_w = radionuclide concentration in water

The k_1 values calculated from data derived from the continuous release studies are shown in Table 7-3. Notably, turbulence affected the k_1 values. Besides, k_1 values

describing uptake were higher than those expressing release. This difference can be explained on the basis that part of the ^{85}Sr transferred into the sediments is bound chemically or physically. Theoretically, k_1 should be expressed by a step function of time as:

$$k_1 = k'_1 - (k'_1 - k'_{1'})\, S_t(t)$$

Where

k'_1 = mass transfer coefficient for the sorption reaction

$k'_{1'}$ = mass transfer coefficient for the desorption reaction

$S_t(t)$ = step function of time

$$= \begin{cases} 0, & t \leq \bar{t} \\ 1, & t \geq \bar{t} \end{cases}$$

$\bar{t}$ = mean flow through time

Based on Table 7-3, the difference of k'_1 and $k'_{1'}$ for ^{85}Sr is very small. Therefore, $k'_1 \approx k'_{1'}$, for the instantaneous release study involving ^{85}Sr.

Effects of Organic Pollutant

Based on data shown in Figs. 5-32, 5-33, and 5-34, organic pollutants might cause a significant change in overall transport of ^{85}Sr. As cited in Table 5-8, lower values of penetration coefficients for the polluted environment indicated higher migration of ^{85}Sr.

In Fig. 7-5, it was also shown that organic pollution seems to increase the sorptive capacity of the sediments. Quantitatively, the ^{85}Sr uptake by sediments was found to be increased by 100 dpm/core/1.0 mg/l of COD added.

Table 7-3. Parameters for the Transport of ^{85}Sr

Reynold's Number	k_1 Value (hr^{-1})		K_s Value (dpm/core/dpm/ml)
	Sorption	Desorption	
Stirrer mixing			140
2400	0.0045	0.0017	120
3700	0.011	0.0085	138

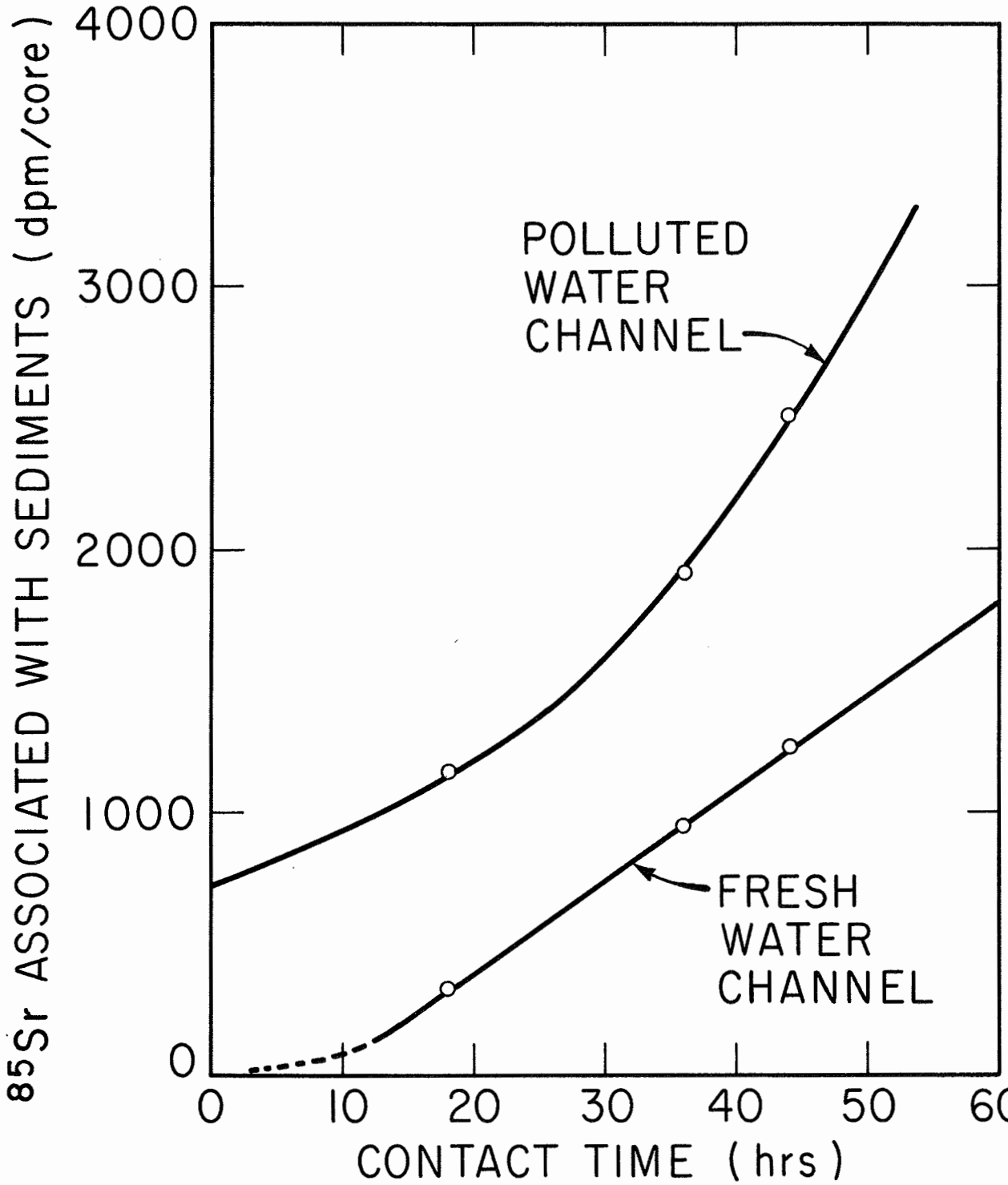

FIG. 7-5. EFFECT OF ^{85}Sr UPTAKE BY SEDIMENTS DUE TO ORGANIC POLLUTANT

APPENDIX I

Fortran Programs

```
  1.  COUNTING EFFICIENCY-- GAMA 3

      PROGRAM GAMA3
C     THIS PROGRAM IS DESIGNED FOR THE CALCULATION OF EFFICIENCY OD GAMA SPECT.
C     PROGRAMED BY C.S. SHIH IN OCTOBER 1965
      DIMENSION JJJ(1300),DPM(40),IBKGD(300)
      COMMON/MM/III(300)
    4 FORMAT(8I10)
    5 FORMAT(5F8.3)
    6 FORMAT(2I10,A8)
    7 FORMAT(1H1)
   10 FORMAT(8F10.2)
   44 FORMAT(9H1BAD BOX=,I4)
   55 FORMAT(5X,A8,14X,I4,25X,F8.6,21X,I4)
   66 FORMAT(//5X,2F10.2)
   77 FORMAT(10X,22HPAPER TAPE BOX NUMBER I6///)
   88 FORMAT(5X,7HISOTOPE,11X,12HSPECT NUMBER,15X,19HCOUNTING EFFICIENCY
     *,11X,16HPEAK CHANNEL NO.//)
  111 FORMAT(I1,79X)
  999 FORMAT(///1X,10I10)
C     READ IN THE NUMBER OF REEL OF TAPES TO BE ANALYZED
      READ 4,NB
      IBOX=0    $  IBADX=0
   11 IF(IBOX-NB)12,100,100
   12 READ 4,NBOX,ISPECT
C     READ IN THE CONCENTRATION OF KNOWN STANDARD FOR EACH SPECTRUM
      READ 10,(DPM(I),I=1,ISPECT)
      READ 6,JKK,IKK,ISO
C     READ IN THE THEORETICAL SUMMATION RANGE AND THE NAME OF STANDARD
      IBAD=0 $ IGOOD=0    $       JSPECT=0
   20 CALL CON(IABC)
C     CHECK THE STOP CODE
      IF(IABC)222,21,222
  222 IF(IABC.EQ.1)27,198
   27 CALL CON(IABC)
      IF(IABC)198,21,198
   21 DO 22 I=1,256
   22 IBKGD(I)=III(I)
C     READ IN THE BACKGROUND COUNTING TIME, SAMPLE COUNTING TIME, DELAYED TIME,
C     AND THE HALF LIFE OF THE STANDARD
      READ 5,BMM,CMM,DAYS,HAFLY,
      PRINT 7
      PRINT 77,NBOX
      PRINT 88
    9 IF(ISPECT-IGOOD-IBAD)199,199,40
   40 CALL CON(IABC)
      IF(IABC)99,23,99
   23 IGOOD=IGOOD+1
      DO 24 I=1,256
C     CALCULATION OF THE NET COUNTS FOR EACH CHANNEL
      JJJ(I)=III(I)-(IBKGD(I)*CMM/BMM)
      IF(JJJ(I))25,25,24
   25 JJJ(I)=0
   24 CONTINUE
C     SEARCH FOR THE PEAK CHANNEL
```

```
      IJ=JKK-1
      DO 28 J=JKK,IKK
      IF(JJJ(IJ)-JJJ(J))26,26,28
   26 TEMP=IJ
      IJ=J
      J=TEMP
   28 CONTINUE
      IPK=IJ
      IA=IPK-7
      IB=IPK+7
      A=0
      DO 30 K=IA,IB
      A=A+JJJ(K)
   30 CONTINUE
      CPM=A*EXPF(0.693/HAFLY*DAYS)
      JSPECT=JSPECT+1
      EFF=CPM/DPM(JSPECT)/CMM
      PRINT 999,(III(M),M=IA,IB)
      PRINT 66,CPM,A
      PRINT 55,ISO,JSPECT,EFF,IPK
      GO TO 9
   99 IBAD=IBAD+1
      JSPECT=JSPECT+1
      GO TO 9
  198 IBADX=IBADX+1
      READ 111,ISKIP
      DO 197, I=1,ISPECT
  197 CALL CON(IABC)
  199 IBOX=IBOX+1
      GO TO 11
  100 CONTINUE
      PRINT 44,IBADX
      CALL TIME
      END
```

2. CONTRIBUTION COEFFICIENT --GAMA 1

```
      PROGRAM GAMA1
C     THIS IS THE PROGRAM DESIGNED FOR THE CALCULATION OF CONTRIBUTION COEFF.
C     PROGRAMMED BY C.S.SHIH IN OCTOBER 1965
      DIMENSION A(10),FRAC(10),IKK(10),JKK(10),IBKGD(300),ISO(10),
     *JJJ(300)
      COMMON/MM/III(300)
    4 FORMAT(8I10)
    5 FORMAT(5F8.3)
    7 FORMAT(1H1)
   10 FORMAT(I4,A8,2I10)
   17 FORMAT(10X,22HPAPER TAPE BOX NUMBER I6///)
   44 FORMAT(9H1BAD BOX=,I4)
   66 FORMAT(19X,10F8.4)
   77 FORMAT(5X,7HISOTOPE,15X,18HCONTRIBUTION VALUE//)
   88 FORMAT(5X,A8,6X,10A8)
  111 FORMAT(I1,79X)
C     READ IN THE NUMBER OF REEL OF TAPES TO BE ANALYZED AND THE TOTAL NUMBER OF
C     ISOTOPES INVOLVED IN THE STUDY
      READ 4, NB,N
      READ 10,(M,ISO(M),IKK(M),JKK(M),M=1,N)
      IBOX=0   $  IBADX=0
   21 IF(IBOX-NB)22,200,200
C     READ IN THE CATELOG NUMBER FOR THE REEL OF PAPER TAPE, NUMBER OF SPECTRA
C     CONTAINED, AND THE GIVEN NUMBER FOR THE ISOTOPE OF THE STANDARD
   22 READ 4, NBOX,ISPECT,IO
      IBAD=0 $ IGOOD=0 $JSPECT=0
   23 CALL CON(IABC)
      IF(IABC)222,24,222
  222 IF(IABC.EQ.1)27,198
   27 CALL CON(IABC)
      IF(IABC)198,24,198
   24 DO 25,L=1,256
   25 IBKGD(L)=III(L)
      READ 5,BMM,CMM,DAYS,HAFLY
      PRINT 7
      PRINT 17,NBOX
      PRINT 77
      PRINT 88,ISO(IO),(ISO(M),M=1,N)
    9 IF(ISPECT-IGOOD-IBAD)199,199,30
   30 CALL CON(IABC)
      IF(IABC)99,33,99
   33 IGOOD=IGOOD+1
      DO 34,I=1,256
      JJJ(I)=III(I)-IBKGD(I)*CMM/BMM
      IF(JJJ(I))35,35,34
   35 JJJ(I)=0
   34 CONTINUE
      DO 48 J=1,N
      A(J)=0
      NI=IKK(J)
      NJ=JKK(J)
      DO 48,K=NI,NJ
      A(J)=A(J)+JJJ(K)
```

```
 48 CONTINUE
    B=A(IO)
    DO 38, J=1,N
 38 FRAC(J)=A(J)/B
    PRINT 66,(FRAC(J),J=1,N)
    JSPECT=JSPECT+1
    GO TO 9
 99 IBAD=IBAD+1
    JSPECT=JSPECT+1
    GO TO 9
198 IBADX=IBADX+1
    READ 111,ISKIP
    DO 197, I=1,ISPECT
197 CALL CON(IABC)
199 IBOX=IBOX+1
    GO TO 21
200 CONTINUE
    PRINT 44,IBADX
    CALL TIME
    END
```

3. SELF-ABSORPTION CORRECTION -- GAMA 4

```
      PROGRAM GAMA4
C     THIS PROGRAM IS DESIGNED FOR THE CALCULATION OF SELF ABSORPTION CONST.
C     PROGRAMED BY C.S. SHIH IN OCTOBER 1965
      DIMENSION JJJ(1300),DPM(40),IBKGD(300)
      COMMON/MM/III(300)
    4 FORMAT(8I10)
    5 FORMAT(5F8.3)
    6 FORMAT(2I10,A8)
    7 FORMAT(1H1)
   10 FORMAT(8F10.2)
   44  FORMAT(9H1BAD BOX=,I4)
   55 FORMAT(5X,A8,14X,I4,25X,F8.6,21X,I4)
   66 FORMAT(//5X,2F10.2)
   77 FORMAT(10X,22HPAPER TAPE BOX NUMBER I6///)
   88 FORMAT(5X,7HISOTOPE,11X,12HSPECT NUMBER,15X,19HSELF ABSORPT. COEFF
     *,11X,16HPEAK CHANNEL NO.//)
  111 FORMAT(I1,79X)
  999 FORMAT(///1X,10I10)
      READ 4,NB
      IBOX=0    $  IBADX=0
   11 IF(IBOX-NB)12,100,100
   12 READ 4,NBOX,ISPECT
      READ 6,JKK,IKK,ISO
      IBAD=0 $ IGOOD=0    $       JSPECT=0
   20 CALL CON(IABC)
      IF(IABC)222,21,222
  222 IF(IABC.EQ.1)27,198
   27 CALL CON(IABC)
      IF(IABC)198,21,198
   21  DO 22 I=1,256
   22 IBKGD(I)=III(I)
      READ 5,BMM,CMM,DAYS,HAFLY,
      PRINT 7
      PRINT 77,NBOX
      PRINT 88
    9 IF(ISPECT-IGOOD-IBAD)199,199,40
   40 CALL CON(IABC)
      IF(IABC)99,23,99
   23 IGOOD=IGOOD+1
      DO 24 I=1,256
      JJJ(I)=III(I)-(IBKGD(I)*CMM/BMM)
      IF(JJJ(I))25,25,24
   25 JJJ(I)=0
   24 CONTINUE
      IJ=JKK-1
      DO 28 J=JKK,IKK
      IF(JJJ(IJ)-JJJ(J))26,26,28
   26 TEMP=IJ
      IJ=J
      J=TEMP
   28 CONTINUE
      IPK=IJ
      IA=IPK-7
```

```
      IB=IPK+7
      A=0
      DO 30 K=IA,IB
      A=A+JJJ(K)
   30 CONTINUE
      CPM=A*EXPF(0.693/HAFLY*DAYS)
      JSPECT=JSPECT+1
      IF(JSPECT.EQ.1)35,36
   35 DPM(1)=CPM
C     CALCULATION OF SELF-ABSORBTION CORRECTIONS
   36 SELF=CPM/DPM(1)
      PRINT 999,(III(M),M=IA,IB)
      PRINT 66,CPM,A
      PRINT 55,ISO,JSPECT,SELF,IPK
      GO TO 9
   99 IBAD=IBAD+1
      JSPECT=JSPECT+1
      GO TO 9
  198 IBADX=IBADX+1
      READ 111,ISKIP
      DO 197, I=1,ISPECT
  197 CALL CON(IABC)
  199 IBOX=IBOX+1
      GO TO 11
  100 CONTINUE
      PRINT 44,IBADX
      CALL TIME
      END
```

4. COMPLEX SPECTRUM ANALYSES -- GAMA 2

```
      PROGRAM GAMA2
C        PROGRAM BY C. S. SHIH  SEPT. 1964
      COMMON/MM/III(300)
      DIMENSION JJJ(300),IJK(8),A(8),KII(8),KJI(8),    FRAC(8,8),F(8,9),
     *COUNT(8),KJJ(8),EFF(8),ISO(8),IX2(8),IX1(8),IKI(8), EV(8),DIS(8),
     *IBACK(300),ABS(8),DECAY(8)
    1 FORMAT( 5X,22HPAPER TAPE ROLL NUMBER  F8.2 )
    2 FORMAT(/50X,I5,6F10.2/    )
    3 FORMAT(2X,3HJOB 5X,7HISOTOPE 5X,12HPOTOPEAK AT 5X,12HUPWARD SHIFT
     *5X,15HDISINTEGRATIONS
     */1X,6HNUMBER 14X,14HCHANNEL NUMBER 4X,12HOF PHOTOPEAK 8X,
     *  10HPER MINUTE///)
    4 FORMAT(8I10)
    5 FORMAT(4I5,A8,F8.5,F8.2,4F6.4)
    6 FORMAT(//10X,4I10)
    7 FORMAT(6F10.3)
    8 FORMAT(2X,I4,6X,A8,7X,I5,12X,I5,5X,F15.3)
  777 FORMAT(///55X,5F12.2)
  888 FORMAT(8F10.2)
  999 FORMAT(1H1 )
      CALL TIME
      READ 4,N,MMN
      M = N + 1
      DO 10 K = 1,N
   10 READ 5,I,KJJ(I),KJI(I),KII(I),ISO(I),EFF(I),DECAY(I),
     *(FRAC(I,J),J=1,N)
   42 IF(MMN)299,299,43
   43 READ 888,CNN,AMM,DAYS,BOX
      READ 7, (ABS(J),J=1,N)
      PRINT 999
      PRINT 1,BOX
      PRINT 3
      IRLM = 0
      CALL CON(IABC)
      IF(IABC)199,44,199
   44 DO 45 I = 1,256
   45 IBACK(I)  = III(I)
   46 CONTINUE
      IRLM = IRLM + 1
      CALL CON(IABC)
      IF(IABC)199,47,199
   47 DO 50 I = 1,256
      JJJ(I)=III(I)-(IBACK(I)*AMM)/CNN
      IF(JJJ(I))48,50,50
   48 JJJ(I) = 0
   50 CONTINUE
C     SEARCH FOR THE PEAK CHANNEL
      DO 20 IX = 1,N
      IJK(IX) = 0
      IX2(IX) = 0
      KI = KJI(IX)
  101 KJ = KI - 1
      IF(JJJ(KI)-JJJ(KJ))11,12,12
```

```
   11 KI = KJ
      GO TO 101
   12 KJ = KI + 1
      IF(JJJ(KI)-JJJ(KJ))13,14,14
   13 KI = KJ
      GO TO 12
   14 I = 0
      IX2(IX) = KI - KJI(IX)
  145 IF(ABSF(IX2(IX)).LT.5)196,156
  156 J=KI-7
      K=KI+7
      GO TO 197
  196 CONTINUE
      J = KJJ(IX)
      K = KII(IX)
      KI = KJI(IX)
  197 IKI(IX) = KI
      DO 20 IA=J,K
      IJK(IX) = IJK(IX) + JJJ(IA)
   20 A(IX) = IJK(IX)
C     TRANSPOSE THE MATRIX OF CONTRIBUTION COEFFICIENTS INTO THE MATRIX OF THE
C     COEFFICIENT OF SIMULTANEOUS EQUATIONS
      DO 23 I=1,N
      DO 23 J=1,M
      IF(J-M)21,22,22
   21 F(I,J) = FRAC(J,I)
      GO TO 23
   22 F(I,J) = A(I)
   23 CONTINUE
      PRINT 777,(A(K),K=1,N)
C     CALCULATION FOR THE SOLUTIONS OF SIMULTANEOUS EQUATIONS
      CALL GAUSS2(N,1,.000001,F,COUNT,LKL)
      PRINT 2,LKL,(COUNT(I),I=1,N)
      DO 24 I=1,N
      DIS(I) = COUNT(I)*EXPF(DAYS   *.693/DECAY(I))/(EFF(I)*AMM*ABS(I))
   24 PRINT 8, IRLM , ISO(I), IKI(I), IX2(I), DIS(I)
      GO TO 46
  199 MMN = MMN - 1
      IF(IABC.EQ.1)339,299
  339 GO TO 42
  299 CONTINUE
      CALL TIME
      PRINT 999
      END
       SUBROUTINE   GAUSS2(N,M,EP,A,X,KER)
      DIMENSION A(8,9),X(1,8)
       NPM=N+M
   10  DO 34 L=1,N
       KP=0
       Z=0.0
       DO 12 K=L,N
       IF(Z-ABSF(A(K,L)))11,12,12
   11  Z=ABSF(A(K,L))
       KP=K
   12  CONTINUE
```

```
    IF(L-KP)13,20,20
13  DO 14 J=L,NPM
    Z=A(L,J)
    A(L,J)=A(KP,J)
14  A(KP,J)=Z
20  IF(ABSF(A(L,L))-EP)50,50,30
30  IF(L-N)31,40,40
31  LP1=L+1
    DO 34 K=LP1,N
    IF(A(K,L))32,34,32
32  RATIO=A(K,L)/A(L,L)
    DO 33 J=LP1,NPM
33  A(K,J)=A(K,J)-RATIO*A(L,J)
34  CONTINUE
40  DO 43 I=1,N
    II=N+1-I
    DO 43 J=1,M
    JPN=J+N
    S=0.0
    IF(II-N)41,43,43
41  IIP1=II+1
    DO 42 K=IIP1,N
42  S=S+A(II,K)*X(K,J)
43  X(II,J)=(A(II,JPN)-S)/A(II,II)
    KER=1
    GO TO 75
50  KER=2
75 CONTINUE
   END
```

5. PAPER TAPE DATA INPUT - SUBROUTINE CON(IABC)

```
      SUBROUTINE CON(IABC)
      COMMON/MM/JJJ(300)
      DIMENSION II(4000)
    1 FORMAT(10I10)
    2 FORMAT(5X,12HBAD SPECTRUM
      PIE = 3.1415926536
      IABC = 0
      DO 5 I=1,4000
 5    II(I) = 0
      DO 6 I = 1,300
 6    JJJ(I) = 0
   11 J = 1
      L = 1
      K = J + 49
      BUFFER IN (20,2)(II(J),II(K))
C     THE UNIT 20 IS ARBITRARILY SELECTED
   12 IF(UNIT,20)12,13,104,13
C     THE PROCESS TO EXCLUDE THE BLANK SPACES ON PAPER TAPE
   13 IF(II(L))17,14,17
   14 L = L + 1
      IF(L-50)13,13,11
   15 CONTINUE
      J = J + 50
      K = K + 50
      BUFFER IN (20,2)(II(J),II(K))
   16 IF(UNIT,20)16,17,104,17
   17 L = 0
      IF(K-4000)18,18,100
C     THE PROCESS TO EXCLUDE THE CONTINUOUS TOP ROW PUNCHES
   18 L = L + 1
      IL = L
      IF(L- K)19,19,15
  185 L = L + 1
      IF(L- K)19,19,15
   19 IF(II(L))20,18,20
   20 IF(II(L)-16)185,21,185
   21 L = L + 1
      IF(L- K)215,215,15
  215 IF(II(L)-16)22,21,22
   22 IF(II(L))23,18,23
C     THE FIRST NONZERO AND NONSIXTEEN BINARY COLUMN IS IY
   23 IY = L  $         I = 0
   29 J = J + 50
      K = K + 50
      L = L + 50
      BUFFER IN (20,2)(II(J),II(K))
      IF(K-4000)30,30,100
   30 IF(UNIT,20)30,31,104,31
   31 IF(II(K))29,33,29
C     THE INTEGER MXN IS THE TOTAL NUMBER OF BINARY COLUMN IN A ACCEPTABLE SPECT
   33 IF(L-IY-1750)100,335,335
  335  L = IY
   34 L = L + 1
```

```
      IF (II(L).EQ.0)37,35
   35 IF(II(L)- 16)34,36,34
   36 I = I + 1
C     TRANSLATION OF THE IMAGES ON PAPER TAPE.
      I6 = (II(L-1)-1)/2
      I5 = (II(L-2)-1)*5
      I4 = (II(L-3)-1)*50
      I3 = (II(L-4)-1)*500
      I2 = (II(L-5)-1)*5000
      I1 = (II(L-6)-1)*50000
      JJJ(I)= I1+I2+I3+I4+I5+I6
      GO TO 34
   37 L = L+ 1
      IF(II(L).EQ.0)40,35
   40 IF(200.LT.I.AND.I.LT.260)41,42
   41 RETURN
   42 IF(L.LT.200)34,43
   43 PRINT 2  $        L1 = L - 25  $        L2 = L + 24
      PRINT 1,L,K,I,(II(N),N=L1,L2)
      GO TO 105
  100 PRINT 2
      PRINT 1,L,K,I
  105 IABC=2
      RETURN
  104 CONTINUE
      IABC = 1
      RETURN
      END
```

6. DISPERSION COEFFICIENT -- DISPRSN

```
DISPRSN.EH011444,SHIH.
RUN(G)

      PROGRAM DISPRSN (INPUT,OUTPUT)
C     PROGRAM DISPRSN
      DIMENSION TIME(100),CONC(100),DISPR(50), VARNS(50),TMEAN(50),
     1UNITM(50),TMASS(50),X(50),VARNX(50)
    1 FORMAT(8I10)
    2 FORMAT(8F10.4)
    3 FORMAT(/,5X,F10.2,2X,5F16.6)
   44 FORMAT(1H1)
   55 FORMAT(8X,16HDYE STUDY NUMBER,I3//)
   66 FORMAT(12X,8HDISTANCE,2X,19HMEAN FLOW THRU TIME,4X,10HVARANCE(X),
     16X,13HDISPRSN COEFF)
      READ 1, MM
      DO 15 L=1,MM
      PRINT 44
      PRINT 55,L
      PRINT 66
      READ 1,M
      DO 15 J=1,M
      READ 2, X(J)
      READ 1,N
      READ 2, TIMO,DELTM
      READ 2, (CONC(I),I=2,N)
      TIME(1)=TIMO
      UNITM(J)=0.
      TMASS(J)=0.
      DO 10 I=2,N
      K=I-1
      TIME(I)=TIME(K)+DELTM
      UNITM(J)=UNITM(J)+CONC(I)
   10 TMASS(J)=TMASS(J)+CONC(I)*TIME(I)
      TMEAN(J)=TMASS(J)/UNITM(J)
      TDEV=0.
      DO 12 I=2,N
   12 TDEV=TDEV+(TIME(I)-TMEAN(J))**2*CONC(I)
      VARNS(J)=TDEV/UNITM(J)
      VARNX(J)=VARNS(J)*X(J)**2/(TMEAN(J)**2)
      IF(J-1)21,21,20
   20 DISPR(J)=(VARNX(J)-VARNX(J-1))/2/(TMEAN(J)-TMEAN(J-1))
      GO TO 15
   21 DISPR(J)=0.0
   15 PRINT3,X(J),TMEAN(J),VARNX(J),DISPR(J),VARNS(J)
      END
```

7. TRANSPORT FUNCTION -- TRNSPRT

```
TRNSPRT,1,500,40000,4000.CE042016,SHIH.
RUN(S).
LGO.
'
      PROGRAM TRNSPRT (INPUT,OUTPUT)
C     THIS PROGRAM IS DESIGNED FOR THE PREDICTION OF RADIONUCLIDES TRANSPORT IN
C     THE STREAM SYSTEM
      DIMENSION TIME(20),B1(80),DELTA(20),TAU(400),X(10),T(40),S1(20),
     1S2(20),S3(20),H1(20),H2(20),H(20),CONC(20),TAMDA(400),F(400)
      PIE=3.1415926536
    1 FORMAT(8I10)
    2 FORMAT(8F10.2)
    3 FORMAT(5X,F1.02,5X,F10.2,5X,F16.8,5X,F16.8)
    4 FORMAT(1H1)
    5 FORMAT(5X,8HDISTANCE,10X,4HTIME,8X,14HINTEGRAL VALUE,5X,10HCONCENT
     1ION///)
    7 FORMAT(E10.2,3F10.6,2E10.2,F10.4)
      READ 1,NP
      READ 7,TMASS,A,DX,VEL,SK,H,DK
      B=VEL**2./4./DX+SK/H*DK-SK
      SA=SK/H
      DO 90 N=1,NP
      PRINT 4
      PRINT 5
      READ 2,X(N)
      READ 1,MN
      DO 90 I=1,MN
      READ 2,TIME(I)
      DELTA(I)=TIME(I)/40.0
      TAU(1)=0.
      DO 80 J=2,40
      TAU(J)=TAU(J-1)+DELTA(I)
      TAMDA(J)=2.*SQRTF(SA*SK*DK*TAU(J)*(TIME(I)-TAU(J)))
      PRINT 2,TAMDA(J)
      CALL BES(1,TAMDA,1,B1,T)
   80 F(J)=B1(J)*SQRTF(SA*SK*DK/(TIME(I)-TAU(J)))/TAU(J)*EXPF(-(X(N)**2
     1/4./DX/TAU(J)+B*TAU(J)))
      S1(I)=S2(I)=S3(I)=0.
      DO 81 L=3,39,4
   81 S1(I)=S1(I)+F(L)
      DO 82 L=5,37,4
   82 S2(I)=S2(I)+F(L)
      DO 83 L=2,40,2
   83 S3(I)=S3(I)+F(L)
      H1(I)=(4*S1(I)+2*S2(I))*DELTA(I)/1.50
      H2(I)=(4*S3(I)+2*S2(I)+2*S1(I))*DELTA(I)/3.0
      H(I)=(16*H2(I)-H1(I))/15.0
      CONC(I)=H(I)*TMASS*X(N)/(2*A*VEL*SQRTF(PIE*DX))*EXPF(VEL*X(N)/2./
     1DX-SK*TIME(I))/28316.0
   90 PRINT 3,X(N),TIME(I),H(I),CONC(I)
      END
      SUBROUTINE BES(NO,X,KODE,RESULT,T)
       DIMENSION T(40)
```

APPENDIX II

Procedures of Sampling and Processing

1. Sediments Sample

A. Sampling Procedures

(1) Preparation

(a) Clean the plunger and lucite tube.

(b) Put grease (Vaseline is recommended) around the rim of the aluminum disc and the central guide wire.

(c) Push the plunger into the lucite tube smoothly. Set the plunger as shown below.

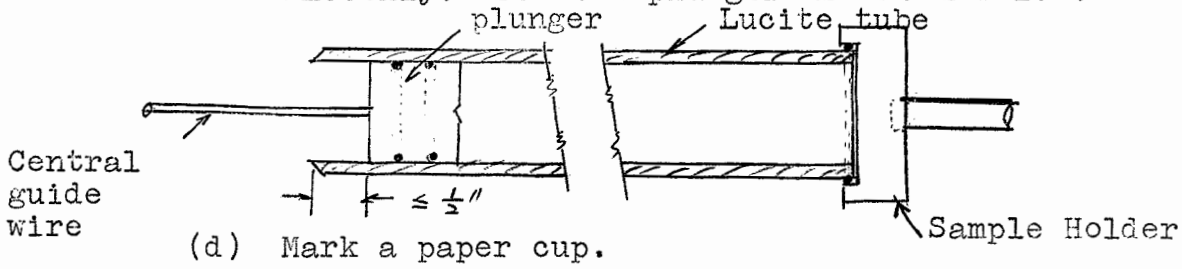

(d) Mark a paper cup.

(e) Push the lucite tube with plunger into the sampling handle.

(2) Sampling

(a) Push the plunger wire into the sediment.

(b) Push the sampling rod downward until the lucite tube reaches the bottom. Then pull the entire sampler out. Gentle rotation and pulling action is recommended.

(3) Sediment Release

(a) After the tube and core are pulled out of the sediments, remove the tube from sample holder.

(b) Put the tube into the premarked paper cup.

(c) During the "removing" action, the sediment core must not be shaken.

B. Processing Procedures

(1) Freezing

(a) The lucite tube with sediment core should be frozen as soon as possible.

(b) More than 8 hours freezing time is required.

(2) Cutting (for regular samples)

(a) After the sample is frozen, the plunger must be pushed out and removed from the lucite tube.

(b) Then the sediment core is pushed out gently. A circular 3/4 in. steel rod may be used.

(c) Finally, the top 3 in. of the frozen core is cut for drying.

(3) Cutting (for penetration samples)

(a) Repeat steps of (2)(a) and (2)(b).

(b) Sections are cut at points 1/4, 1/2, 1, and 3 in. from the top of the original core.

Note: It is recommended that the sediment core be pushed out in steps along with the cutting process.

(4) Heating, Grinding, and Weighing

(a) Put sections of the sediment core in the premarked crucibles and heat at 110°C for more than 8 hours.

(b) Grind the dried sediments into powder.

(c) Weigh the ground sediments and place in a planchet.

(d) If the sediment is more than what a planchet can accommodate, transfer only 2 gms. to the planchet and record the total weight.

(e) Spread the sediment on the planchet evenly, using a binder such as dilute lucite.

2. Vallisneria Sample

A. Sampling Procedures

(1) Samples are removed by tongs from test bed one leaf at a time.

(2) After the leaf has been cut, rinse it with tap water while still holding.

(3) Place the leaf in an appropriately marked cup.

B. Processing Procedures

(1) Dry leaves under heat lamps for at least 48 hours.

(2) Chop the dried leaves with a spatula while the leaves are still in the cups.

(3) Transfer the sample into an appropriate planchet.

(4) Determine sample weight and enter into the log book.

(5) "Tack" down sample with lucite.

3. Water Sample

A. Sampling Procedures

(1) Set up vacuum system and the depth of drawoff.

(2) Mark the 100-ml polyethylene bottles appropriately.

(3) Turn on the vacuum and suck the water into the bottles.

B. Processing Procedures

(1) Transfer 10 ml of water solution into the appropriate planchet from each bottle.

(2) Dry the planchet under infrared lamps.

APPENDIX III

Analytical Solution for Sorption-Desorption Model

Appendix III

FORMULA DERIVATION

1. The assumption is made that the sorption of radionuclides by sediments is greater than that of plants. Based on mass balance principle

$$\frac{\partial (CA\ x)}{\partial t} = AN\Big|_x - AN\Big|_{x+\Delta x} + QC\Big|_x - QC\Big|_{x+\Delta x} + \Delta x W N_s \quad (A\text{-}1)$$

Where

N = $-D_x \frac{\partial C}{\partial x}$

N_s = $k_1 (C_s - K'_s C)\ D \cdot \rho_s$

K'_s = constant to define average

$$\frac{\text{dpm in unit weight of sediments}}{\text{dpm in unit volume of water}}$$

ρ_s = the density of sediments

A = W (width) · H (depth)

and

D = total depth of sediments

Take limits as $\Delta x \rightarrow 0$ and divide the Eq. A-1 by $(A\Delta x)$, then Eq. A-1 becomes

$$\frac{\partial C}{\partial t} = D_x \frac{\partial^2 C}{\partial x^2} - U \frac{\partial C}{\partial x} + \frac{1}{H} k_1 (C_s - K'_s C)\ (D\rho_s) \quad (A\text{-}2)$$

The radionuclides associated with sediments usually are expressed in terms of total radionuclides in unit surface area. Here, the total radionuclides in the sampling core, m, of the sediments are used as the basis for comparison; and the relationship between the C_s value and the m value is according to

$$m = D \cdot a \cdot \rho_s \cdot C_s$$

Then Eq. A-2 can be expressed as,

$$\frac{\partial C}{\partial t} = D_x \frac{\partial^2 C}{\partial x^2} - U\frac{\partial C}{\partial x} + \frac{1}{H \cdot a}(m - K_s C) \qquad (A\text{-}3)$$

Where K_s = $K'_s \times D \times \rho_s \times a$

= $\frac{\text{total dpm in each sediment core}}{\text{dpm in unit volume of water}}$

The changing rate of the radionuclides associated with the sediments can be functionized by the non-equilibrium reactions.

$$\frac{\partial m}{\partial t} = \frac{\partial C_s}{\partial t} \cdot D \cdot a \cdot \rho_s = K_1 \frac{As}{\forall s} \cdot D \cdot a \cdot \rho_s (K'_s C - C_s)$$

$$= \frac{K_1}{D}(K_s C - m) \qquad (A\text{-}4)$$

Where $\forall s$ = volume of sediments in the infinitesimal compartment

Let $k_1 = \frac{K_1}{D}$ = mass transfer coefficient per unit depth of sediments

Then, Eqs. A-3 and A-4 become:

$$\frac{\partial C}{\partial t} = D_x \frac{\partial^2 C}{\partial x^2} - U\frac{\partial C}{\partial x} + \frac{k_1}{H \cdot a}(m - K_s C) \qquad (A\text{-}5)$$

$$\frac{\partial m}{\partial t} = k_1 (K_s C - m) \qquad (A\text{-}6)$$

with the following boundary conditions

$$C(x, 0) = \quad ; \quad x > 0 \qquad (A\text{-}7)$$

$$\lim_{t\to\infty} C(x,\ t)\to 0+ \quad ; \quad \lim_{x\to\infty} C(x,\ t)\to 0 \qquad \text{(A-8)}$$

$$m(x,\ 0) = 0 \quad ; \quad x>0 \qquad \text{(A-9)}$$

and the initial condition

$$C(0,\ 0) = \frac{M}{AU}\,\delta(t-0) \qquad \text{(A-10)}$$

The simultaneous partial differential Eqs. A-5 and A-6 are solved by use of Laplace transforms. Their transformed equations are:

$$sC(x,\ s) = D_x\frac{\partial^2 C(x,\ s)}{\partial x^2} - U\frac{\partial C(x,\ s)}{\partial x} - \frac{k_1}{H\cdot a}\left[K_s C(x,\ s) - m(x,\ s)\right] \qquad \text{(A-11)}$$

and

$$sm(x,\ s) = k_1\left[K_s C(x,\ s) - m(x,\ s)\right] \qquad \text{(A-12)}$$

By solving Eqs. A-11 and A-12 with the aid of boundary conditions,

$$C(x,\ 0) = 0 \quad ; \quad s>0$$

$$\lim_{s\to\infty} C(x,\ s)\to 0 \quad ;$$

the solution of the transformed equation is:

$$C(x,\ s) = \frac{M}{AU}\, e^{\frac{Ux}{2D_x}}\, e^{-x\sqrt{\frac{U^2}{4D_x^2} + \frac{1}{D_x}\left[dK_s + s - \frac{dk_1K_s}{s+k_1}\right]}} \qquad \text{(A-13)}$$

Meanwhile, let

$$e^{-x\sqrt{\frac{U^2}{4D_x^2} + \frac{1}{D_x}\left[dK_s + s - \frac{dk_1K_s}{s+k_1}\right]}} = e^{-\sqrt{p}\,x} = \frac{se^{-\sqrt{p}\,x}}{s+k_1} + \frac{k_1 e^{-\sqrt{p}\,x}}{s+k_1} \qquad \text{(A-14)}$$

The inversion of Eq. A-13 has involved the rarely used formula

$$L\left\{\int_0^t J_o\left[2\sqrt{x(t-x)}\right] F(x)dx\right\} = \frac{1}{s} f(s+\frac{1}{s}) \qquad (A\text{-}15)$$

By the insertion of constant terms and the substitution of (s+D), Eq. A-15 becomes:

$$L\left\{e^{-Dt} \int_0^t J_o\left[2\sqrt{Ex(t-x)}\right]F(x)\, dx\right\}$$

$$= \frac{1}{s+D} f(s+D+\frac{E}{s+D}) \qquad (A\text{-}16)$$

Now, the $(s+\frac{1}{s})$ becomes $\exp(-A(s+\frac{1}{s})^{\frac{1}{2}}$, then

$$f(s+D+\frac{E}{s+D}) = e^{-A\sqrt{s+D+\frac{E}{s+D}+B}} \qquad (A\text{-}17)$$

Comparing $e^{-\sqrt{p}\,x}$ and $e^{-A\sqrt{s+D+\frac{E}{s+D}+B}}$, the following equations are derived.

$$A = \frac{x}{\sqrt{D_x}}$$

$$E = -d\, k_1 K_s$$

$$B = \frac{U^2}{4D_x} + dK_s - k_1$$

$$D = k_1$$

$$L^{-1}\left\{\frac{e^{-\sqrt{p}\,x}}{s+k_1}\right\} = e^{-k_1 t} \int_0^t I_o\left[2\sqrt{dk_1 K_s(t-\tau)\tau}\right] e^{-(\frac{x^2}{4D_x\tau})-(\frac{U^2}{4D_x}+dK_s-k_1)\tau} \frac{x}{2\sqrt{\pi D_x \tau^3}}\, d\tau \qquad (A\text{-}18)$$

If, $L^{-1}\left\{\frac{e^{-\sqrt{p}\,x}}{s+k_1}\right\} = k_1\, G(x, t)$

Then, $L^{-1}\left\{\frac{s\, e^{-\sqrt{p}\,x}}{s+k_1}\right\} = L^{-1}\left\{s\, g(x, s)\right\}$

But, $L\left\{G'(x, t)\right\} = s\, g(x, s)$

So, $L^{-1}\left\{\frac{s\, e^{-\sqrt{p}\,x}}{s+k_1}\right\} = G'(x, t)$ (A-19)

With the aid of Leinitz formula and the differentiation of Bessel function, $\frac{\partial}{\partial z} I_0(z) = I_1(z)$,

$$L^{-1}\left\{e^{-\sqrt{p}\,x}\right\} = \frac{x}{2\sqrt{\pi D_x}}\, e^{-k_1 t} \int_0^t I_1\left[2\sqrt{dk_1 K_s (t-\tau)\tau}\right]\sqrt{\frac{dk_1 K_s}{t-}}\,\frac{1}{\tau}\, e^{-\left(\frac{x^2}{4D_x\tau} + B\tau\right)}\, d\tau \quad \text{(A-20)}$$

Substituting Eq. A-20 into the inversion of Eq. A-13, Eq. 6-26 is derived.

2. The assumption is made that the sorption of radionculides by an aquatic plant is greater than that of sediments. The radionuclide mass in the water phase is balanced as

$$\frac{\partial(CA\Delta x)}{\partial t} = AN\Big|_x - AN\Big|_{x+\Delta x} + QC\Big|_x - QC_{x+\Delta x} + A\Delta x N_p \qquad \text{(A-21)}$$

Where

N_p = $m_b K_2 (C_p - K_c C)$

m_b = biomass in unit volume of stream

K_2 = the constant to define the mass transfer mechanism through the interface of water and the aquatic plant

K_c = equilibrium concentration factor for the radionuclides associated with the aquatic plant

and C_p = radionuclides associated with unit weight of biomass of the aquatic plant

For the radionuclides variation associated with the aquatic plant, the mass can be balanced

$$\frac{\partial M_p}{\partial t} = m_b \, A\Delta x \, K_2 (C_p - K_c C) \qquad \text{(A-22)}$$

Where

M_p = total mass of radionuclides associated with the aquatic plant in unit compartment

But, by definition, it is realized that

$$M_p = m_b \, A\Delta x \, C_p \qquad \text{(A-23)}$$

Therefore, Eq. A-21 and Eq. A-22 limits can be taken as $\Delta x \longrightarrow 0$ and their partial differential equations derived:

$$\frac{\partial C}{\partial t} = D_x \frac{\partial^2 C}{\partial x^2} - U\frac{\partial C}{\partial x} - m_b K_2 \left[C_p - K_c C\right] \qquad \text{(A-24)}$$

$$\frac{\partial C_p}{\partial t} = K_2 \left[C_p - K_c C\right] \qquad \text{(A-25)}$$

With the following boundary conditions

$$C(x, 0) = 0 \quad ; \quad x>0 \qquad \text{(A-26)}$$

$$\lim_{x \to \infty} C(x, t) \quad 0^+ \quad ; \quad \lim_{x \to \infty} C(x, t) \to 0 \qquad \text{(A-27)}$$

$$C_p(x, 0) = 0 \quad ; \quad x>0 \qquad \text{(A-28)}$$

and the initial condition

$$C(0, 0) = \frac{M}{AU} \delta(t-0) \qquad \text{(A-29)}$$

The solution for C(x, t) is solved as presented in Eq. 7-5.

BIBLIOGRAPHY

1. Ames, L. L., "Effect of Base Cation on the Casium Kinetics of Clinoptilolite," U.S.A.E.C. Report HW-SA-2452, General Electric Co., Hanford Atomic Products Operation, Richland, Wash. (Feb. 1962).

2. Aris, R., "On the Dispersion of Solute in Fluid Flowing Through a Tube," Proceedings Ser. A, Royal Soc. of London, 235 (1956).

3. Bennett, C. O., and Meyers, J. E., "Momentum, Heat, and Mass Transfer," McGraw-Hill Book Co., New York (1962).

4. Bhagat, S. K., "Transport of Nitrosylruthenium in an Aquatic Environment," Ph. D. Dissertation, The University of Texas (1966).

5. Bowen, V. T., and I. Ketchum, "Biological Factors Determining the Distribution of Radioisotopes in the Sea," 2nd U. N. International Conference of Peaceful Use of Atomic Energy (September 1-15, 1958).

6. Boegly, W. J., Jr., et al, "Disposal in Natural Salt Formations," Health Physics Division Annual Progress Report for Period Ending July 31, 1962, USAFC ORNL, 13-17 (Nov. 12, 1962).

7. Brey, W. S., "Principles of Physical Chemistry," Appleton-Century-Crofts, Inc., New York, 245 (1958).

8. Burkholder, Paul P., "Radioactivity in Some Aquatic Plants," Nature, 198, No. 4880, 601-603 (May 11, 1963).

9. Canter, L. W., "Transport of ^{51}Cr in the Model River," Unpublished Dissertation, The University of Texas (1967).

10. Churchill, R. V., "Operational Mathematics", McGraw-Hill Book Co., New York (1963).

11. Daniels, F., "Outlines of Physical Chemistry," John Wiley and Sons, Inc., New York, 255 (1948).

12. Diachichin, Alex N., "Dye Dispersion Studies," Journal of ASCE, SED, 89, SA, (Jan. 1963).

13. "The Disposal of Radioactive Waste on Land," Natl. Acad. of Sci., Natl. Research Council, Div. of Earth Sci. (1956).

14. Elder, J. W., "The Dispersion of Marked Flow in Turbulent Shear Flow," J. of Fluid Mech., 5, 544-560 (1959).

15. Fischer, H. B., "A Note on the One-Dimensional Dispersion Model," Air and Water Pollution Inst. J., Pergamon Press, London, 10, 443-452 (1966).

16. Fischer, H. B., "Longitudinal Dispersion in Laboratory and Natural Stream," Keck Lab. of Hyd. and Water Resources, Cal. Tech., Pasadena, Calif. (1966).

17. Fröberg, G., "Introduction to Numerical Analysis," Addison-Wesley Co., New York (1956).

18. Fujita, L., et al, "The Behavior of ^{85}Sr in a Normal Man Following a Single Injection," Health Physics, 9, 407-415 (April, 1963).

19. Gloyna, E. F., et al, "Transport of Radionuclides in a Model River," IAEA Symposium, Vienna, Austria (May, 1966).

20. Grim, R. E., "Clay Mineralogy," McGraw-Hill Book Co., New York, 27 (1953).

21. Hayes, F. R. and Phillips, J. E., "Radiophosphorous Equilibrium Mud, Plants, and Bacteria under Oxidized and Reduced Conditions," J. Limn. and Oceanog., 4, 459-475 (Oct. 1948).

22. Hays, J. R., "Mass Transport Mechanism in Open-Channel Flow," Ph. D. Dissertation, Vanderbilt Univ. (1966).

23. Helfferich, F., "Ion Exchange," McGraw-Hill Book Co., New York (1962).

24. Jacobs, D. G., et al, "Soil Column Studies," Health Physics Division Annual Progress Report for Period Ending July 31, 1960, U.S.A.E.C., ORNL, 78-95 (Oct. 24, 1960).

25. Krenkel, P. A. and Orlob, G. I., "Turbulent Diffusion and Reaeration," J. of ASCE, SEC, 87, 20-35 (March 1962).

26. Krumholz, L. A., et al, "Etiological Factors Involved in the Uptake, Accumulation, and Loss of Radionuclides by Aquatic Organisms," The Effects of Atomic Radiation on Oceanography and Fisheries, Natl. Acad. of Sci., Natl. Research Council, Pub. No. 551, Washington, D. C., 77 (1957).

27. Krumholz, L. A., et al, "Accumulation and Retention of Radioactivity from Fission Products and Other Radiomaterials by Fresh-water Organism," The Effects of Atomic Radiation on Oceanography and Fisheries, Natl. Acad. of Sci., Natl. Research Council, Pub. No. 551, Washington, D. C.,91 (1957).

28. Lacy, W. J., "Decontamination of Radioactivity Contaminated Water by Slurrying with Clay," Ind. and Engin. Chem., 46, 5, 1061 (May 1954).

29. McHenry, J. R., "Adsorption and Retention of Strontium by Soils of the Hanford Project," U.S.A.E.C. HW34499 (Feb. 1, 1955).

30. Morton, P. J, et al, "Status Report No. 2 on Clinch River Study," ORNL, 34 (Apr. 13, 1962).

31. Morton, P. J., et al, "Status Report No. 4 on Clinch River Study," ORNL, 25-32 (Sept. 25, 1963).

32. Orlob, G. I., "Eddy Diffusion in Homogenous Turbulence," J. of ASCE, HY9, 85 (Sept., 1959).

33. Pickering, R. J. and Carrigan, P. H., "Radioactive Materials in Bottom Sediments of Clinch River: Part B, Inventory and Vertical Distribution of Radionuclides in Undisturbed Cores," Health Physics Final Progress Report, U.S.A.E.C., ORNL, 5-60 (March, 1967).

34. Purushothaman, K., "Transport of ^{137}Cs in Turbid Environment," Unpublished Dissertation, The University of Texas (1967).

35. Patterson, C. C. and Gloyna, E. F., "The Dispersion of Radionuclides in Open Channel Flow," Tech. Report - 2, U.S.A.E.C. Contract At(11-1)-490 (June 1, 1960).

36. Raymond, H., "Uptake of Strontium by Roots of Zea Mayo," Plant Physiology, 38, 180-184 (March, 1963).

37. Reynolds, T. and Gloyna, E. F., "Radioactivity Transport in Water--Treatment of Strontium and Cesium by Stream and Estuarine Sediments," Tech. Report - 1, U.S.A.E.C. Contract AT(11-1)-490, 7, The University of Texas (1963).

38. Richardson, L. F., "Atmospheric Diffusion Shown on a Distance-Neighbor Graph," Royal Society of London, (Nov. 1925).

39. Richardson, L. F., "Note on Eddy Diffusion in the Sea," J. of Meterology, 5, 238-240 (Oct. 1949).

40. Rowe, D. R. and Gloyna, E. F., "Radioactivity Transport in Water--Transport of ^{65}Zn in an Aqueous Environment," Tech. Report 4, U.S.A.E.C. Contract AT(11-1)-490, The University of Texas (1964).

41. Sayre, W. W., et al, "Progress Report: Dispersion and Concentration of Radioactive Wastes by Streams," U.S.G.S. CER59ARC26, Denver, Colorado, 35 (1959).

42. Shih, C. S., "Transport of ^{85}Sr and ^{137}Cs in an Aquatic Environment," Master's Thesis, The University of Texas (1966).

43. Story, A. H. and Gloyna, E. F., "Radioactivity Transport in Water--Environment Behavior of Nitrosylruthenium," Tech. Report 3, U.S.A.E.C. Contract AT(11-1)-490, The University of Texas (1963).

44. Struxness, E. G., et al, "Clinch River Studies," Health Physics Division Annual Progress Report for Period Ending July 31, 1960, U.S.A.E.C., ORNL, 48 (Oct. 24, 1960).

45. Sverdrup, H. V., "Oceanography for Meteorologists," Prentice-Hall, Inc., New York (1943).

46. Tamura, T., et al, "Ion Exchange of Minerals," Health Physics Division, ORNL (July 31, 1962).

47. Tamura, T. and Struxness, E. G., "Reactions Affecting Strontium Removal from Radioactive Wastes," Unpublished Paper, Health Physics Division, Oak Ridge National Laboratory.

48. Tamura, T., et al, "Sorption and Retention by Minerals and Compounds," Health Physics Division Annual Progress Report for Period Ending July 31, 1960, U.S.A.E.C., ORNL, 58-78 (Oct. 24, 1960).

49. Taylor, Sir G. I., "Diffusion by Continuous Movements," Proc. London Mathematical Soc., Ser. 2, 20, 196-212 (1921).

50. Thackston, E. L., "Longitudinal Mixing and Reaeration in Natural Stream," Ph. D. Thesis, Vanderbilt University (1966).

51. Thomas, I. E., "Dispersion in Open Channel Flow," Ph. D. Dissertation, Northwestern University (1958).

52. Western, F., "Problems of Radioactive Waste Disposal," Nuc. Sci. Abst., 1, 7 (Sept. 30, 1948). Original article in Nucleonics, 3, 2, 43-49 (Aug. 1948).

53. Yotsukura, Nobubiro and Fiering, "Numerical Solution to Dispersion Equation," Proceedings ASCE, Hyd. Div. 90, HY5 (Sept. 1964).

54. Yousef, Y. A. and Gloyna, E. F. "The Transport of ^{58}Co in an Aqueous Environment," Tech. Report - 7, U.S.A.E.C. Contract AT(11-1)-490 (Dec. 1, 1964).

55. Mclachlan, N. W. and Humbert, P., "Mem. des Science Math.," 100, 12 (1941).

56. Watson, G. N., "A Treatise on the Theory of Bessel Functions," 2nd Ed., Cambridge University Press, London (1944).